A systematic review
Enhancing cementitious composites through additively manufactured lattice structures

El Etri, Hamza; Ghanbari-Ghazijahani, Tohid; Abbassi, Rouzbeh; Schlangen, Erik

DOI
10.1080/15376494.2025.2585150

Publication date
2025

Document Version
Final published version

Published in
Mechanics of Advanced Materials and Structures

Citation (APA)
El Etri, H., Ghanbari-Ghazijahani, T., Abbassi, R., & Schlangen, E. (2025). A systematic review: Enhancing cementitious composites through additively manufactured lattice structures. *Mechanics of Advanced Materials and Structures*, Article 2585150. https://doi.org/10.1080/15376494.2025.2585150

Mechanics of Advanced Materials and Structures

ISSN: 1537-6494 (Print) 1537-6532 (Online) Journal homepage: www.tandfonline.com/journals/umcm20

A systematic review: Enhancing cementitious composites through additively manufactured lattice structures

Hamza El Etri , Tohid Ghanbari-Ghazijahani , Rouzbeh Abbassi & Erik Schlangen

To cite this article: Hamza El Etri , Tohid Ghanbari-Ghazijahani , Rouzbeh Abbassi & Erik Schlangen (08 Dec 2025): A systematic review: Enhancing cementitious composites through additively manufactured lattice structures, Mechanics of Advanced Materials and Structures, DOI: 10.1080/15376494.2025.2585150

To link to this article: https://doi.org/10.1080/15376494.2025.2585150

MECHANICS OF ADVANCED MATERIALS AND STRUCTURES
https://doi.org/10.1080/15376494.2025.2585150

Taylor & Francis
Taylor & Francis Group

ORIGINAL ARTICLE

A systematic review: Enhancing cementitious composites through additively manufactured lattice structures

Hamza El Etri[a], Tohid Ghanbari-Ghazijahani[a], Rouzbeh Abbassi[a], and Erik Schlangen[b]

[a]Faculty of Science and Engineering, School of Engineering (Civil), Macquarie University, Sydney, Australia; [b]Faculty of Civil Engineering & Geosciences – Section of Materials & Environment, Delft University of Technology, Delft, The Netherlands

ABSTRACT

Additive manufacturing (AM) has revolutionized the fabrication of complex geometries, enabling efficient material use and innovative applications across sectors such as biomedical, automotive, and aerospace. A significant development is the emergence of 3D-printed lattice structures (LSs), which combine lightweight design with tailored mechanical properties, making them highly suitable for civil engineering applications, including bridge elements, façade systems, and reinforcement of concrete structures. Recent research has increasingly explored the integration of LSs into cementitious composites, though findings remain diverse and primarily experimental. This paper provides a comprehensive review of lattice structures in cement-based materials, examining both their classifications – by dimensionality (2D vs. 3D) and configuration (cellular vs random) – and their role in enhancing ductility, reducing weight, and improving overall performance. It also surveys materials commonly used in 3D printing, such as polymers (PLA, PEEK, ABS), ceramics, and composites, along with relevant printing techniques. Evidence demonstrates that LSs significantly improve the mechanical behavior of cementitious composites, transforming failure modes from brittle to ductile and increasing energy absorption. These findings highlight the potential of 3D-printed lattices as effective reinforcements, offering promising pathways for advancing structural performance in construction.

ARTICLE HISTORY
Received 9 April 2025
Accepted 28 October 2025

KEYWORDS
Cementitious composites; lattice structures; 3D printing; mechanical properties; composites

Abbreviations

AM	Additive manufacturing
CAD	Computer-aided design
SLA	Stereolithography
STL	Standard tessellation language
PLA	Polylactic acid
PC	Polycarbonate
PA	Polyamide
ECC	Edge-centered cubic
SC	Simple cubic
TPMS	Triply periodic minimal surface
PP	Polypropylene
TPE	Thermoplastic elastomers
EBAM	Electron beam additive manufacturing
SLM	Selective laser melting
FDM	Fused Deposition Modeling
GFRP	Glass fiber reinforced plastic
HDPE	High-density polyethylene
PTFE	Polytetrafluoroethylene
SU	Large surface-based sea urchin
FPMA	Flat plate modified auxetic
FPT	Fixed-parameter tractable
FPV	Shortest vector problem
MJF	Multi-jet fusion
PDED	Powder-directed energy deposition
PBBJ	Powder-bed binder jetting
CFRCLSs	Continuous fiber-reinforced composite lattice structures
LUCIE	Unit-cell Characterization Interface for Engineers
NLS	Nested lattice structures
BDL	Bending-dominated lattice
NBCC	Novel body-centered cubic
FPMA	Flat plate modified auxetic
FPV	Flat plate ventile
FPT	Flat plate tesseract
TPE	Thermoplastic elastomers
UHPFRC	Ultra-high-performance fiber-reinforced concrete
PA6	Polyamide 6
CBC	Reinforced cement-based composites
DIC	Digital image correlation
OR	Ordinary resin
ACCs	Auxetic cementitious composites
RE	Reentrant
CR	Chiral
SA	Sand-sprinkled epoxy
SF	Short steel fibers in epoxy
NPR	Negative Poisson's ratio
NRC	Non-reinforced cementitious beam
LRCCs	Lattice-reinforced cementitious composites
AE	Acoustic emission
LS	Lattice structure
ABS	Acrylonitrile butadiene styrene
PEEK	Polyether-ether-ketone
3D	Three dimensions
IWP	Isotropic woodpile
FRD	Förstner random dots
BCC	Body-centered cubic
FCC	Face-centered cubic
ULTEM	Polyetherimide
CFRCLSs	Continuous fiber-reinforced composite lattice structures

CONTACT Tohid Ghanbari-Ghazijahani tohid.ghanbari@mq.edu.au, tohid.ghanbari@utas.edu.au, tohidghanbari@gmail.com Faculty of Science and Engineering, School of Engineering (Civil), Macquarie University, Sydney, Australia.

CF/PA6	Carbon fiber-reinforced polyamide 6
CNC	Computer numerical control
3DCP	3D concrete printing
PPSF	Polyphenyl sulfone
ASA	Acrylonitrile styrene acrylate
CFRP	Carbon fiber-reinforced polymer
LOM	Laminated object manufacturing
UAM	Ultrasonic additive manufacturing
NLS	Nested lattice structures
PAEK	Polyaryletherketone
LSs	Lattice structures
LMD	Laser metal deposition
DLP	Digital light processing
DIW	Direct ink writing
EBF 3	Electron beam freeform fabrication
TPU	Thermoplastic polyurethane
PC	Polycarbonate
BDPL	Bending-dominated periodic lattice
SDL	Stretching-dominated
PALS	Programmable active lattice structure
RVE	Representative volume element
UBCC	Uniform cell BCC
UBCCz	Uniform with z-axis reinforced cell
GBCC	Graded cell
L-PBF	Laser powder bed fusion Lattice-reinforced composites
3D-PPL	3D-printed polymer lattice
CT	Computed tomography
TR	Transparent resin
NY	Nylon
RS	Rotating-square
MR	Missing rib
w/b	Water-to-binder ratios
EP	Epoxy resin
CTB	Composite tailings backfill
FS	Fractal-square
FE	Finite element
OTEC	Octet-truss engineered concrete
mPCM	Micro-encapsulated phase change material

1. Introduction

Commonly known as 3D printing, additive manufacturing (AM) stems from the 1980s rapid prototyping technologies. It directly creates complex structures from 3D Computer-Aided Design (CAD) models, reducing costs and production times while optimizing products for lightweight design, energy absorption, and heat transfer [1]. AM produces parts layer by layer, bypassing the demand for molds or traditional machining. Techniques involved in AM include selective laser sintering (SLS), 3D inkjet printing, powder bed fusion (PBF), lap assembly, laser cutting, stereolithography (SLA), investment casting, stamping, selective laser melting (SLM), stretched mesh folding, and fused deposition modeling (FDM), among others [2–4]. AM utilizes a wide variety of polymers, including thermoplastics (PLA [5], ABS [6], Nylon [7], etc.), thermosets like epoxy resins [8], elastomers (TPU [9], TPE [10], etc.), functional polymers [11], polymer blends [12, 13], etc. [14].

Recent advancements in AM now allow for the fabrication of intricate, small-scale parts with optimized, lightweight forms, such as cellular and lattice structures. These lattice configurations bring substantial advantages, including enhanced mechanical strength and efficient energy absorption, due to their lightweight, high durability, and flexible geometry. They have gained popularity as an innovative structural design, providing both high load-bearing capacity and customizable mechanical responses through their unique porosity and structural adjustments [1, 15–18]. The mechanical behavior of LSs is primarily affected by various parameters, including relative density, volume fraction, design parameters, materials used, and the structure category (stretched/bending-dominated LSs). LSs have found applications in a diverse array of fields in aerospace, automotive, biomedical, heat exchangers, protective equipment, and structural sectors due to their unique characteristics [16, 19, 20].

In civil engineering applications, such as concrete reinforcements [21–23] cementitious composites reinforced with lattice structures are utilized due to their ability to enhance the structural integrity, ductility, and load-bearing capacity of concrete structures. Studies on the mechanical characteristics of 3D-printed lattice-reinforced concrete and the impact of various lattice designs have been gaining significant interest recently [22, 24, 25]. However, 3D LSs face challenges in terms of high costs, scalability, bonding, durability, and environmental impact compared to traditional reinforcements.

1.1. Motivation and organisation of paper

The rising interest in 3D-printed LSs is significantly altering the landscape of the construction industry by introducing groundbreaking solutions that improve both the strength and environmental viability of concrete implementations. These structures are engineered to be lightweight yet possess exceptional strength, enabling the fabrication of complex geometries that traditional construction methods often cannot achieve. The integration of LSs into concrete permits a significant reduction in material usage, which not only lowers costs but also diminishes environmental impact. These lattices enhance the mechanical characteristics of concrete, particularly in terms of ductility and its capacity to support loads, thereby increasing the safety and resilience of buildings. This innovative technology is paving the way for more efficient, sustainable, and cost-effective construction practices, addressing critical global challenges like housing shortages and the pursuit of sustainable development [15, 26, 27].

Studies indicate that the implementation of 3D-printed polymer lattices can reduce concrete usage while preserving structural integrity [28]. Consequently, there is growing attention on the application of 3D-printed LSs for both reinforced concrete and serving as molds in construction applications. This paper presents an overview of 3D-printed LSs incorporated into cementitious composites, as well as the application of novel concrete structures, including concrete poured into lattice-shaped molds and 3D-printed concrete lattice models. Section 1 includes a general introduction to the concept and the motivation behind the investigation of 3D-printed lattice structures incorporated into cementitious composites. Section 2 introduces AM lattice structures. Moreover, it provides a comprehensive overview of the role of 3D-printed LSs as reinforcement in cementitious

composites. It highlights how these structures enhance the mechanical properties of cement-based materials, improving ductility and reducing weight, ultimately boosting their performance. The use of 3D-printed lattice molds is emphasized for enabling complex geometric designs that are difficult to achieve through traditional methods. Additionally, it underscores the potential of 3D printing technology to optimize material usage and maintain structural integrity, offering innovative solutions for lightweight concrete components. Key conclusions are drawn from the literature, reinforcing the effectiveness of lattice structures in cement-based composites. Section 3 presents the future scopes and research gaps of the manuscript, and Section 4 presents an overall summary of the research findings. Figure 1 illustrates the VOSviewer network of all papers used in this paper, demonstrating the shown keywords as the main clusters.

1.2. Significance of paper

This review bridges the gap between AM techniques and their practical applications in enhancing cementitious composites. By presenting a comprehensive analysis of 3D-printed LSs and their mechanical behavior, this article aims to inform and inspire researchers and practitioners in the fields of materials science and civil engineering. Unlike other review papers that focused on presenting the application of auxetic materials in cementitious composites, our paper highlights the use of various types of LSs (TPMS lattices, Strut-based, auxetic, shell-based, hybrid lattices, etc.) as concrete reinforcements, molds, in addition to printing concrete in the form of cellular/lattice shapes. Table 1 shows a comparison between our manuscript and recent review papers.

2. Additively manufactured lattice structures

The AM technique is the procedure of assembling materials to produce customized and unique products for end customers. The technology has been widely popular among manufacturers and scholars in the last 20 years because of its immense capacity to design and manufacture complex designs, which may not be achievable using conventional methods [19, 37, 38]. For instance, AM allows for the rapid production of personalized biomedical implants with various intricacies, surpassing the speed of already established conventional methods [39]. One clear benefit of additive manufacturing compared to traditional production is its capacity to create complicated LSs with specifically engineered porosities [37]. An ideal AM process is establishing a CAD model of a part by transmitting the model to a printer and constructing the component incrementally [40–43]. The first SLA technologies were launched by Charles Hull in 1987 [41, 43]. Subsequently, other approaches have been devised with the continued advancement of novel additive manufacturing processes. To date, the total count of AM methods has surpassed 20. These techniques may be categorized in several ways, such as based on the kind of fabrication (indirect or direct) and the material condition (liquid, solid, or powder) (Table 2) [43, 68, 72–75]. AM facilitates the construction of personalized components incorporating metals, polymers, composites, cement, and ceramics, eliminating the need for molds or the usual machining processes used in traditional formative and subtractive manufacturing [14].

2.1. 3-D printing

3D printing is a mechanical method that assembles materials to generate items according to three-dimensional model

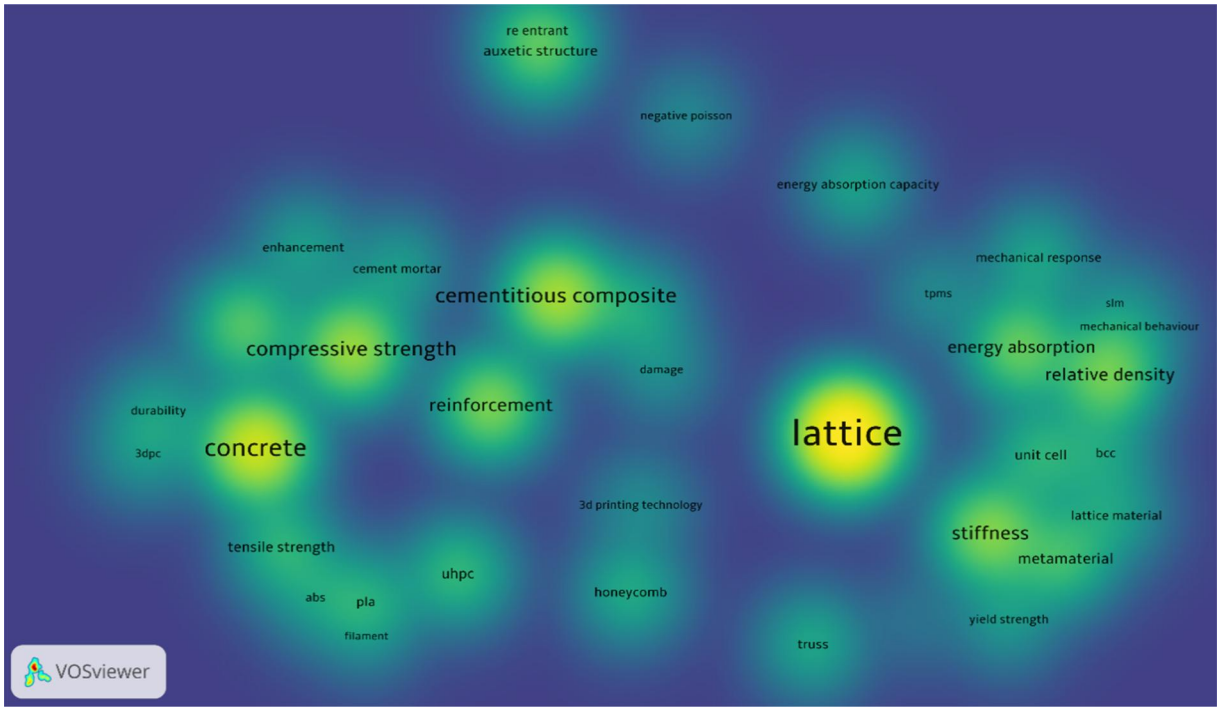

Figure 1. 3D cluster of the crucial keywords from the papers used in this review.

Table 1. A comparison between our manuscript and recent review papers.

Ref	Author (s)	Journal	Review paper title	Nb. of papers reviewed	Focus	Distinction from our RP paper
[19]	Chen Pan, Yafeng Han, and Jiping Lu	Applied Sciences, 2020 – mdpi.com	Design and optimization of lattice structures: A review	207	This paper focuses on the **design and optimization** of uniform/non-uniform lattices used in various applications.	Our manuscript focuses on LSs used in the **civil and construction** sectors.
[17]	H. Yin, W. Zhang, L. Zhu, F. Meng, J. Liu, and G. Wen	Composite Structures, 2023 – Elsevier	Review of lattice structures for energy absorption properties	221	This paper focuses on the **energy absorption** characteristics of lattices used in general applications.	Our manuscript highlights the influence of LSs on the mechanical behavior of **cementitious composites** only.
[29]	N. Khan and A. Riccio	Progress in Aerospace Sciences, 2024 – Elsevier	A systematic review of design for additive manufacturing of aerospace lattice structures: Current trends and future directions	448	This paper illustrates the applications, **materials, properties, and manufacturing methods** of lattices used in the **aerospace** industry.	The focus of the manuscript is **not only** on lattices but also on the behavior of **cementitious composites after incorporating LSs.**
[30]	M. Helou and S. Kara	International Journal of Computer Integrated Manufacturing, 2017 – Taylor and Francis	Design, analysis and manufacturing of lattice structures: an overview	106	This paper presents the **manufacturing process of lattices**, in addition to their design and applications.	Our manuscript presents a general overview of LS types, applications, and materials. However, the manuscript focused on lattices used in **civil engineering** applications (cementitious composites).
[31]	CJ. Hunt, F. Morabito, C. Grace, Y. Zhao, BKS. Woods	Composite Structures, 2022 – Elsevier	A review of composite lattice structures	132	This paper focuses on the concept of composite lattice structures, such as composite **lattice beams, stiffened panels, and sandwich panels.**	The focus is on general LS types used to **enhance the mechanical behavior of cementitious composites.**
[32]	I. Echeta, X. Feng, B. Dutton, R. Leach, and S. Piano	The International Journal of …, 2020 – Springer	Review of defects in lattice structures manufactured by powder bed fusion	133	This paper reviews **defects in LSs** from **powder bed fusion**, emphasizing how lattice design impacts dimensional accuracy, surface texture, and porosity.	The focus is on lattices used in cementitious composites produced by various **3D printing methods, and not only powder bed fusion.**
[1]	B.K. Nagesha, V. Dhinakaran, M. Varsha Shree, K.P. Manoj Kumar, D. Chalawadi, T. Sathish	Materials Today, 2020 – Elsevier	Review on characterization and impacts of the lattice structure in additive manufacturing	80	This paper explores modern methods for designing lattices and analyzing their mechanical behavior.	The manuscript shows how various parameters affect the mechanical behavior of lattices. However, the focus is also on the **mechanical behavior of cementitious composites.**
[33]	E. Momoh, A. Jayasinghe, M. Hajsadeghi, R. Vinai, K. Evans, P. Kripakaran, J. Orr	Thin-Walled Structures, 2024 – Elsevier	A state-of-the-art review on the application of auxetic materials in cementitious composites	163	This paper reviews the state-of-the-art use of **auxetics in cementitious construction**, highlighting challenges, opportunities, and future research recommendations to promote their adoption by engineers.	Our manuscript presents the use of various LSs (**auxetic, non-auxetic, TPMS-based, etc.**) incorporated in cementitious composites.
[34]	C. Amaechi, E. Adefuye, I. Kgosiemang, B. Huang, and E. Amaechi	Materials, 2022 – MDPI	Scientometric review for research patterns on additive manufacturing of lattice structures	190	This paper focuses on bibliometric analysis (**scientometric science**) to establish research maps and **visualization maps**.	Our paper focuses on the mechanical behaviors of **cementitious composites** by incorporating LSs.
[35]	T. Maconachie, M. Leary, B. Lozanovski, X. Zhang, M. Qian, O. Faruque, and M. Brandt	Materials & Design, 2019 – Elsevier	SLM lattice structures: Properties, performance, applications and challenges	141	This paper focuses on lattice structures produced through **SLM 3D printing**.	Our manuscript addresses lattices used in civil engineering applications produced *via* **various 3D printing methods**.
[36]	A. Kantaros and D. Piromalis	Applied Mechanics, 2021 –MDPI	Fabricating Lattice Structures via 3D Printing: The Case of Porous Bio-Engineered Scaffolds	77	This paper reviews **lattice scaffolds for tissue regeneration** and highlights their evolution as 3D printing is integrated into their fabrication.	Our manuscript focuses on lattices used for **construction applications**.

The bold font is only to draw attention to the most relevant concepts and differences between the existing reviews and our paper.

Table 2. AM methods based on base materials.

	Powder	Liquid	Solid
AM base material	Selective layer melting (SLM) [35, 44] Selective layer sintering (SLS) [49, 50] Laser metal deposition (LMD) [55, 56] Electron beam melting (EBM) [61] Multi jet fusion (MJF) [66, 67] Powder directed energy deposition (PDED) [68, 69] Powder-bed binder jetting (PBBJ) [70, 71]	Material jetting (MJ) [45, 46] Stereolithography (SLA) [51, 52] Digital light processing (DLP) [57, 58] Direct ink writing (DIW) [62, 63]	Wire and arc additive manufacturing (WAAM) [47, 48] Laminated object manufacturing (LOM) [53, 54] Electron beam freeform fabrication (EBF3) [59, 60] Fused deposition modeling (FDM) [64, 65]

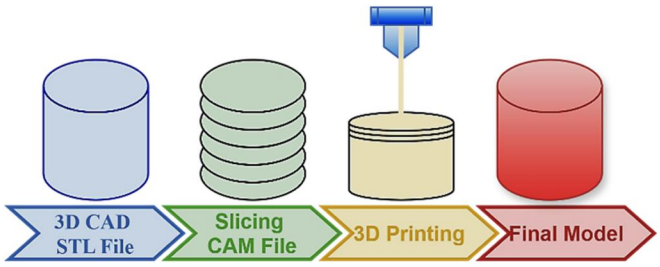

Figure 2. 3D printing procedure.

specifications [76]. The AM process of 3D printing begins with the core design of the component being modeled [77]. Using compatible software with 3D printers, a design is created and converted into a specialized file. This file is then transferred to the printer, which reads the instructions and constructs the object by layering material [78]. Layers are used in almost all 3D printing processes to create parts. 3D printers interpret components as a single 2D layer, not the whole part. 3D printers, as shown in Figure 2, operate by reading Standard Tessellation Language (STL) files [79].

In 3D printing applications, both thermoplastic polymer materials like polylactic acid (PLA) [80] and thermosetting polymer materials, such as epoxy resins, are used [81–83] while polycarbonate (PC) [84], polyamide (PA) [85], and acrylonitrile butadiene styrene (ABS) [81, 82, 86] are processed. Other materials include carbon fiber-reinforced polymer composites [87], Polyether-ether-ketone (PEEK) [88], carbon fiber-reinforced PEEK composite [89], and particle-reinforced composites [88], which are often made from reinforced composites. These may include platelets (like graphene), hollow spheres, short fibers (like fiberglass), or specialized materials (like fullerene and carbon nanotubes) [90]. Moreover, 3D printing can make ceramic and concrete objects without holes or fractures by adjusting parameters and mechanical properties. Strength and fire resistance characterize ceramics. Industrial and component designers now have more options than ever before thanks to 3D printing. 3D printing of complex parts that are both lightweight and energy and material-efficient could have applications in the aerospace industry [91]. Alloys based on nickel are often 3D printed and used in aviation because of their high tensile strength and resistance to damage [92]. There have been notable developments in the medical field as a result of 3D printing, also known as bio-fabrication, especially the development of customized medication tablets and patient-specific medical models, including brain tissues, vascular tissues, joints, and bones, which are just a few of the many kinds of tissues that have found new uses in 3D printing[93–100]. The construction sector stands to gain a great deal from this technology, which has the potential to boost personalization, decrease building time, and lower overall construction costs [101], and the shortage of skilled labor for tasks like complex formwork has driven countries to invest in 3D concrete printing (3DCP). An expanding selection of technologies has emerged that allows for the 3D printing of concrete fragments, and their use in building projects is on the rise. Benefits of 3DP in concrete buildings include geometric flexibility, speed, formwork-less printing, reduced waste creation, eco-friendliness, cost-saving, and safety. Dwellings in space are attracting interest as a potential use of 3D printing technology beyond Earth [102]. Examples of the usage of 3D printing technology in the construction industry include Canal House in Amsterdam, In-situ Contour crafting, and Win Sun Company buildings [103]. Figure 3 shows the main materials and applications of 3D printing technology.

2.2. Lattice structures (LSs)

LSs are prised in biomedical, structural, and mechanical engineering for their high strength and stiffness, efficient heat dissipation, and lightweight design [19, 104, 105]. Cellular structures are also beneficial for energy absorption purposes owing to their deformation properties [35, 106, 107]. A variety of fabrication methods allow for the creation of a wide variety of cellular structures. LSs are distinguished from other cellular materials by the consistent regularity in the arrangement of their unit cells [108]. According to Ashby [109], LSs are distinguished from large-scale designs like trusses or frames by the millimeter or micrometre scale of their unit cells [109]. The term *"an interconnected network of struts or plates"* is used by Gibson to describe cellular materials [110]. LSs can be made using a range of techniques, such as investment casting [111], an extrusion and electro-discharge machining combination [112], or a variety of composite fabrication techniques like textile weaving [113], interlacing, interlocking hot-press [114], or filament winding [115]. LSs can be 2.5D or 3D [35, 116]. In recent years, growing interest has been seen in the fabrication, modeling, and design of lattices that AM constructs. Additionally, many methodologies have been presented to forecast the mechanical behavior of LSs [117, 118]. The mechanical properties of LSs are influenced by factors such as cell type, orientation, size, thickness, material used, and cross-section. Numerous studies have been carried out to explore these characteristics using

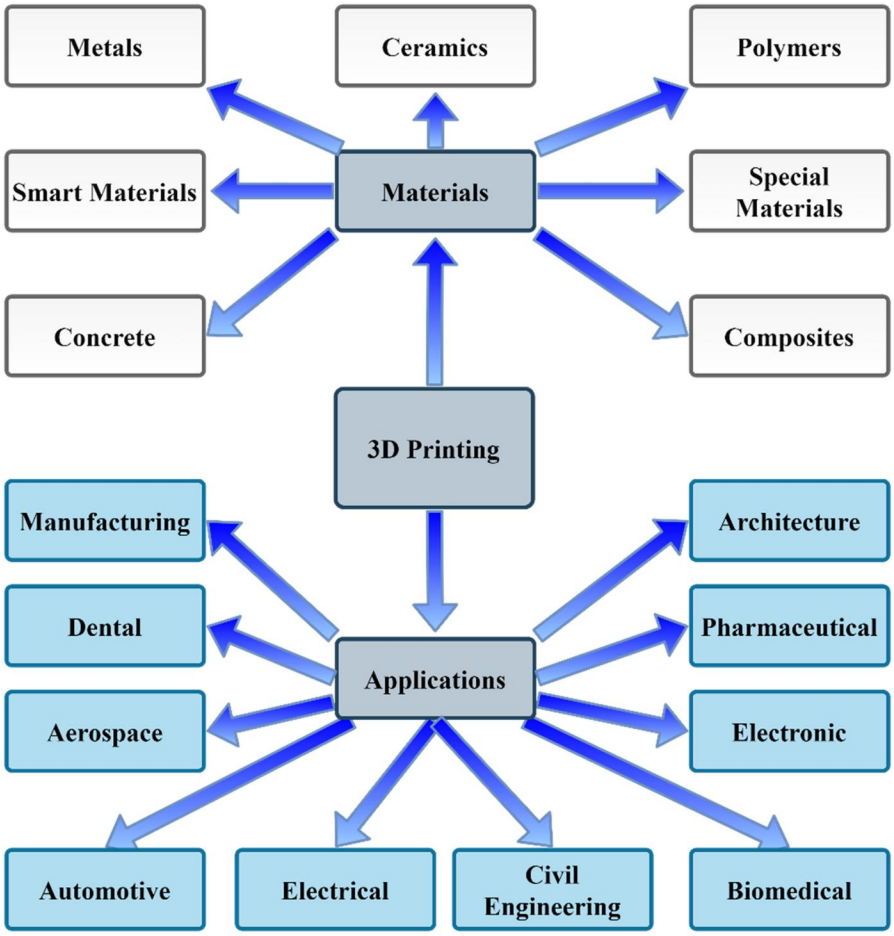

Figure 3. Applications and materials of 3D printing technology.

experimental, numerical, machine learning, and analytical approaches [119–134].

2.2.1. Classification of LSs

LSs may be systematically categorized as either 2D or 3Dbased on their structural configuration characteristics.

2.2.1.1. 2D Structures. Honeycomb structures [31, 135–143], hierarchical two-dimensional [144–152], and auxetic [153–161] LSs are the prominent forms of two-dimensional LSs [17]. The 2D auxetic structures include various shapes such as tri-chiral, star-shaped, anti-tri-chiral, hexa-chiral, reentrant hexagon, tetra-chiral, rotating triangle/quadrangle, bio-inspired reentrant, etc. [157, 158, 160, 162–166]. Hierarchical 2D structures include hexagonal shapes, hierarchical, triangular hierarchical 1 and 2, reentrant hexagonal, vertex-based, spiderweb-based, square-based, etc. [167–172]. General 2D LSs include square, triangle, hexagon, octagon, rhomb, petal-shaped, six/Quadri-arc, honeycomb structures, etc. [17, 173–177]. Figure 4 shows an example of 2D auxetic LSs.

2.2.1.2. 3D structures. 3D LSs primarily consist of plate-structured, shell-structured, truss-structured, and hierarchical-structured elements [178–188]. Plate-based 3D lattices, made from panels, mostly uses planform configurations such simple cubic (SC), hexagonal prism, SC-BCC, FCC, BCC, octet, tetrakaidecahedron, and SC-FCC for cell shapes [182, 183]. Shell-based 3D LSs (Figure 5), often curved, exhibit triply periodic minimum surfaces, such as Schwarz, Split-P, Primitive, Neovius, Gyroid [189], Isotropic Woodpile (IWP), and Förstner Random Dots (FRD) [186, 190–192]. Truss-based 3D LSs (Figure 6), such as solid and hollow trusses, have various cell shapes, comprising face-centered cubic (FCC), reentrant honeycomb auxetic, body-centered cubic (BCC), edge-centered cubic (ECC), cross-chiral, octagonal truss, SC, octahedron, diamond, double pyramid dodecahedron, tetrakaidecahedron, rhombic dodecahedron, etc. [178, 193–200]. The 3D hierarchical lattice structure begins with the nesting of one or two types of 3D spatial unit combinations, such as FDC, FCC, BCC, SC, octet, octahedron, etc. [17, 180, 188]. Honeycomb and foam-based LSs are shown in Figure 7. A 3D auxetic reentrant lattice is shown in Figure 8.

2.2.1.3. Random structures. Random, also known as stochastic (triangle-shaped and Voronoi-shaped) LSs, involve non-periodic, non-recurring cells, creating a distinctive framework of interconnected plates, surfaces, and struts, enhancing performance under compressive and shear loads [201, 202]. The mechanical characteristics of the stochastic lattice microstructure are approximately isotropic when the number of struts in the microstructure is

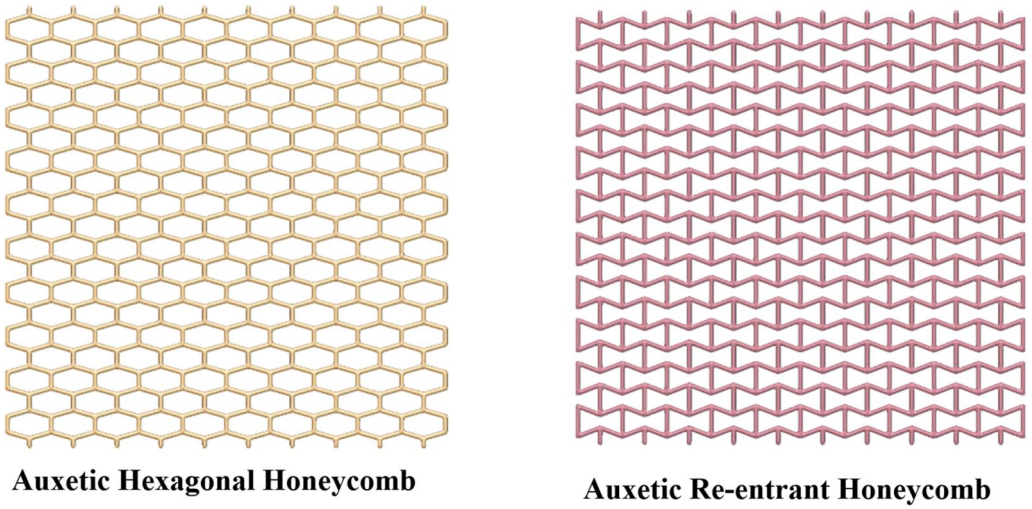

Figure 4. 2D auxetic LSs.

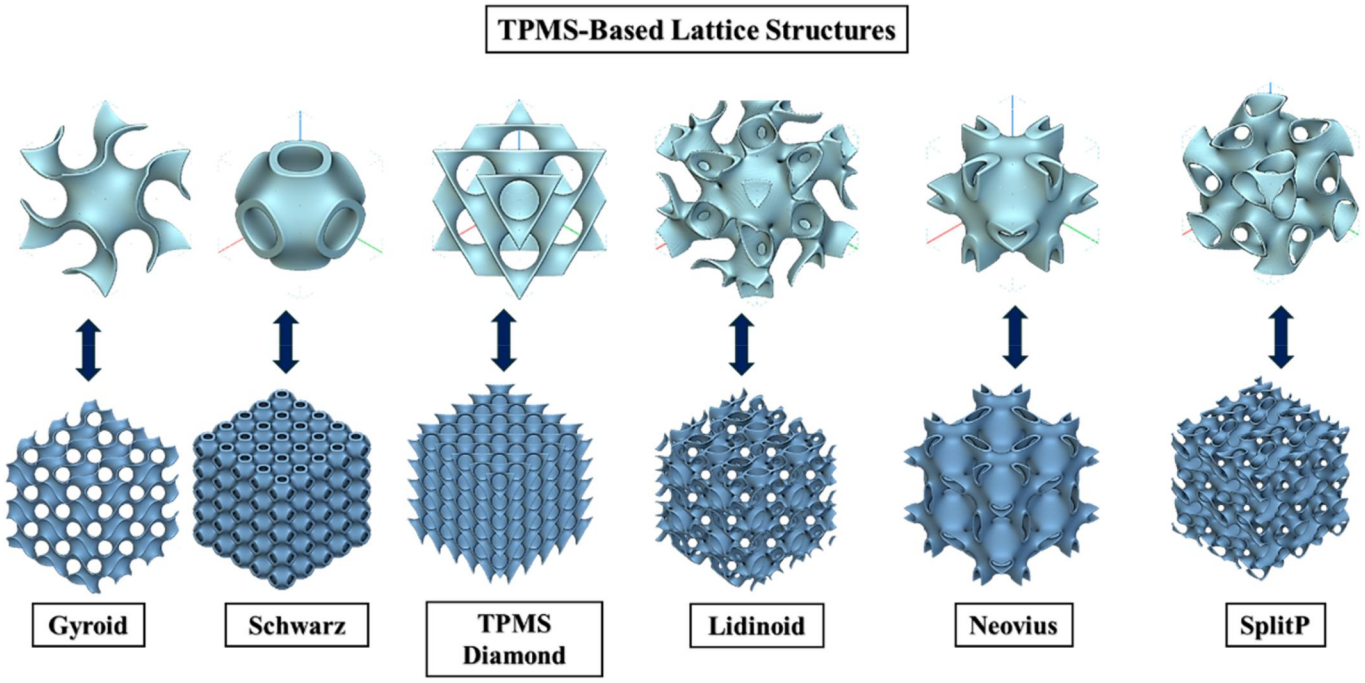

Figure 5. TPMS-based LSs.

sufficient [203]. Figure 9 shows an illustration of a stochastic structure.

2.2.1.4. Cellular structures. A common feature of most cellular structures is a 3D assembly of unit cells that repeats throughout. The unit cells are linked at positions called nodes and may have several shapes, such as struts, walls, or plates. Applications in structural engineering, aerospace, and materials science often make use of LSs due to their overall strength and lightweight nature. Stiffness, strength, and energy absorption are just a few of the mechanical characteristics that may be enhanced by their shape. Subsequently, periodic (Figure 10) and pseudo-periodic lattices differ from cellular lattices by having variable unit cell sizes, while periodic lattices maintain a consistent size. In heterogeneous lattices, the strut and wall thicknesses vary, whereas in homogeneous lattices, they are uniform [118, 201]. All LS illustrations shown in Figure 4–11 are designed using nTop (© nTopology Inc. 2024)

2.2.2. Hybrid/novel LSs

Researchers have suggested several approaches to improve the structural integrity and stability of additively generated LSs, hence solving the issue of instability. One approach is to use hybrid or novel (innovative) LSs [204]. Novel or hybrid LSs use innovative designs that combine different geometric patterns or materials to enhance mechanical

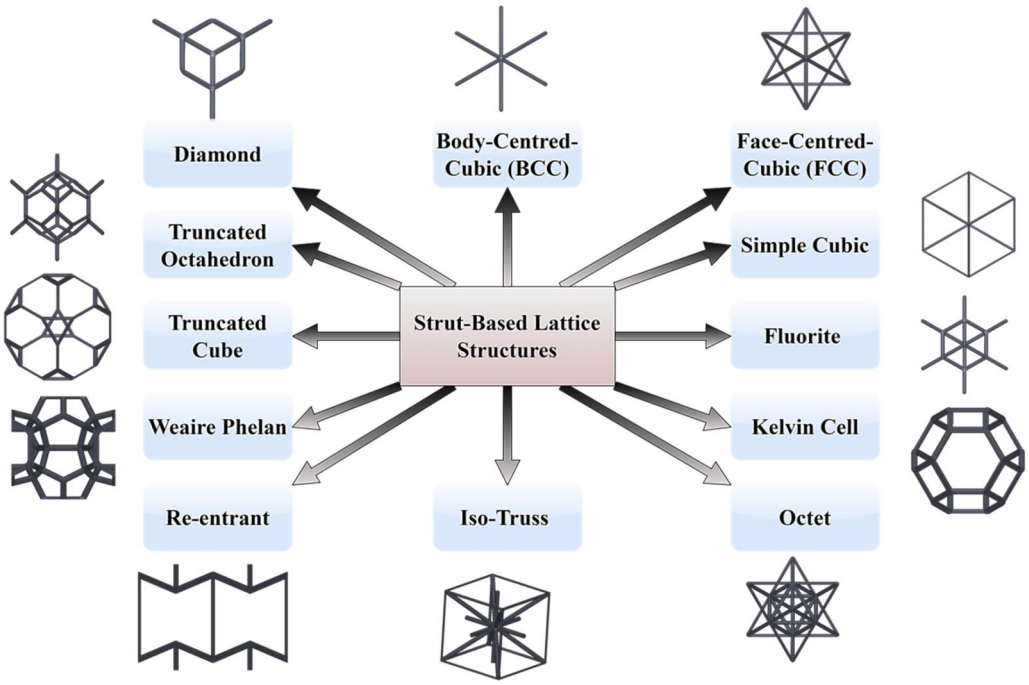

Figure 6. Strut/truss-based LSs.

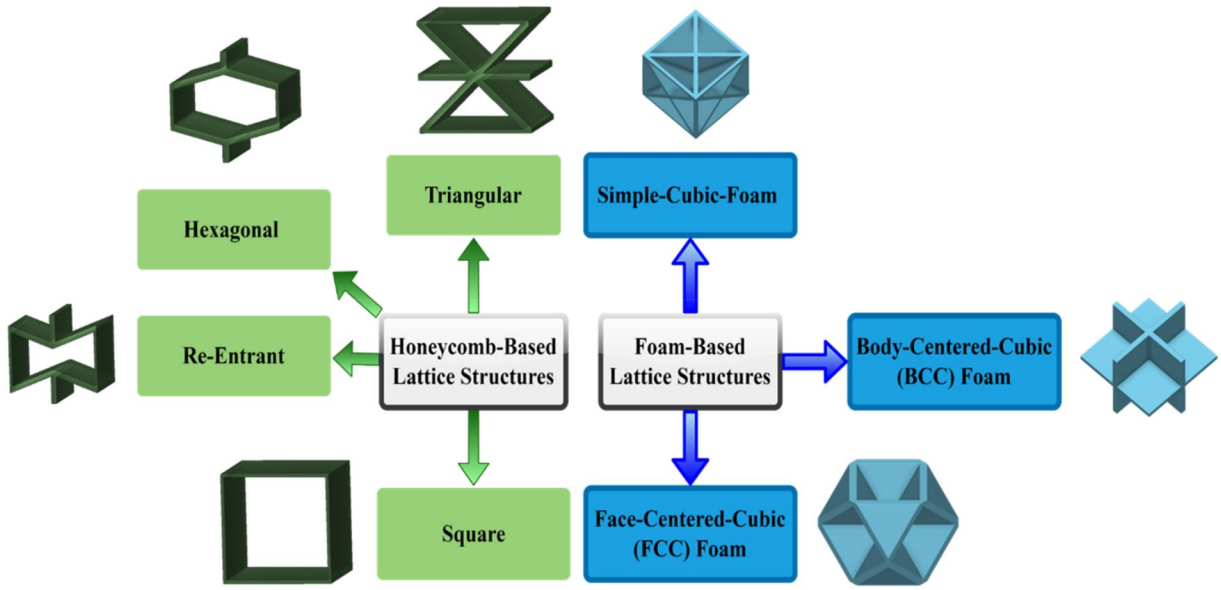

Figure 7. Honeycomb and foam-based LSs.

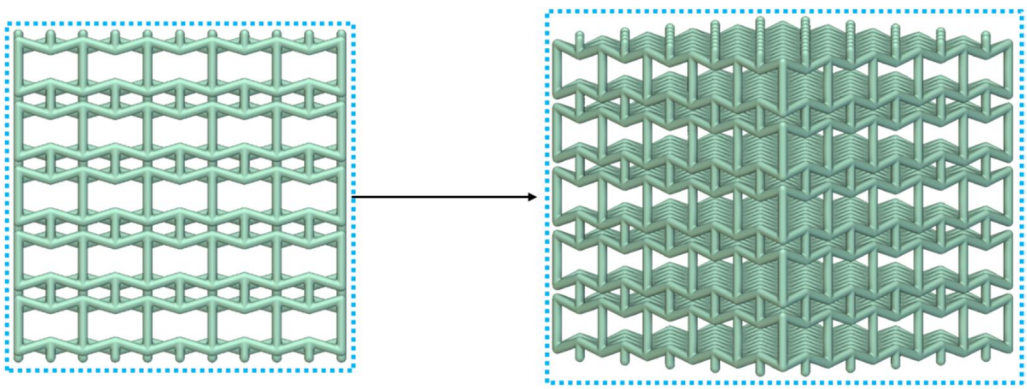

Figure 8. 3D Auxetic reentrant lattice structure.

characteristics like stiffness, energy absorption, and strength. To achieve an optimal balance between weight and strength, hybrid structures integrate several lattice types or materials, whereas innovative LSs include unconventional geometries tailored for specific performance requirements. Key elements of the designs include optimization for 3D printing, energy absorption, and control of density to enhance stress distribution. Bhat et al. [205] have constructed hybrid LSs that are referred to as "nested LSs ". Large surface-based sea urchin (SU) unit cells with internal truss lattice nests make up these nested LSs. To fit the vacuum area of the SU lattice structure, three distinct trusses, fluorite (bending-dominated), octet (stretch-dominated), and BCC (bending-dominated), have been adapted [205]. Alawwa et al. [206] developed and investigated several innovative lattice topologies relevant to additive manufacturing [206].

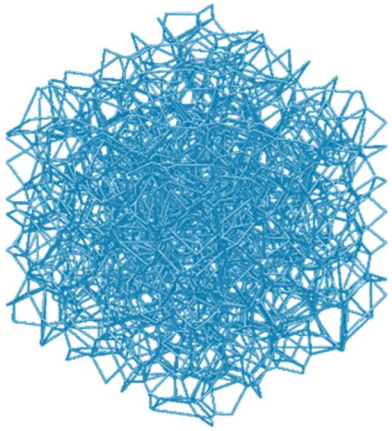

Figure 9. Stochastic lattice structure.

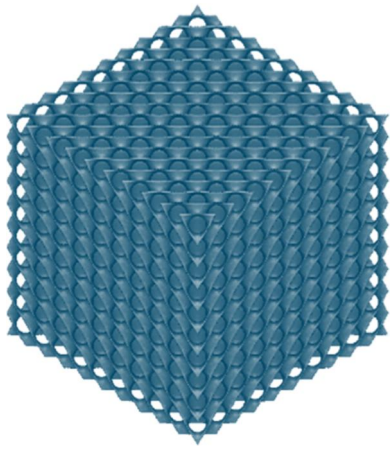

Figure 10. Periodic lattice structure.

Zhang et al. [207] created an innovative topology optimization approach for LSs that features highly anisotropic lattice characteristics [207]. Chen et al. [208] presented an innovative way to design LSs that yield predictable mechanical characteristics by altering the three-dimensional posture and mirror arrays of cells [208]. Armanfar and Gunpinar [209] developed an innovative strut-based LS known as G-Lattices, as well as a technique for generating them [209]. Han and Yu [210] proposed a novel technique for designing nonuniform LSs using topology optimization [210]. Deng et al. [211] suggested an innovative approach to mixed structural design, especially concentrating on the development of innovative mixed LSs. Both experimental evaluation and numerical analysis have been performed to confirm the consistency of the suggested design approach [211]. A novel NBCC design, combining BCC structure with a bionic fractal approach, was introduced by Ma et al. [212].

Based on the rotating stiff mechanism, Gao et al. [163] have constructed a class of innovative 3D auxetic LSs [163]. Zhao et al. [213] developed a parametric method for a graded BCC lattice structure with a closed shell of triangular facets, directly producing STL files for AM [213]. Hassanieh et al. [214] developed vintile (FPV), tesseract (FPT) hybrid-plate, and flat-plate modified auxetic (FPMA) LSs (LSs) from standard truss-based lattices. SLA AM was used to create tensile, compressive, and LS samples with varying relative densities [214]. A unique surface-based LS called the O-surface structure was developed by Nazir et al. [215], using inspiration from the existing Triply Periodic Minimal Surface morphologies seen in a specific sea urchin structure [215]. Figure 11 shows an example of hybrid LSs created using Ntop.

Table 3 presents various LS types and their applications in various sectors.

Table 3. Different sorts of LSs and their applications.

Ref	Type of LS	Application
[22]	Rhombicuboctahedron (RO) Cubic Circular Octagonal Strengthened octagonal	Reinforced concrete
[216]	Auxetic	Cementitious composite reinforcement
[217]	Diamond TPM	Damage tolerance and energy absorption
[218]	Hexagonal	Lightweight applications

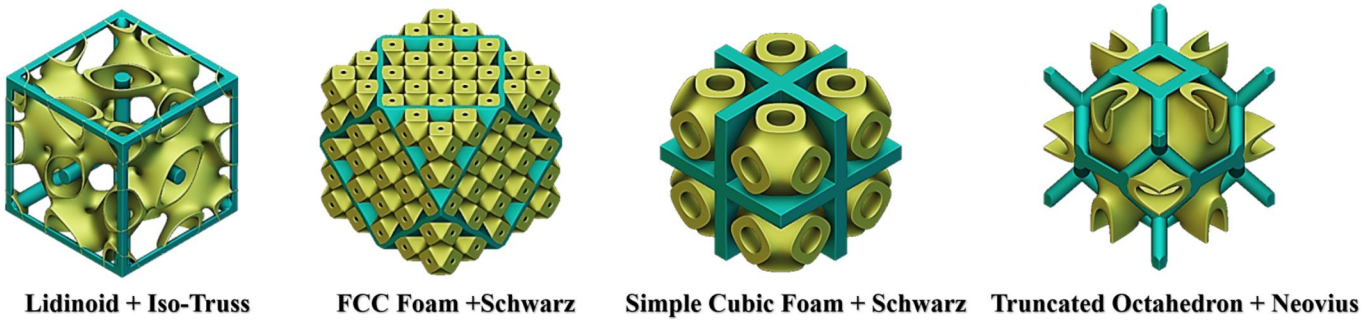

Figure 11. Hybrid/custom-based LSs.

Table 4. The 3D printing techniques for LSs with the corresponding materials, procedures, advantages, and drawbacks of each method.

Method type	Materials	Weakness	Advantage	Reference
Stereolithography appearance (SLA)	• Photopolymer • Resin • ABS • Polycarbonate (PC)	• High cost • Complicated curing procedure	• Can be used to print polymer-ceramic composites • Creates precise, high-quality components. • Can be used for printing complex nanocomposites	[15,41, 76,79, 224–226]
Selective laser sintering (SLS)	• Polymers • PEEK • Nylon PA 11 and PA 12 (polyaryletherketone (PAEK), polycarbonates, polyamides, thermoplastic elastomer (TPE), fused silica, borosilicate glass, etc.)	• Requires elevated temperatures for sintering. • Parts come out covered in powder and need cleaning. • Machines and powders are expensive.	• Excellent dimensional accuracy • Easy modification, -design adaptability • Versatility in material selection • Fast production • High-resolution parts	[227–234]
Inkjet printing	• Ceramics/ photopolymers • Thermoset (poly-iso-butylene) • Polyaniline • Polyacrylate	• Parts are often brittle. • Supports are required and post-processing is needed. • Ensuring strong layer adhesion.	• Fast • Effective • Flexible designs • Capable of printing complex structures	[41,224, 235,236]
Fused deposition modeling (FDM)	• Polymer matrix composites • Thermoplastic polymer filaments • Green ceramic/Binder mixture • (Polycarbonates (PC), glass fiber reinforced plastic (GFRP), polylactic acid (PLA), high-density polyethylene (HDPE), nylon 12, polytetrafluoroethylene (PTFE), etc.)	• Inter-layer distortion • Poor mechanical characteristics • Weak surface –supports are often needed.	• Cheap method • High speed • Simple procedure • Suitable for large parts.	[41,78,79,224, 226,237–243]

2.3. Manufacturing methods

Manufacturing of LSs depends on the material to be used (metal or nonmetal). The fabrication of LSs may be achieved by conventional techniques like waterjet cutting, weaving, and braising, as well as by more sophisticated manufacturing techniques like Electron Beam Additive Manufacturing (EBAM), SLM, and SLS. The advantages of conventional manufacturing methods lie in their widespread use and specialized knowledge, since each unit cell has to be produced and built separately [30].

In this paper, only additively manufactured methods are discussed for nonmetal LSs, such as 3D inkjet printing [41, 219], fused deposition modeling (FDM) [220, 221], SLS [222, 223], and SLA [219]). Table 4 shows the 3D printing techniques for LSs with the corresponding materials to be printed, procedures, advantages, and drawbacks of every technique.

2.4. Mechanical properties of LSs

LSs exhibit exceptional mechanical properties and can be optimized through modifications to their cellular architecture. These structures are characterized by their lightweight nature, high specific strength, stiffness, and thermal insulation capabilities, which have garnered increasing attention and highlighted their extensive potential for industrial applications [244–248]. Substantial research has been dedicated to assessing the mechanical behavior of LSs over the past thirty years, with mathematical models developed to link relative density to mechanical characteristics like ultimate strength and elastic modulus, particularly in foams [249, 250]. Key factors influencing the performance of cellular structures include material properties, array mode, topology, unit cell size or count, volume fraction, structure geometry, relative density, and strut dimensions [127, 251–259].

LSs are often categorized by their mechanical behavior into two types: bending and stretch-dominated. Bending-dominated structures are characterized by bending moments, resulting in increased flexibility and compliance. Conversely, stretch-dominated structures endure axial stresses, leading to enhanced stiffness and strength relative to bending-dominated structures [127, 260]. This categorization is crucial in structural engineering applications, since the selection between these two categories may markedly affect performance results, particularly in sophisticated material systems such as composites. A strong correlation exists between the graded density and the mechanical characteristics of LSs [261]. Additionally, the alignment and arrangement of unit cells relative to the direction of load significantly affect mechanical performance, particularly influencing the anisotropic behavior of the structures [127, 262]. An additional key factor when analyzing LSs' mechanical behavior is their isotropy. The mechanical response, particularly in anisotropic lattices, is impacted by the alignment of unit cells with the loading direction [262]. In the following subsections, the mechanical performance of LSs based on several parameters will be discussed.

2.4.1. Bending and stretch-dominated structures

Wang et al. [263] analyzed the elastic stability and buckling behavior of bending-dominated periodic lattice (BDPL) structures with curved cell walls using finite element analysis and experimental testing. Results revealed that raising strut

curvature reduces critical buckling loads for the out-of- or in-plane modes, with strut spacing and panel thickness also having a significant impact [263]. Parisien et al. [264] evaluated 24 lattice topologies in bone ingrowth simulations across 10 relative densities (5–50%) and four pressure levels (0.5–2 MPa). Focusing on SDL and BDL lattices, including AFCC, Auxetic, and BCC topologies, the study enhances the understanding of mechanical responses in lattice designs for tissue engineering. Compared to SDL, BDL topologies showed increased deformation and flow, which helped stimulate mature bone development more effectively, according to the study. The most advantageous BDL configurations were Diamond, BCC, FBCC, Octahedron, and G7, whereas the most desired SDL alternatives were Tetrahedron and Tesseract [264].

Wagner et al. [265] presented a programmable active lattice structure (PALS) designed to undergo a regulated topological change in response to thermal stimulus. The transformation was achieved by including active programmable joints that facilitate the transition between a BDL and an SDL topology by altering the nodal connection in the lattice structure. Furthermore, the research establishes a foundational framework for creating an advanced generation of programmable, multifunctional LSs that can dynamically alter their mechanical properties in response to external stimuli [265].

Eren et al. [266] investigated the influence of LS design (bending/stretched dominated models) on the mechanical behavior of AM structures. Truss-based LSs composed of three different unit cell configurations: centered, octet, and diagonal, were utilized. The researchers found that the stretch-dominated diagonal model showed superior strength characteristics (up to 250%), while the bending-dominated centered model enhanced elongation (up to 120%) [266].

2.4.2. Relative density

Relative density significantly influences the mechanical characteristics of LSs, characterized by the ratio of the parent material inside a Representative Volume Element (RVE) of the LS [267]. Changes in relative densities correlate with lattice structural dominance, where lower densities favor bending-dominated structures and higher densities result in stretch-dominated structures [29, 268]. Stretch-dominated structures have better initial stiffness and yield strength than bending-dominated structures at comparable densities but are prone to unexpected shear failures. Bending-dominated structures are more compliant and can disperse deformation and control loads, making them ideal for flexible and efficient load distribution applications [29, 269]. Extensive research was performed on the effect of relative density on the quasi-static mechanical characteristics of different lattices. Becerra et al. [120] investigated the mechanical performance of LS made of polylactic acid by highlighting the influence of relative density. The authors examined the tensile and compressive behaviors of honeycomb, triangular, and square LSs at varying relative densities. It is generally accepted that triangular lattices are stronger than square lattices at the same relative density. However, in this study, the authors noted the opposite trend. This discrepancy may be attributed to stress concentrations at the joints of the struts and the alignment of the 3D printer extruder, which could create favorable directions that minimize defects, thereby enhancing the strength of the square lattice [120]. Ling et al. [270] fabricated three octet-truss LSs with different densities using two polymer resins via SLA printing and tested under compressive loading. The results showed that higher densities improved yield and compressive strengths, while the material choice influenced the toughness, with one material being brittle and the other tougher [270]. Kandasamy et al. [271] investigated how relative density and strain rate affect Young's modulus and energy absorption in Kelvin LSs made of PA12 *via* SLS. Higher densities (20 and 30%) improved both properties, while the 10% density structures showed reduced performance at higher strain rates due to early strut deformation from smaller cross-sectional areas [271]. Dar et al. [272] explored the effects of relative density and unit cell configuration on the energy absorption and compression behavior of flexible polymeric BCC LSs, created using digital light processing 3D printing. The configurations (GBCC, UBCC, and UBCCz (with z-axis reinforcement))were tested under compression. Results showed that increasing relative density improved modulus and collapse strength, with UBCCz outperforming the others in energy absorption, modulus, and strength [272]. In another study, the elastic modulus of 3D lattices increased linearly with relative density [273]. Ye et al. [274] tested 3D-printed pyramidal structures with varying strut diameters to examine the effect of relative density on compression performance and energy absorption. Results showed that higher relative density increased strength and elastic modulus, with optimal energy absorption at a specific density [274]. Al Khalil et al. [275] introduced a variable-density design and optimization framework for LSs [275]. Research on graded-density lattices indicates they can yield endoprostheses with mechanics similar to the femur, and their porosity promotes tissue ingrowth [276].

2.4.3. Process parameters

The mechanical properties of 3D-printed samples are heavily influenced by key parameters, such as layer thickness, printing speed, and temperature. Despite their importance, these properties frequently fail to meet expected standards. Therefore, it is crucial to examine how these factors impact the mechanical characteristics of tensile samples and LSs [119]. Table 5 presents the impact of process parameters on the mechanical behavior of LSs (LSs).

2.4.4. Volume fraction

In LSs, the volume fraction is the ratio of solid material volume to the total structure volume. It plays a key role in determining mechanical properties, such as stiffness, strength, and weight. A smaller volume ratio produces a lighter structure, although it may be less rigid or sturdy. In applications such as impact resistance, LSs with varied volume fractions have variable energy absorption properties [29, 252, 280]. Yang et al. [281] examined the impact of unit cell size and volume fraction on the compressive properties

Table 5. An overview of the influence of process parameters on the mechanical behavior of LSs.

Ref	Process parameter (s)	Outcome
[277]	• Layer thickness (0.1–0.2–0.3 mm) • Printing temperature (195–205–215 °C) • Infill density (80–90–100%)	Optimal tensile strength and density are achieved with: • Infill density of ∼80% • Layer height of 0.1 mm • Extrusion temperature of 215 °C • Key factors for tensile strength/density: (1) infill density, (2) layer thickness, and (3) printing temperature
[278]	• Layer heights of 0.1, 0.2, and 0.3 mm. • Printing temperatures of 190, 200, and 210 °C. • Printing speeds of 50, 75, and 100 mm/s.	The optimal design factors for improved tensile strength include: • Layer height of 0.1 mm • Printing temperature of 190 °C • Printing speed of 100 mm/s This combination results in a 25.4% increase in tensile strength.
[279]	• Printing speeds of 600, 1200, 1800, And 2400 Mm/Min. • Layer heights of 0.1 and 0.2 mm. • Nozzle temperatures of 225, 235, 245, and 255 °C. • Fan speeds of 0, 50, and 100%.	Optimal settings for horizontal struts: • Nozzle temperature: 245 °C • Print speed: 600 mm/min • Fan speed: 0% • Layer height: 0.2 mm Optimal settings for inclined struts: • Nozzle temperature: 255 °C • Print speed: 1200 mm/min • Fan speed: 50% • Layer height: 0.1 mm

of Ni-Ti Gyroid TPMS lattices made by L-PBF. A positive correlation was found between compressive properties and volume fraction, while larger unit cell sizes showed a negative correlation. Martensitic transformation and shape recovery were largely unaffected by these factors. [281]. Chen et al. [282] explored how volume fraction affects the mechanical and shape memory properties of gyroid LSs made by laser powder bed fusion. Results revealed that higher volume fractions improved compressive modulus and yield strength [282]. Maskery et al. [283] focused on the design and modeling of surface-based LSs using volume fraction and cell-type grading. The authors identified moduli along three loading directions, linked to volume fractions and showed that modulus-volume fraction correlations accurately predicted the moduli of graded lattice systems [283].

2.4.5. Heat treatment

Heat treatment methods applied to LSs are additional factors that influence the mechanical behavior of structures. Nie et al. [284] studied the influence of heat treatment on the energy absorption, failure modes, and mechanical performance of TPMS lattices. They concluded that heat treatment was successful in controlling the failure degree of skeletal structures [284]. Galati et al. [285] investigated the impact of heat treatment and cell size on the cellular structure's compressive behavior. They stated that the heat-treated sample showed a ductile compressive performance rather than brittle performance [285]. Li et al. [286] carried out a study on the compression characteristics and microstructure evolution of LSs subjected to heat treatment. They noted that the sample with artificial aging and heat treatment showed a stable deformation mode and the best compression characteristics [286]. Ali et al. [287] studied the influence of annealing heat treatment on the mechanical characteristics of PA-12 lattices. The authors concluded that heat treatment enhanced the strength performance of various lattices used in the study [287]. Liu et al. [288] investigated the impact of heat treatment on the gradient microstructure of a BCC LS. They concluded that a gradient microstructure causes hardness variation in as-manufactured and 300 °C annealed specimens, while a homogeneous microstructure at 530 °C results in uniform hardness [288].

2.4.6. Lattice geometry

Altering unit cell characteristics such as unit cell dimensions, length, and strut thickness or their combinations may result in varied densification patterns, thereby yielding distinct mechanical characteristics [29]. Wang et al. [289] stated that by mapping the equivalent stress to the strut wall thickness, the optimization of strut design is achieved. In addition, more material is distributed to struts experiencing higher stress, improving material utilization and enhancing overall mechanical performance [289]. Park et al. [290] noted that lattice shapes such as truncated octahedrons, truncated cubes, octahedrons, and simple cubic have higher axial compression yield forces than diamond and BCC structures at constant relative density. This shows the former group performs better under axial compression. At stress concentrations, LSs fractured first. Optimized nodes, struts, and fillets redistributed stress and increased compressive strength, improving structural integrity [290].

Abdulhadi et al. [291] noted that a body-centered cubic lattice structure (BCC LS) with variable strut lengths at a 40° angle maximizes specific strain energy absorption and stiffness while minimizing weight, whereas a fixed strut length BCC LS at a 100° angle achieves the highest modulus [291]. Britt et al. [292] explored how strut dimensions and processing parameters affected LSs' microstructure and hardness. Thicker struts, with smaller sub-grain cell diameters, showed higher hardness, while 0.5 mm struts, with larger cells and more elongated grains, exhibited lower hardness [292]. Fan et al. [293] stated that strengthened edges greatly influence equivalent specific stiffness, which is lower in lattices with few unit cell layers compared to infinite lattices. Increasing edge thickness further reduces stiffness, but this effect diminishes with more than 10-20 cell layers.

Additionally, strong edges function like elastic foundation beams, distributing loads effectively and reducing local strain and stress concentrations, while maintaining the deformation mechanism of stretching-dominated struts. In conclusion, changes in strut diameter in AM LSs can significantly influence both collapse stress and elastic modulus [293].

Syam et al. [294] stated that alterations to strut-based LSs, driven by variations in orientation and strut length, significantly influence the mechanical behavior of such structures [294]. Geometric design factors, such as unit cell type and strut diameter, do not impact dimensional accuracy; however, they have a strong effect on the elastic constant of LSs [295]. Hanks et al. [130] noted that the Lattice Unit-cell Characterization Interface for Engineers (LUCIE) enables users to comprehend the topology of unit cells and LS mechanical characteristics for better selection. Build orientation affects microstructure and mechanical characteristics, with inclined struts having higher grain sizes and better properties [130]. Shin and Chang [296] concluded that an increase of 26% in compressive stiffness was noted when the unit cell size was decreased from 150 to 100 μm. In topology-optimized LSs, the compressive strength and dynamic elastic modulus relationship are affected by porosity and variations in unit cell size. The mechanical performance tends to decrease as the size of the unit cell increases [296]. The mechanical characteristics of a structure are significantly influenced by the arrangement and orientation of unit cells with regard to the applied load, particularly with regard to anisotropic behavior [262].

2.5. Critical review of mechanical properties of LSs and recommendations

Investigation into the mechanical behavior of LSs has advanced significantly in recent years, particularly with the advent of AM technology. The study has managed to categorize LSs into bending-dominated and stretch-dominated LSs and comprehend their relative strength, stiffness, and energy absorption capacities. However, future research could explore hybrid LSs, which combine these two forms of behavior for optimized mechanical performance. Additionally, while relative density remains a primary parameter for controlling strength and stiffness, ongoing research is needed on graded-density structures, where density is spatially varied within the lattice to maximize localized performance criteria. Process parameters, such as print speed, layer thickness, and temperature, are well documented in affecting mechanical properties, but ongoing research can focus on real-time monitoring and adaptive control systems to minimize defects like porosity and delamination. Numerical modeling, in the form of finite element analysis (FEA) and machine learning-based predictive models, can be advanced to improve design optimization and failure prediction. Furthermore, multi-material LSs, where more than one material is combined in a single LS, provide an exciting avenue in the creation of mechanical properties for a specific application. Post-processing and heat treatment techniques have shown promise for enhancing LS performance, although further work is required to establish optimum processing parameters for various material systems. In addition, dynamic loading conditions, including fatigue, impact resistance, and thermal cycling, must be investigated more thoroughly to ensure LSs perform adequately under real-world use. Future opportunities can also aim at bio-inspired LSs, utilizing nature's own designs, to develop highly efficient and adaptive mechanical systems. Integrating experimental, computational, and theoretical approaches will be crucial in pushing the performance boundaries of LS and broadening its applications to a broad spectrum of engineering disciplines.

2.6. Mechanical testing of LS

Mechanical testing in AM LSs aims to evaluate their response to different loads, such as compression and buckling. These tests ensure the structure's ability to handle operational stresses and refine design and material choices to improve performance and safety in practical applications. When it comes to testing LSs, there are several key mechanical tests that researchers use to understand their properties under different conditions. Each test follows specific standards and has a lot of research backing it up. Compressive properties [297] are usually the first thing to be tested. Standards like ISO/ASTM DIS 52959 [298] and ISO 13314 [299] provide guidelines on how to prepare the specimens, control the strain rate, and interpret the data. Researchers have extensively studied how factors like strut thickness, cell shape, and density affect the compressive strength and stiffness of LSs [300]. Flexural testing [301] is another important method, typically done according to ASTM D790. This test helps us understand how LSs resist bending loads, which is crucial for applications where the material needs to withstand out-of-plane deformations or bending stresses [302]. Fatigue testing [29] is essential for understanding how LSs perform under repeated or cyclic loads. This is often based on ISO 13314 [299], and researchers have looked into various factors like load amplitude, frequency, and environmental conditions (such as corrosive environments or high temperatures) to determine the fatigue life and identify failure mechanisms [260]. Tensile testing varies depending on the material. For metallic LSs, ASTM E8-04 [303] is commonly used, while plastics [304] and other polymers follow ASTM D638 [305]. Studies have shown how different lattice designs, microstructural features, and material anisotropy can affect tensile strength, yield behavior, and elongation at break [306]. To complement these experimental tests, numerical analyses using FEA in software like Abaqus [307] or Ansys [308] are often performed. These simulations allow researchers to conduct parametric studies, alter lattice cell geometry, relative density, or material properties virtually, and predict stress distribution, potential failure sites, and energy absorption before physical testing. Energy absorption [309] is a critical factor for applications like crashworthiness and protective structures. Various studies have focused on how lattice architecture, material selection, and manufacturing processes influence the ability of these

Table 6. The characteristics of different 3D printing polymers.

Material	Density [g/cm^3]	Tensile strength [MPa]	Melting point °C	Young modulus [MPa]	Flexural strength [MPa]
PLA [329]	1.24	60	145–160	3100	108
PP [330–332]	0.90	28	146	1300	40
ABS [333]	1.04	51	250	2750	78.5
PEEK [334, 335]	1.3	100	343	3900	162
PC [336, 337]	1.2	65.5	Amorphous	2738.6	93
TPU [338, 339]	1.23	36	216	1800–3000	60–97

structures to dissipate impact energy [310]. Finally, buckling behavior [311] is a predominant failure mode in slender or thin-walled lattice components. This is characterized using ASTM F2971-13 [312], and related research explores how geometric imperfections, anisotropic material behavior, and complex loading scenarios affect lattice stability. These studies offer strategies to enhance the buckling resistance and overall reliability of these advanced cellular systems [313].

2.7. Materials and applications of LSs

Three-dimensional printed LSs may be fabricated utilizing a diversity of materials such as polymers, ceramics, and concrete [314], metals, composites, liquid resins, and alloys. Nevertheless, this study will specifically address LSs made of polymers, composites, and concrete.

2.7.1. Polymers

Polymers that are produced using 3D printing [15, 315] incorporate an extensive range of materials, such as polypropylene (PP) [316], ABS [317, 318], PLA [319, 320], PEEK [321], thermoplastic elastomers (TPE) [322], polyetherimide (ULTEM) [323], thermoplastic polyurethane (TPU) [324, 325], Nylon [326, 327] and PC [328]. Table 6 illustrates the characteristics of several polymers used in the 3D printing process.

In recent years, lattice and auxetic structures [340, 341] have been used with various shapes and types to improve the ductility of concrete, which is a widely employed engineering material with high compressive strength but low tensile strength, requiring reinforcement to improve ductility due to its fracture propagation resistance [342–344]. Steel rebar cages are traditional reinforcement methods, but they may not be sufficient for extreme loads like blast or seismic loads due to the trend toward thinner beams and stronger concrete columns. Additionally, construction with large ratios of reinforcing bars requires significant effort and is challenging to penetrate with concrete [28]. One method to improve the concrete's ductility involves the incorporation of discrete polymer or steel fibers. Nevertheless, the arrangement of these fibers within fiber-reinforced concrete composites is challenging to regulate, which may result in certain areas being susceptible to crack propagation [345–350].

2.7.2. Polymer LSs in concrete

In recent years, civil engineering has seen a rising trend toward digitalized construction. Within this shift, AM, or 3D printing, became a key area of focus, especially for its potential to fabricate cementitious materials [351–354]. This technology offers new possibilities for innovative designs and construction techniques, improving efficiency and customization in the field [21, 355–358]. Recently, the utilization of cementitious composites [359] reinforced by lattices has been recognized as a promising strategy to enhance the fracture toughness and quasi-brittleness of cementitious composites [360–363], and due to their ultra-lightweight structures, enhanced energy absorption, high impact resistance, toughness, programmable characteristics, various designs, improved ductility, and diverse material compositions [364–372]. Researchers aiming to resolve issues of brittleness, cracking, and deficient tensile properties in cement-based materials have concentrated their efforts on three-dimensional (3D) printing, commonly referred to as AM. This technique offers significant advantages, including a wide variety of material selections, increased material efficiency, and the ability to design and construct complex components [373–375]. Currently, AM methods can create nearly isotropic parts, which include metal, composite, concrete, and polymer components fabricated through direct printing processes [376–378]. Furthermore, polymer reinforcements produced through 3D printing can be integrated into cement-based materials, resulting in strain-hardening composites. This integration enhances the toughness of the material while simultaneously decreasing its brittleness [28, 379–381].

Zhang et al. [342] designed and generated 4 lattice TPMS-based structures (Fischer-Koch S, Diamond, IWP, and Gyroid) and incorporated them as reinforcement elements for cement-based beams. Each of the four TPMS structures featured a 20 mm unit cell size and three unique relative density gradients: 60%-20%, 50%-30%, and 40%-40%. The mesh density points of all structures were set to 60, and the dimensions to $40 \times 40 \times 160$ mm. ABS-like resin raw material was used for the 3D printing process by using a photo-curing 3D printer. The ABS-like resin combines the benefits of TPE with the mechanical strength and toughness of ABS, making it more suitable for alkaline situations like concrete [382]. A total of 36 test components were created, with three specimens for each of the four TPMS structures and three gradient variants. As control samples, three beams made of non-reinforced cement (Specimen-C) were also produced. The G50-30 notation is used for gyroid structures having a 50%-30% gradient variation, and other structures with similar notations are also used. The dimensions of each cement beam specimen were $50 \times 50 \times 170$ mm. After 28 days, samples were prepared for mechanical testing. Black speckles were applied for DIC analysis. Three-point bending tests were conducted with a 100 kN load capacity, applying a constant displacement rate of 1 mm/s at the mid-span with

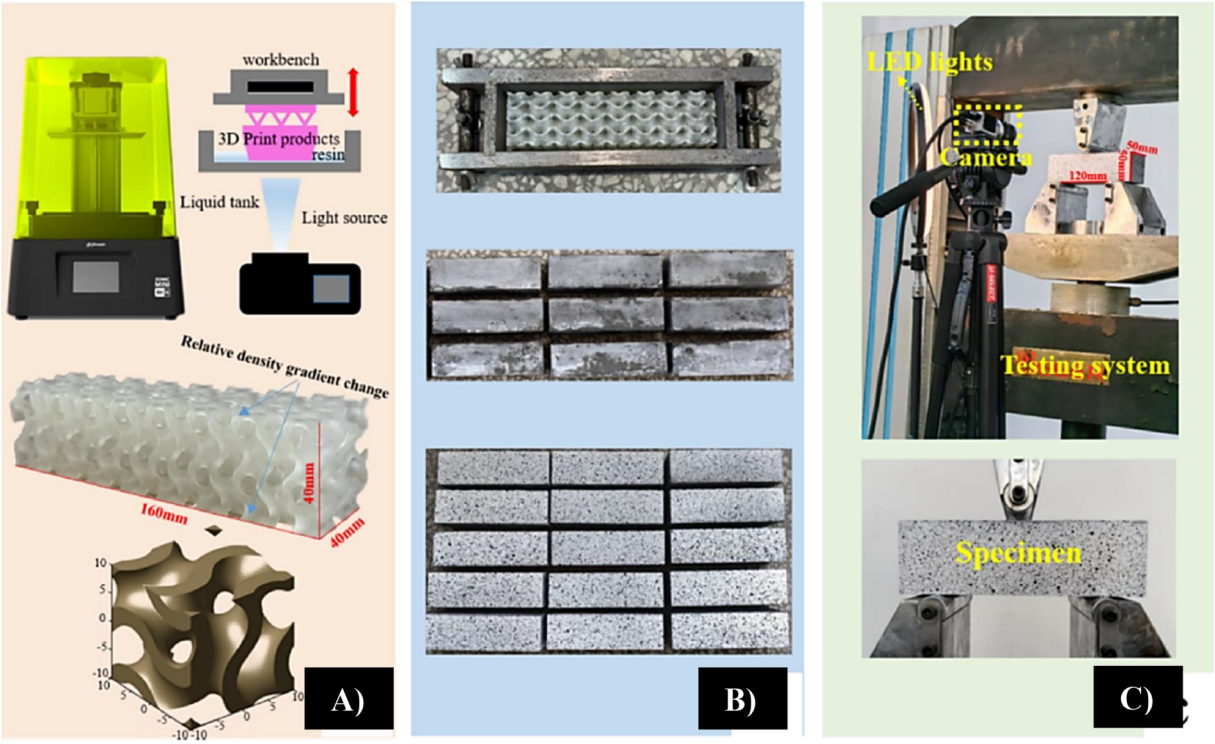

Figure 12. 3D Printing process and lattice samples (A), the casting and DIC processes (B), and the experimental setup (C) [342].

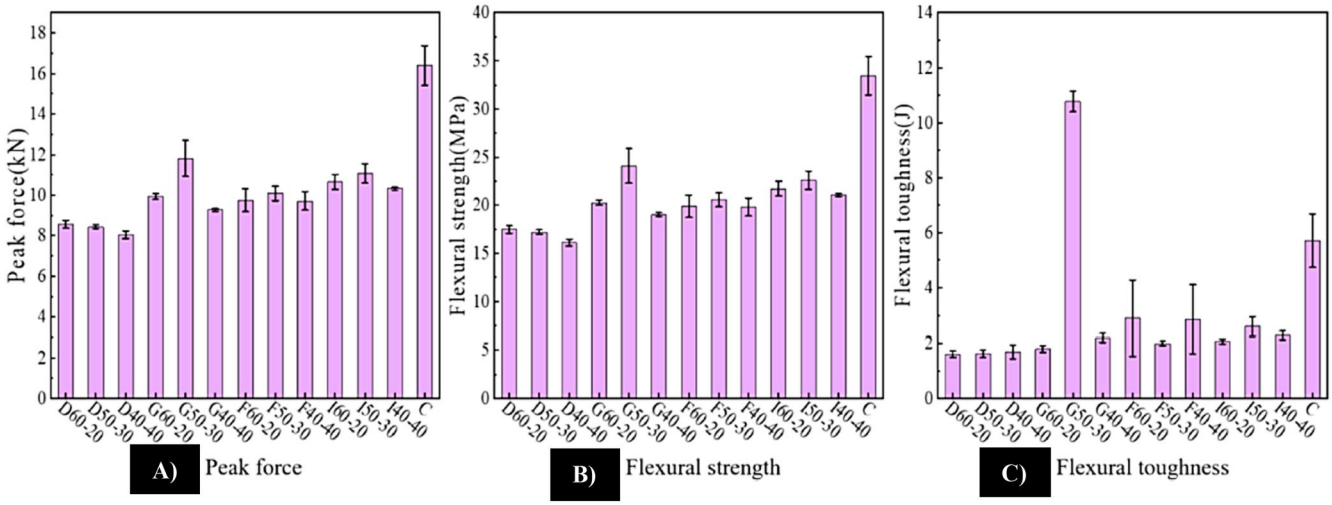

Figure 13. The experimental results of all samples: peak force (A), flexural strength (B), and flexural toughness (C) [342].

a 120 mm span to simulate a quasi-static load. Figure 12 shows the 3D printing process and lattice samples (A), the casting and DIC processes (B), and the experimental setup (C).

The G50-30 group showed the best flexural performance, with an 88.6% increase in flexural toughness over standard cement specimens. Compared to the G60-20 and G40-40 groups, toughness improved by 499.2 and 389.8%, respectively. However, the reinforced specimens had lower maximum destructive force and flexural strength than the cement Specimen-C group (Figure 13(A,B)). The authors stated that the disruption of the UHPC matrix's dense structure by the 3D-printed lattice might be the cause of this strength reduction [342].

Salazar et al. [28] introduced a novel technique to enhance concrete ductility using 3D-printed ABS or PLA lattices to reinforce ultra-high-performance concrete. Two octet lattice configurations were created with 19.2% and 33.7% reinforcement ratios. Cube and beam-shaped lattices were 3D printed, filled with concrete, and tested for compression and bending. PLA prisms and ABS cubes were printed using LulzBot TAZ 6 and Stratasys Dimension 1200es machines. The mechanical behavior of these beams was compared to that of UHPFRC and plain UHPC beams. Samples were cured for 7 days before testing with a Universal Testing Machine. Eight compression tests followed ASTM C109 standards [383]. Nine beam samples were exposed to four-point bending experiments by ASTM C1609

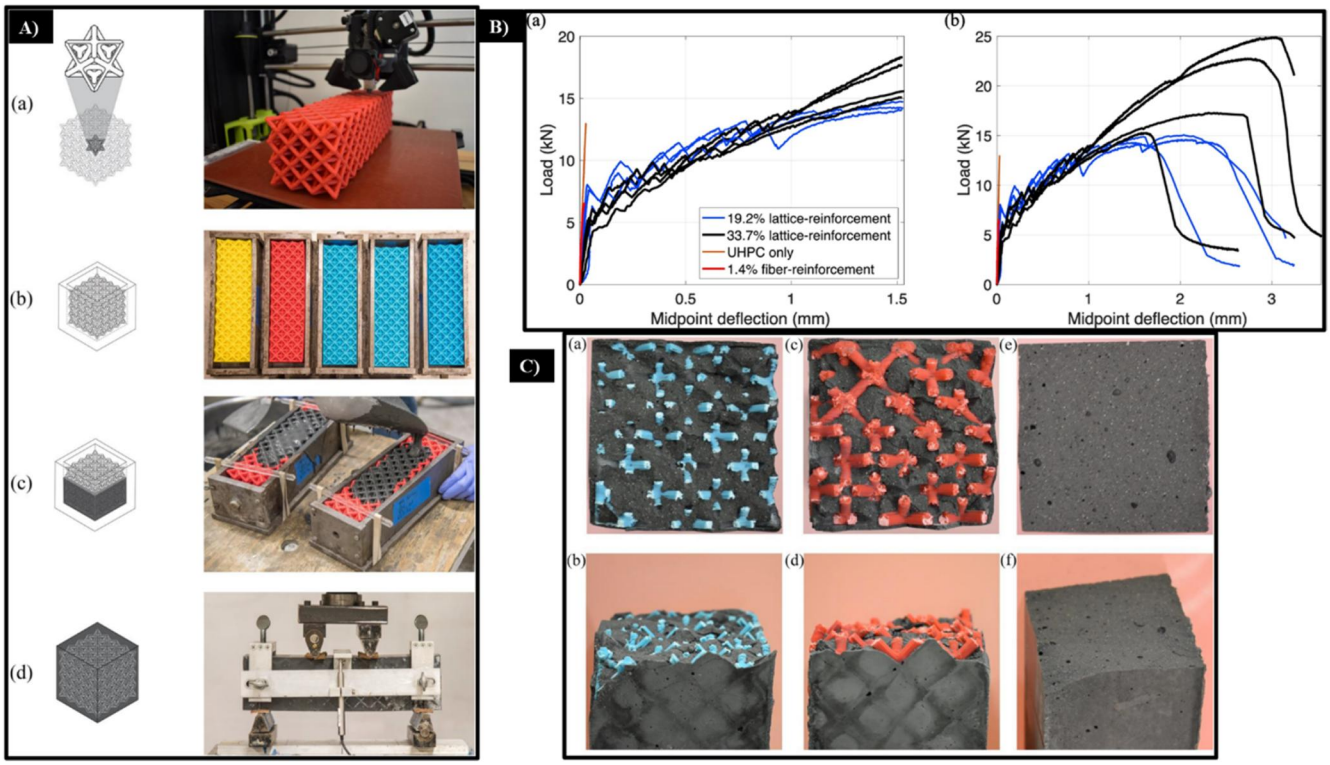

Figure 14. (A) The 3D printing process, placement, infiltration with UHPC, and flexural testing of polymeric lattice-reinforced beams, (B) presents flexural load-deflection curves, and (C) compares fracture surfaces of beams with different lattice and fiber reinforcement ratios [28].

[384], with a span length of 22.9 cm. The authors concluded that the lattices transformed brittle UHPC into a ductile material with strain-hardening characteristics. In compression, all samples showed gradual softening. Raising the ABS reinforcement ratio to 33.7% decreased the compressive strength by 22%. In flexural tests, raising the PLA reinforcement ratio from 19.2% to 33.7% increased the average peak load by 38%. Flexural specimens consistently exhibited multiple cracks and strain-hardening behavior until peak load. Figure 14(A) shows the 3D printing process, lattice placement, UHPC infiltration, and flexural testing. Figure 14(B) presents flexural load-deflection curves for different reinforcement amounts. Figure 14(C) depicts fracture surfaces in flexure specimens, comparing 19.7 and 33.7% lattice-reinforced beams, and fiber-reinforced beams [28].

Hao et al. [351] created six types of PA6 lattices 3D-printed by the Multi Jet Fusion (MJF) to use them as cementitious reinforcements and studied their compressive behavior. Samples without lattice reinforcements served as the control group. Lattice-reinforced specimens, all with the same volume fractions, showed higher compressive strength than the control group. The six lattices significantly improved cementitious composite compressive strength. The enhanced octagonal lattice sample has a 71.36% higher compressive capacity than the control sample. Although the RO lattice-reinforced sample had the lowest compressive capacity, it nevertheless increased 30.80% above the control. Their findings highlight the potential of 3D-printed lattices to strengthen compressive properties in cement-based materials, providing a substitute for steel bars in corrosive conditions and promoting energy efficiency, emission reduction, and sustainable building practices. Additionally, they noted that their paper offers valuable insights in this area. Figure 15 shows the (A) PA6 3D-printed samples and the formed and cured cementitious composite samples (B). Figure 16 illustrates the load-displacement curves of the cementitious samples subjected to uniaxial compression experiments [351].

Xu et al. [21] reinforced cementitious composites with four different 3D-printed ABS octet LSs, each with varying unit cell sizes, to improve ductility. Four-point bending tests were performed on both the reinforced specimens and the plain mortar, and the experiments were numerically simulated using a finite element model. The authors found that reinforcing cementitious composites with 3D-printed LSs altered their failure behavior from brittle to ductile. This reinforcement significantly improved the ductility and overall failure strength of the composites compared to the plain cementitious material [21].

In their research, Xie et al. [385] adopted a "materials by design" strategy to create architected lattice-reinforced composites (LRC) featuring a range of geometric attributes. By conducting experimental tests alongside simulations, they studied the reinforcing mechanisms in LRC specimens under axial compression and three-point bending. Their research highlighted how geometric variations significantly influence the energy absorption, ductility, and strength of these specimens. Furthermore, they explored how the lattice volume ratio and spatial configurations affect the flexural behavior of LRC beams. Figure 17 shows the fabrication and characterization of LRC samples and beams. Part A outlines the creation steps of LRC samples. Part B describes the DIC

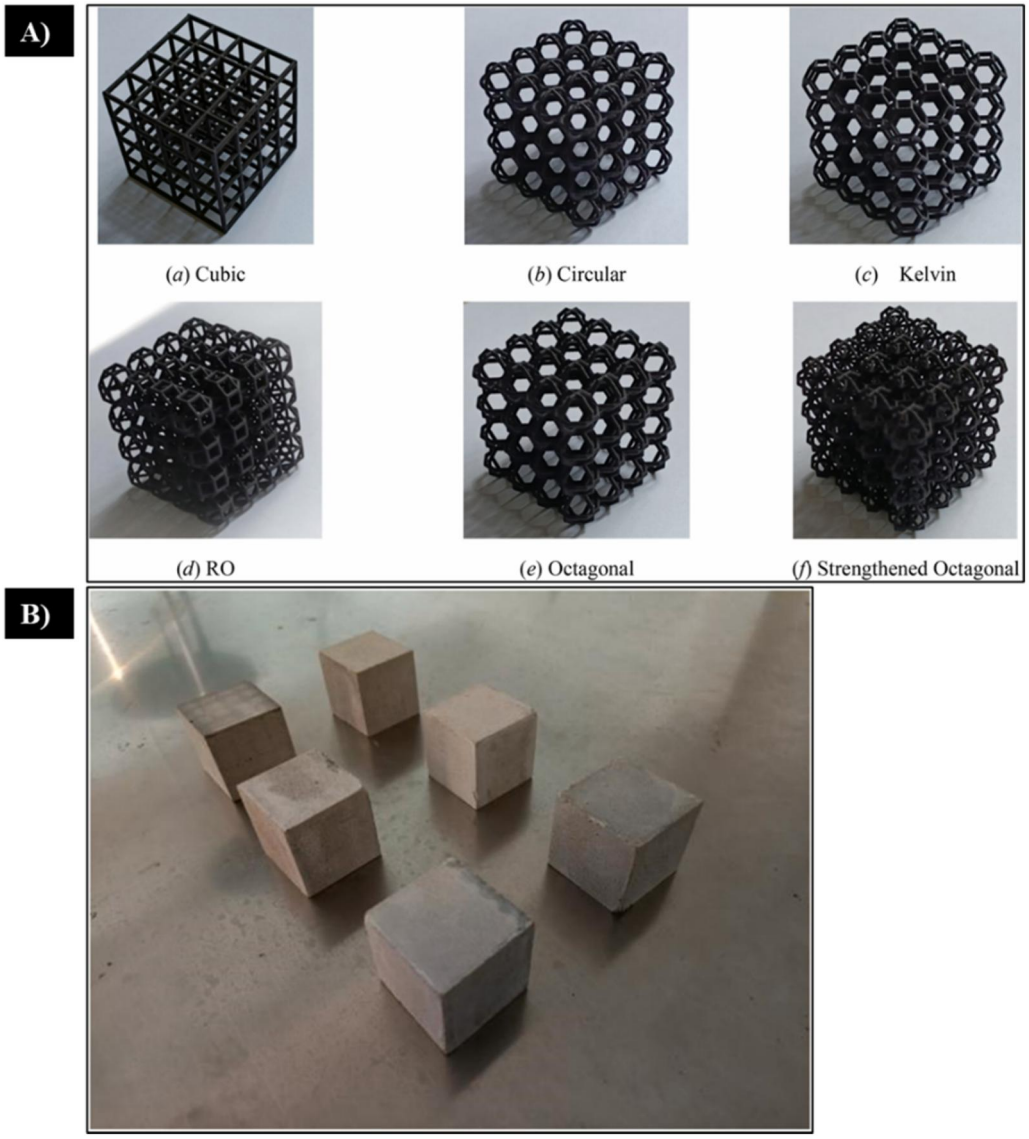

Figure 15. The (A) PA6 3D-printed samples and the formed and cured cementitious composite samples (B) [351].

and experimental procedures for three-point flexural analysis. Part C details the finite element model for an LRC beam. The authors found that the tesseract (T) lattice LRC beam had the highest flexural strength, the octet (O) lattice beam had greater energy absorption, and the reentrant (R) lattice beam was the most ductile. It was shown that raising the volume ratios of lattice reinforcement could improve the energy absorption, flexural strength, and ductility of LRC beams; however, further investigation is needed to establish the upper limit of these ratios [385].

Li et al. [386] created nine 3D-printed polymer lattice (3D-PPL) reinforced cement-based composites (CBC) using three different materials (transparent resin (TR), ordinary resin (OR), and nylon (NY)). They tested the flexural performance through three-point bending, CT scans, and DIC. Their goal was to enhance CBC's bending characteristics with 3D-PPL structures. Figure 18 shows the lattice designs and test process. They found that 3D-PPL reinforcement significantly improves ductility, with the OR-3D-PPL structure being the most effective, increasing ductility by 136-413 times compared to non-3D-PPL. The reinforcement also shifted CBC behavior from single crack to multi-crack failure, with the cube structure promoting multi-crack formation. Tensile and shear cracks were mainly observed, demonstrating 3D-PPL's potential to enhance CBC's bending performance and structural resilience [386].

Tang et al. [379] analyzed the flexural performance of graded lattice-reinforced 3D-printed cementitious composites utilizing six varieties of lattice cells with differing volume fractions, principally subjected to bending and tensile deformation. The lattices were fabricated using 3D printing with PA6 polymer utilizing multi-jet fusion (MJF) technology, while the cementitious composites were produced via mixing, grouting, and a 28-day curing process. The authors found that graded LSs improved the flexural capacity, ductility, and crack distribution of the cementitious matrix, shifting its failure mode from brittle fracture to ductile failure. Despite these enhancements, the 3D-printed lattices did not significantly raise the cement matrix cracking load. The functionally graded lattice design reduced material usage

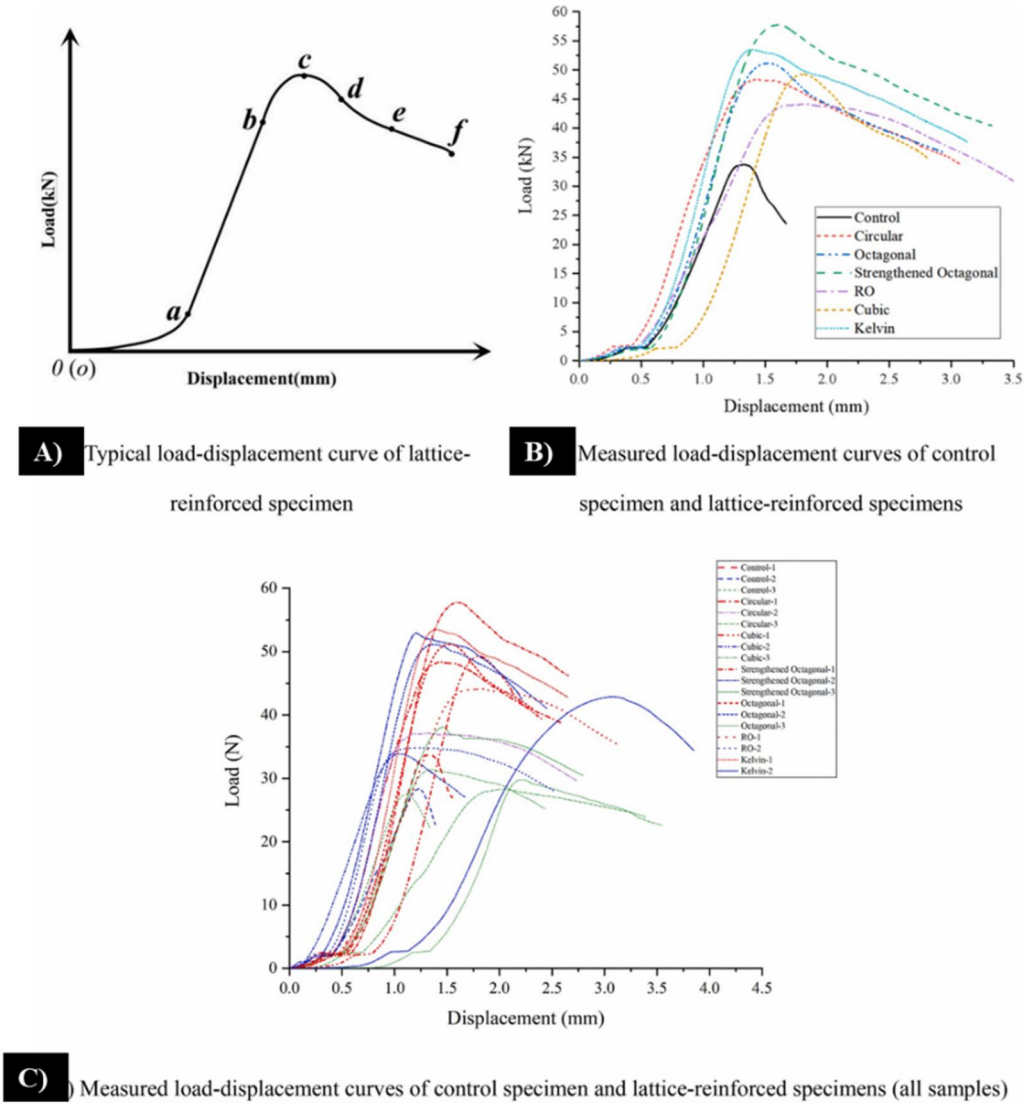

Figure 16. The load-displacement curves of the cementitious samples subjected to uniaxial compression experiments [351].

while still achieving multiple cracking behaviors. A key challenge found in the study is the weak interfacial adhesion between the 3D-printed polymer and cement, which requires further research for improvement [379].

Xu and Savija [24] indicated that using 3D-printed polymeric reinforcement significantly enhances both the tensile strain capacity and deflection of cementitious composites compared to the control material [24]. Moreover, Xu et al. [25] aimed to improve the bonding and mechanical performance of reinforced cementitious composites by modifying the surface of 3D-printed reinforcement. Using epoxy resin (EP), sand-sprinkled epoxy (SA), and short steel fibers in epoxy (SF), they conducted pull-out experiments to test bonding properties. Uniaxial tensile and four-point bending tests followed. Results showed SA and SF reinforcements had nearly double the bonding strength of uncoated and EP reinforcements. Additionally, composites with SA and SF reinforcements exhibited significantly enhanced ductility, showing strain-hardening and deflection-hardening behavior [25]. Qin et al. [387] used 3D-printed U-shaped polymer (NY, OR, and TR) structures (hexagons, squares, and rhombuses) to enhance the flexural performance of cementitious tailings backfills. Three-point bending tests were conducted on composite tailings backfill (CTB) samples, with scanning electron microscopy analyses to assess their flexural and microstructural properties. Figure 19(A) shows the polymer configurations used in the experiments. Figure 19(B) details the preparation process for U-shaped 3DPPL reinforced CTB specimens. Figure 19(C) illustrates the load application mechanism for the three-point flexural experimental setup.

Using "Square-OR" as a case study, where "Square" refers to the 3DPPL geometry and "OR" denotes ordinary resin, observations showed primary cracks within the flexural span of all CTB specimens. The main crack in the N-3DPPL reinforced CTB specimen aligned with the applied load direction. TR material weakened CTB's flexural strength, while the rhombus shape and OR material were ideal. U-shaped 3DPPL with OR and NY polymers significantly increased flexural strength and shifted CTB's failure mode from brittle to ductile, showing a notable increase in flexural deflection compared to N-3DPPL samples. [387]. Figure 20(A) depicts the correlation between load and deflection, alongside the deformation properties of N-3DPPL reinforced CTB specimens. Conversely, Figure 20(B) showcases the load versus

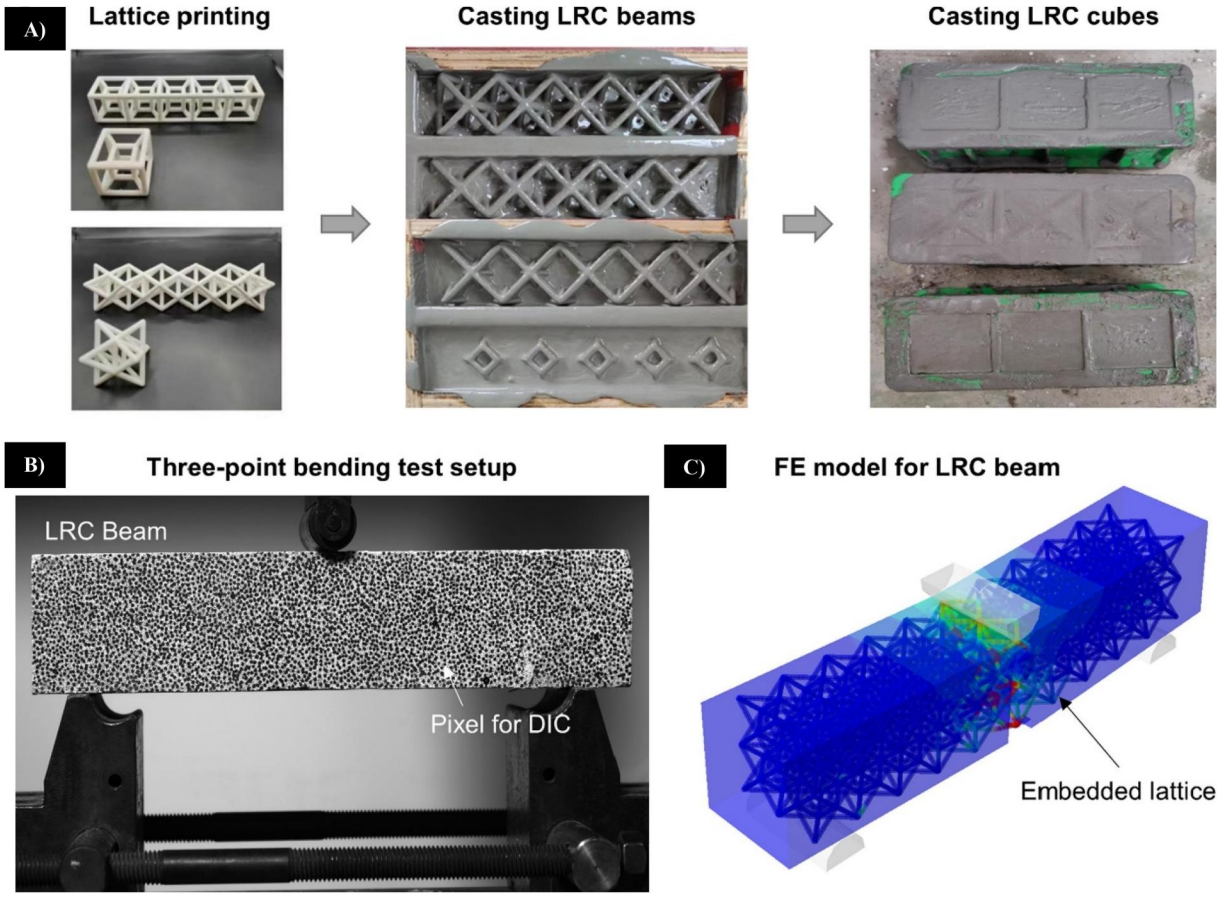

Figure 17. The processes of fabricating and characterizing LRC units and beams [385].

deflection and fracture curves for the U-shaped 3DPPL reinforced CTB specimen.

Liu et al. [22] developed and fabricated five unique LSs using selective laser sintering technology, embedding them within concrete. After a 28-day curing period, three-point flexural tests were conducted using Polyamide 6 (PA6) lattices. The study examined the mechanical characteristics of these reinforced concrete structures. Acoustic Emission (AE) and (DIC) techniques assessed internal damage and strain distribution. Results showed that LSs significantly enhance concrete's mechanical properties, with the rhombicuboctahedron (RO) lattice notably increasing the maximum load-bearing capacity, as shown in Figure 21 [22].

The flexural properties of cement-treated base (CTB) materials reinforced with various types of 3D-printed polymers (3D-PP) were evaluated using three-point bending tests conducted by Zou et al. [388]. A microscopic examination was performed to analyze the failure modes and strain distribution patterns of the CTB samples, while further examining the filled specimens using SEM-EDS, it was found that the bending strength of CTB structures with 3D-printed polymers reached 1.72 MPa, a 409% increase over reference samples (N-3D-PP). The maximum value of deflection was 17.6 mm, showing a significant performance improvement in the CTB structures [388].

Nguyen-Van et al. [389] introduced a method to enhance the bending stiffness of cementitious beams using 3D-printed TPMS-Primitive scaffolds. Three beams (50 mm × 50 mm × 250 mm) were created with FDM 3D-printed ABS molds. The beams included a non-reinforced beam (NRC), a two-layer TPMS-Primitive reinforced beam (PC2), and a one-layer TPMS-Primitive reinforced beam (PC1). The reinforcement used TPMS-Primitive structures with a 10% volume ratio. PC1 had five-unit cells in one layer. The study aimed to assess the effectiveness of these scaffolds in improving beam performance. Results showed that the two-layer reinforced beam's peak load capacity was 35% higher than the one-layer beam and 125% higher than the non-reinforced beam. Additionally, the reinforced beams exhibited improved ductility with a smooth softening response during bending. Figure 22 shows the setup of a one-layer TPMS-Primitive reinforced beam (PC1) and a two-layer TPMS-Primitive reinforced beam (PC2). It also includes an image of the PC2 beam undergoing a three-point bending test [389].

Singh et al. [390] introduced a method that combines 3D-printed complex zeolite-based biodegradable polymer porous structures and schwarzites to reinforce cement matrices, addressing the brittleness of cement. The composites showed significant improvements in resilience, with primitive schwarzites and gyroids achieving 128.1 and 121.3% increases, respectively. Zeolite-based structures exhibited a 125.63% increase in resilience compared to cement cubes and an extraordinary 505.33% improvement over pristine 3D-printed structures. This method, according to the authors, enhances the ductility and energy absorption

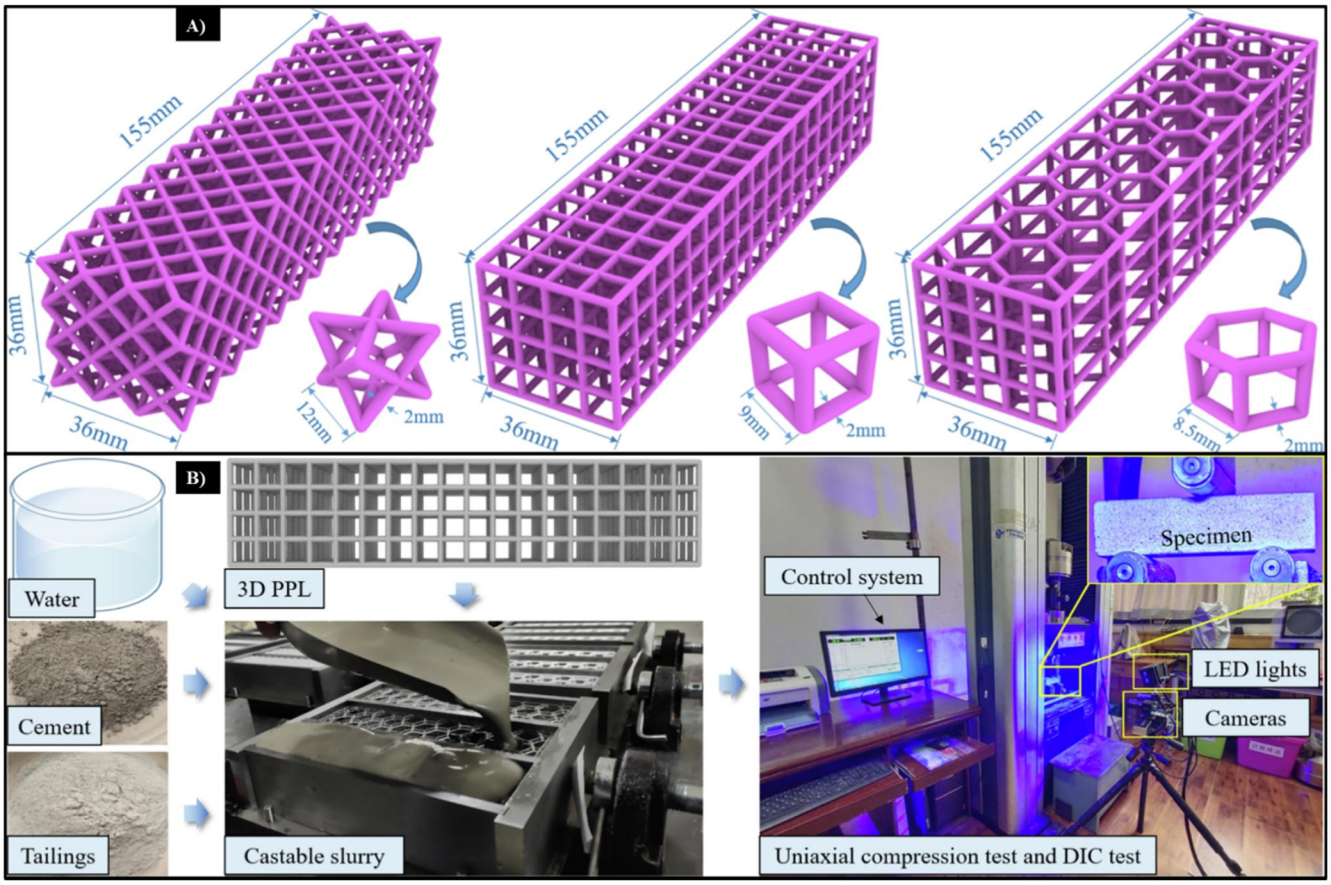

Figure 18. A) The three lattice structure designs and the cell structure, with the 3D-printed polymer lattice (3D-PPL) measuring 35 mm × 35 mm × 155 mm, as well as B) the testing procedure [386].

capabilities of composite blocks compared to conventional cement [390].

Wu et al. [391] focused on creating lightweight cementitious cellular composites (LCCCs) by combining digitally designed cellular structures with cementitious mortar, including micro-encapsulated phase change material (mPCM). Various Voronoi structures with different randomness levels were developed. LCCCs were produced using standard mortar and mPCM mortar through indirect 3D printing. After 28 days, compressive strength tests showed that highly randomized Voronoi structures and mPCM had a minimal negative impact on strength. LCCCs with mPCM had significantly higher relative compressive strength than traditional foam concrete, making them promising for thermal insulation in construction [391].

Pelanconi and Ortona [392] carried out a study that was published on a very lightweight construction inspired by nature (made of gyroid geometry, reinforced with external ribs) that is intended to maximize density and stiffness under bending stresses. The 3D printed model is illustrated in Figure 23(A), and the connection technique seen in Figure 23(B) was used to join the tubes to the core structure and the completed 3D model of the suggested construction, where the CFRP casings are magnified. Quasi-static three-point bending experimental tests were conducted to assess the mechanical behavior of the constructions using a 5 kN cell load. The experimental three-point bending device is seen in Figure 23(C). Figure 24 shows the force-bending deformation curves (experimentally and numerically) of the samples without and with CFRP reinforcements. The authors determined that the structure incorporating CFRP rods exhibited a stiffness more than double that of the non-reinforced structure, measuring 46 ± 4.32 N/mm compared to 20 ± 3.10 N/mm, respectively. Additionally, the maximum load capacity of the reinforced structure was approximately 280 ± 10.05 N, in contrast to 100 ± 8.11 N for the non-reinforced variant. Both structures ultimately failed at a displacement of 10 mm; however, the reinforced panel sustained a load 3.6 times greater than that of the non-reinforced structure (280 N versus 77 N) [392].

Chen et al. [393] implemented a composite design strategy using cementitious units reinforced with 3D reentrant (3DR) lattices, created through single and dual-material 3D printing. By employing digital fabrication, experimental testing, and numerical simulations, the researchers assessed how different materials, printing parameters, combinations, and spatial arrangements affected the compressive strength and energy absorption of the 3DR lattices and the resulting lattice-reinforced cementitious composites (LRCCs). They found that even with weaker 3D-printed materials, LRCC units achieved similar ultimate strengths and better energy absorption. This trend was also observed in LRCC columns with various geometric designs [393].

Aghdasi et al. [394] article focuses on ultra-high-performance fiber-reinforced concrete (UHP-FRC) and sustainable "green" UHP-FRC (G-UHP-FRC) in the

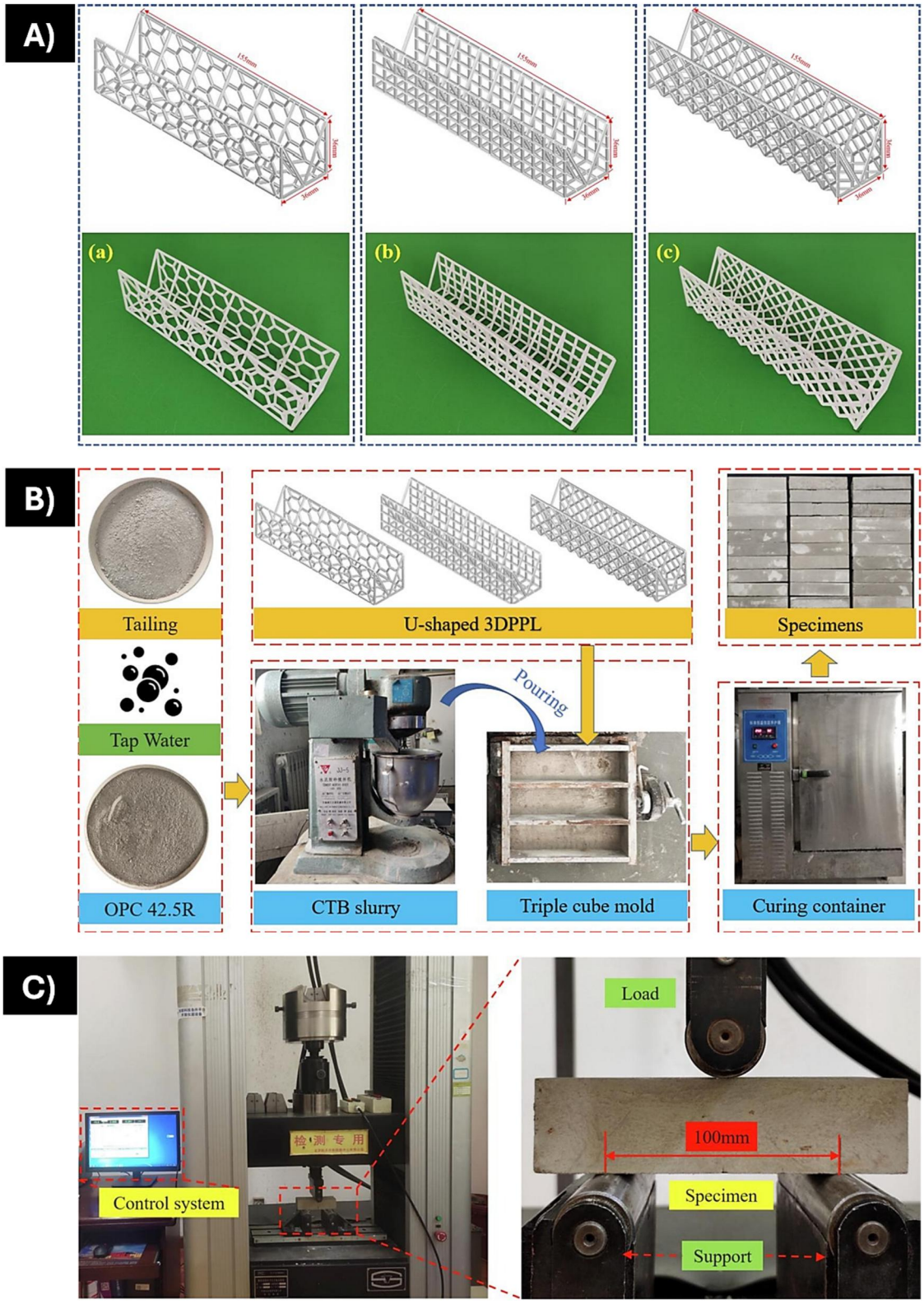

Figure 19. (A) The polymer configurations used in the experiments. The cubic rigid mold measured 40 mm in width, 160 mm in length, and 40 mm in height. (B) The preparation process for U-shaped 3DPPL reinforced CTB specimens. (C) The load application mechanism for the three-point flexural test [387].

development of Octet-Truss Engineered Concrete (OTEC). These mixtures were poured into 3D-printed ABS molds, which were later dissolved. Specimens were stored in a high-humidity fog room for 28 days before testing. The study examined the effects of different curing methods on the compressive strength of OTEC unit cells. Results showed that OTEC unit cells had higher compressive strength than control foam green (G-UHP-FRC) concrete samples. High humidity curing improved compressive strength, flexural capacity, stiffness, and

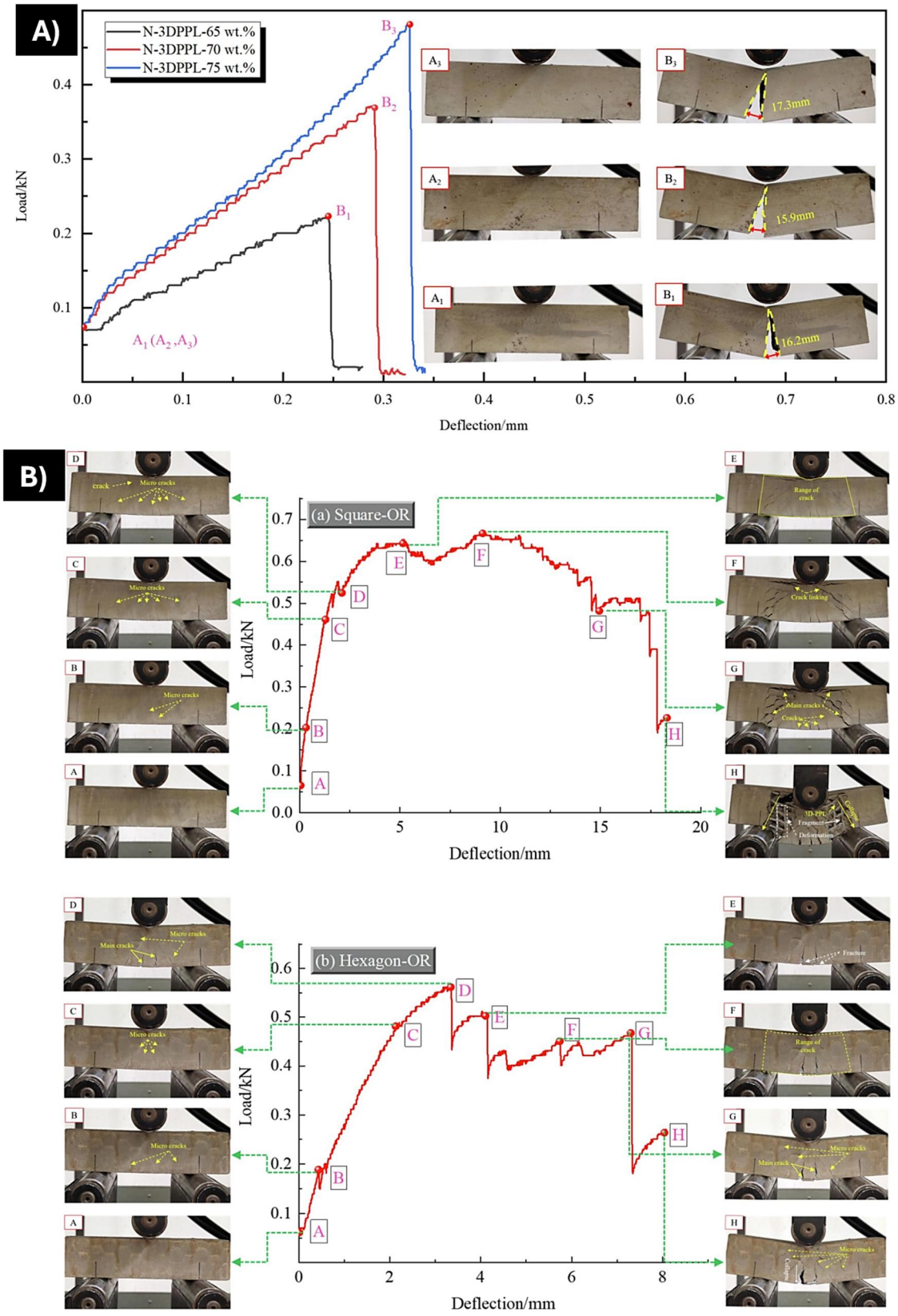

Figure 20. A) The correlation between load and deflection, alongside the deformation properties of N-3DPPL reinforced CTB specimens and B) the load versus deflection and fracture curves for the U-shaped 3DPPL reinforced CTB specimen [387].

toughness. G-UHP-FRC OTEC flexural specimens, despite lower mass, exceeded solid UHP-FRC and standard concrete in toughness and peak load. UHP-FRC OTEC unit cells also outperformed foam G-UHPC cubes under compression, highlighting their potential for lightweight construction [394].

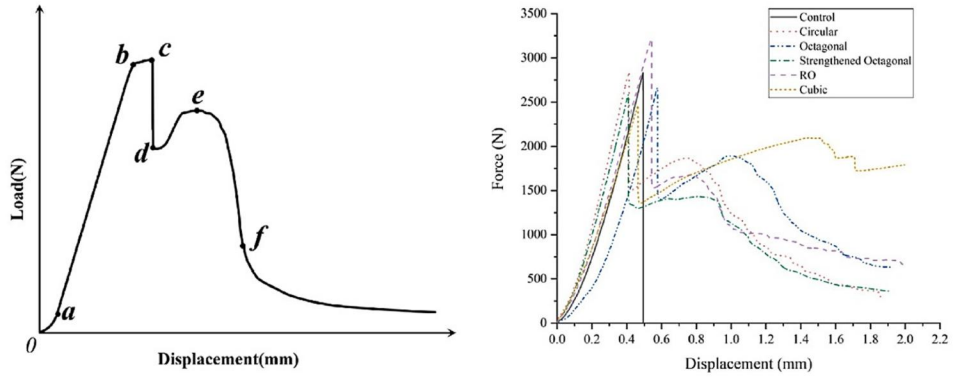

Figure 21. Load-displacement curves of the samples [22].

Tang et al. [23] investigated the compressive behavior of cement mortar reinforced with 3D-printed spiral and skin LSs produced via MJF technology. Six specimens, including a control, and 4 sorts of lattices (spiral) were tested with varying reinforcement ratios to assess bonding and skin reinforcement effects. The findings indicate that 3D-printed lattices improved the ductility and energy absorption of cementitious materials. However, the compressive strength and elastic modulus were reduced due to the reinforcing polymers' lower elasticity compared to cement [23]. Chen et al. [393] analyzed cementitious composites with 3D reentrant (3DR) lattices, printed through dual and single material printing methods. Their findings demonstrated how manufacturing parameters influence the mechanical characteristics of flexible and rigid lattices. They assessed the compressive properties of LRCC featuring 3DR lattices in various spatial configurations. The study concluded that LRCC units achieved enhanced energy absorption and similar ultimate strength, despite incorporating weaker 3D-printed materials [393]. Xie et al. [395] used PLA and TPU polymers to print lattice reinforcements for asphalt concrete and cementitious beams. They concluded that Pla reinforcements improved both energy absorption and ultimate strength [395]. Dong et al. [396] developed topology-optimized LSs as flexible nylon reinforcements in cementitious composites. Testing revealed that these lattices significantly improved strength and ductility, outperforming homogeneous lattices in ductility. Smaller cell sizes reduced enhancement effects, while a larger optimization volume fraction further boosted strength and ductility [396].

2.7.3. Polymer auxetic structures in concrete

Xu and Savija [397] presented the development of auxetic cementitious composites (ACCs) designed to improve mechanical characteristics by embedding 3D-printed polymeric reinforcement structures within cementitious mortar. Four distinct types of ACCs were created, incorporating unique auxetic mechanisms (rotating-square (RS), reentrant (RE), missing-rib (MR) and chiral (CR)). The compressive behavior of these samples was thoroughly investigated via a combination of both experiments and finite element modeling, highlighting the potential of ACCs for enhanced performance in construction applications. The findings demonstrate that all ACCs exhibit significant compressive ductility. Notably, the RE variant displays the highest level of ductility, achieving energy absorption rates that are 853% and 708% greater than those of the reference mortar and the auxetic structure, respectively. Additionally, both the RE and RS variants show enhanced crack-arresting capabilities under compression. The ductility of the resulting system decreases by 32.2% when the volumetric ratio of the auxetic structure is halved [397]. Figure 25 illustrates the four ACC types.

In their study, Choudhry et al. [216] examined four specific auxetic LSs to enhance the energy absorption and ductility properties of cementitious composites using AM polymeric auxetic lattices [164, 381, 398], which possesses a negative Poisson's ratio (NPR) that varies from −0.431 to −0.038. Maxwell's stability factor (M) confirms that all lattice designs exhibit bending-dominated deformation. Fabricated with a commercial FDM printer, the chosen ABS polymer offers superior durability, strength, toughness, minimal shrinkage, cracking, and design flexibility [28, 389, 399]. Specimens were compressed at 2 mm/min using a 250 kN Universal Testing Machine under room temperature [400]. LRCC composites were made by pouring cement-based mortar into an acrylic mold with AM LSs. Figure 26(A,B) show the fabrication process and shear failure patterns, respectively.

Figure 27(A) shows that LRCC specimens have a 35.65 to 64.16% lower Young's modulus than plain concrete. Figure 27(B) highlights the compressive strength, with LRCC 4 at 35.82 MPa, LRCC 2 at 32.38 MPa, LRCC 3 at 28.64 MPa, and LRCC 1 at 27.63 MPa. Figure 27(C) indicates higher peak strain in LRCC specimens, with LRCC 3 showing an 85.71% increase, followed by LRCC 4 (80.95%), LRCC 1 (47.62%), and LRCC 2 (9.52%). Figure 27(D) displays Young's modulus and normalized peak response for various LDs, with LRCC 2 having the highest Young's modulus due to LD2 auxetic reinforcement. The reductions in Young's modulus for LRCC 3, LRCC 1, LRCC 4, and LRCC 2 are

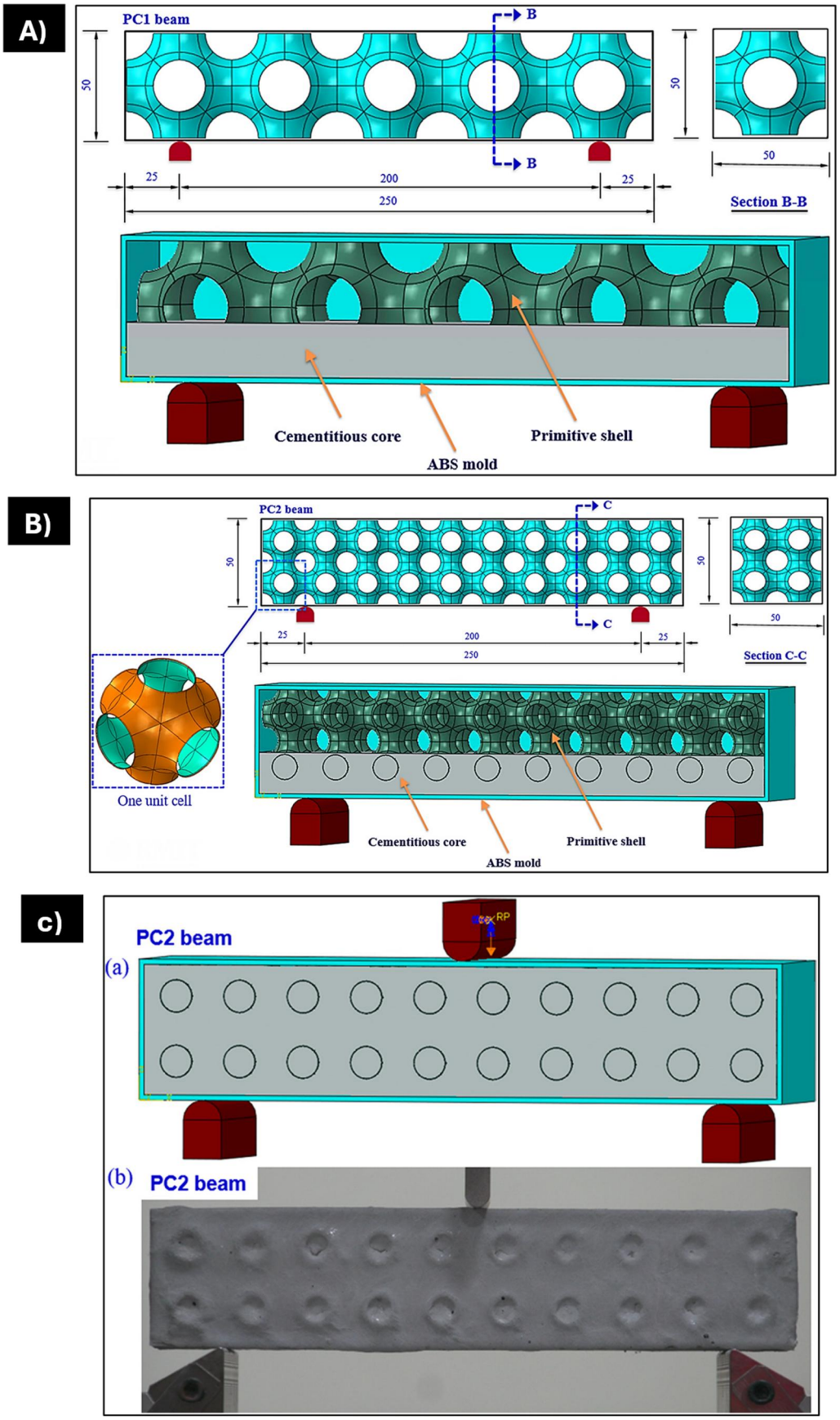

Figure 22. (A) The setup of a one-layer TPMS-Primitive reinforced cementitious beam (PC1), (B) the setup of a two-layer TPMS-Primitive reinforced cementitious beam (PC2), and (C) the PC2 beam during a three-point bending test [389].

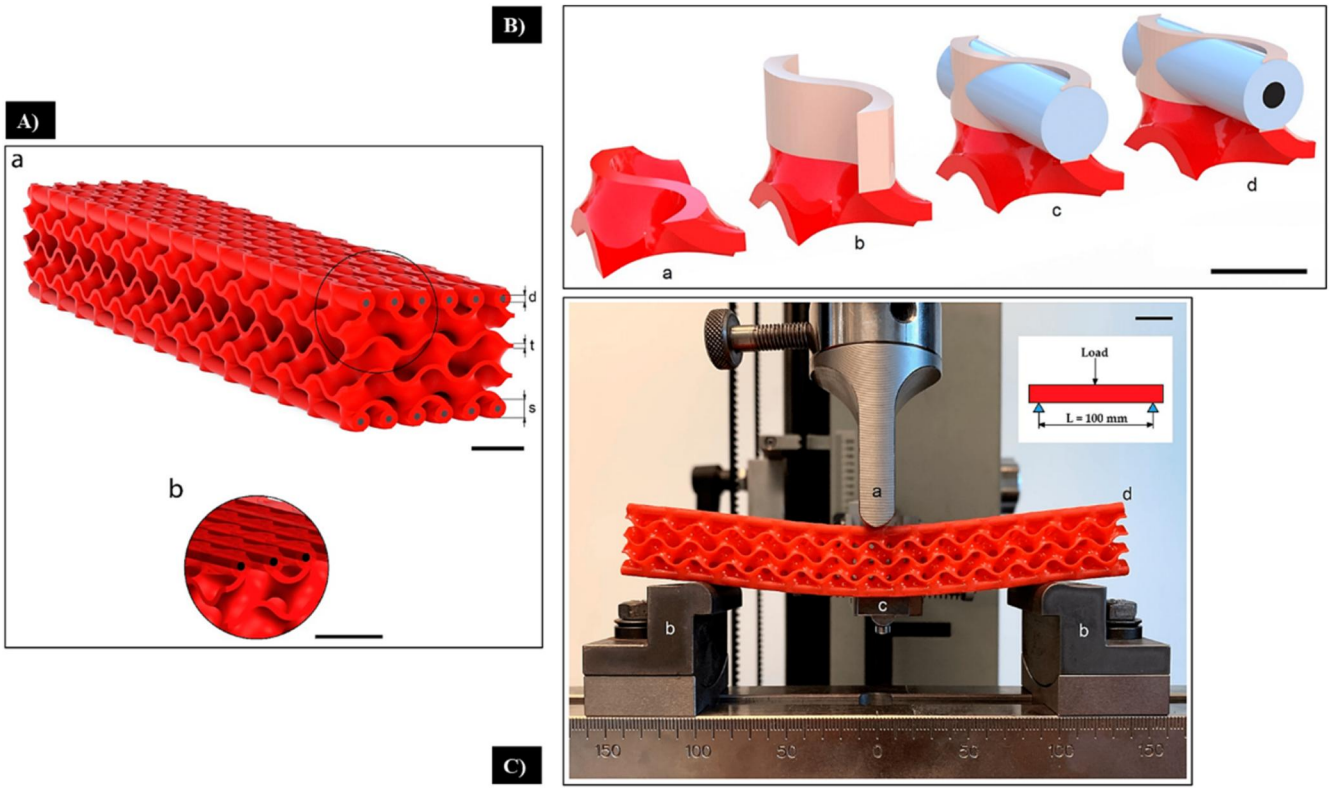

Figure 23. (A) The 3D printed model, (B) the connection technique used to join the tubes to the core structure and the completed 3D model, and (C) the experimental setup [392].

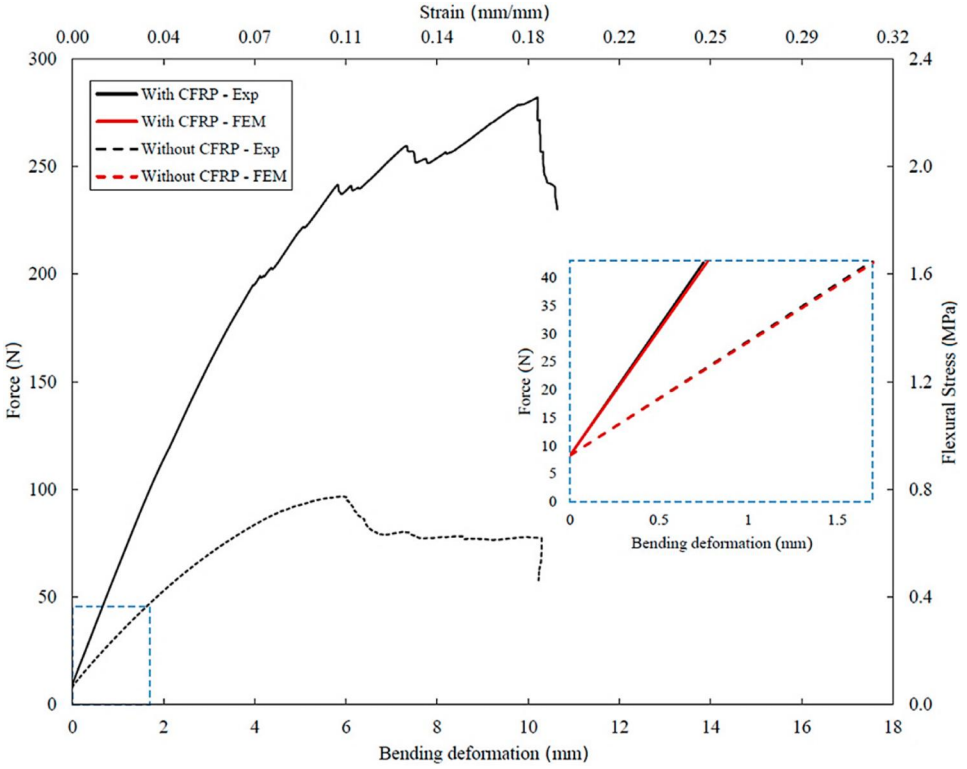

Figure 24. The force-bending deformation curves (experimentally and numerically) of the samples without and with CFRP reinforcements [392].

64.16, 60.98, 52.88, and 35.65%, respectively. The auxetic design enhances ductility by 100–200% for peak load reductions of 15–50%, and energy absorption at failure is nearly eight times that of conventional mortar [216].

Xu et al. [401] presented findings on a novel auxetic cementitious composite (ACC) to reveal its spring-like compressive behavior. Using a 3D-printed TPU auxetic structure with cementitious mortar as a filler, the ACC shows superior

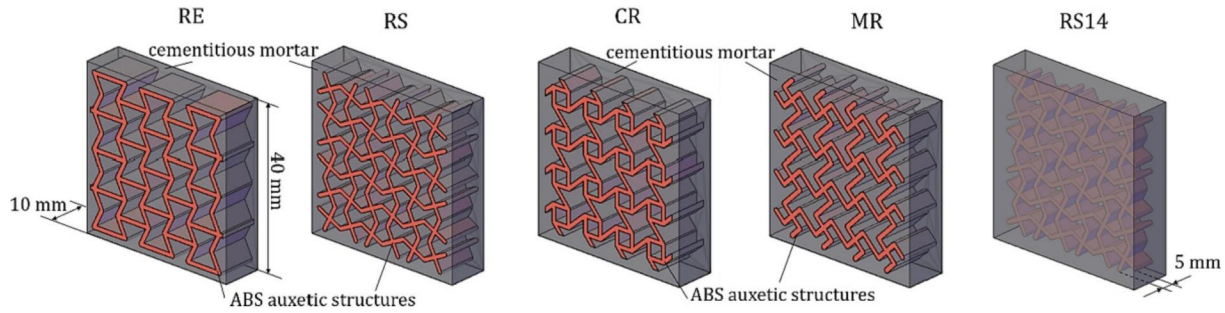

Figure 25. The four ACC types [397].

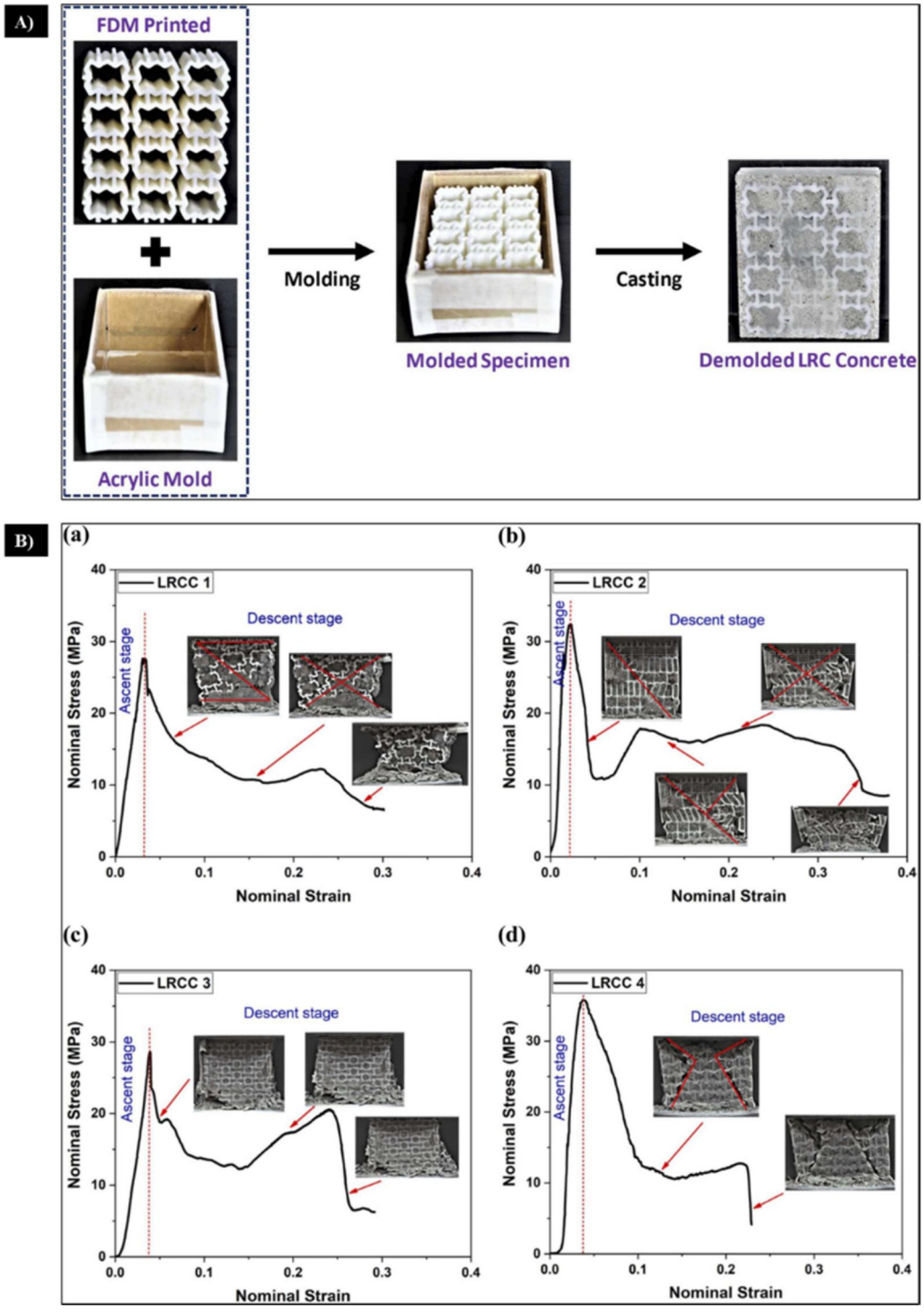

Figure 26. (A) The fabrication process for LRCC composites and (B) the shear failure pattern formations in the LRCC samples [216].

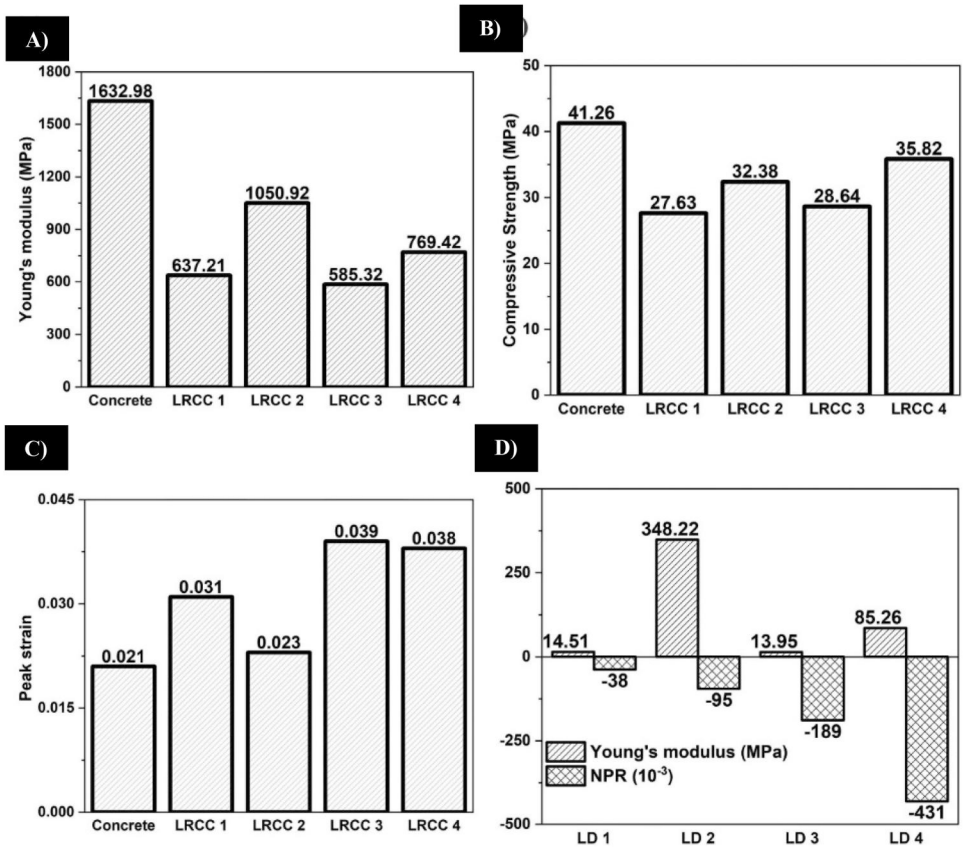

Figure 27. (A) Young's modulus, (B) compressive strength, (C) peak strain observed in concrete and lattice-reinforced concrete (LRCC) specimens, and (D) Young's modulus alongside the normalized peak response of the lattice reinforcement integrated into the concrete structure [216].

energy absorption due to strain-hardening. It absorbed 6300% more energy than the TPU frame and 4200% more than the reference mortar. The ACC's spring-like behavior allows significant recoverable deformability during cyclic loading, achieving a strain amplitude 20 times better than standard mortar. Despite fatigue damage, the ACC demonstrated greater stiffness and energy absorption compared to the auxetic frame [401].

Xu et al. [341] performed a study on the compressive behavior of auxetic cementitious cellular composites (CCCs) through a blend of investigational methods and (FE) simulations. The study implemented a conventional auxetic centrosymmetric geometry for the unit cells that constituted the cellular structure, utilizing fiber-reinforced cementitious mortar as the material component. By varying the geometry of the cells, three CCCs (P0, P25, and P50) were created and subjected to both experimental and numerical testing under uniaxial compression, considering different boundary conditions. The authors concluded that auxetic cellular composite materials (CCCs) exhibit remarkable characteristics regarding density, energy dissipation capacity, and Poisson's ratio, thereby positioning them as highly advantageous for diverse applications within the field of civil engineering [341].

Xu et al. [355] developed a new type of cementitious auxetic material with a unique crack-bridging mechanism, differing from the usual local buckling. By using 3D printing, they created cementitious cellular composites (CCCs) with auxetic structures and varied fiber contents. Tests under uniaxial compression and cyclic loading revealed that these CCCs can show auxetic behavior, including strain hardening and high energy absorption. Remarkably, they achieved 2.5% reversible deformation after 25,000 cycles, despite initial fatigue damage in the first 3,000 cycles. This innovative auxetic mechanism presents a promising design strategy for enhancing brittle materials [355].

An article by Zahra and Dhanasekar [402] presented findings on the fabrication and evaluation of cementitious polymer mortar-auxetic foam composites, which are deemed suitable for wall rendering purposes. The study experimentally assessed the deformation behavior of composites featuring auxetic foam with a high negative Poisson's ratio (NPR), embedded within a polymer cement mortar matrix. These were compared to standard mortar composites reinforced with fiberglass mesh layers, known for their positive Poisson's ratio. The findings showed that the auxetic foam-enhanced composite outperformed the standard version by preventing delamination and reducing brittleness [402].

Rosewitz et al. [381] conducted an integrated experimental and numerical investigation into bioinspired architected composites. These composites were developed using a cement mortar matrix combined with auxetic polymer components and brick-and-mortar. The investigation provides an in-depth assessment of how the unit-cell polymer phase affects mechanical properties with a particular focus on the role of architected geometry. The study analyzed five types of architected composites with different polymer phase geometries. A basic concrete beam without a polymer phase was the reference. Three polymer phases were 3D printed and arranged in unit cells. Results showed that architected

composites outperformed control samples in strength due to reduced localized deformation [381].

Chen et al. [403] conducted a comprehensive testing and numerical investigation into the compressive and flexural characteristics of engineered cementitious composites (ECC) that are utilized in auxetic structures produced *via* 3D printing. The results reveal that the auxetic specimens analyzed show significant auxetic behavior when exposed to compressive loading, whereas this behavior is not apparent during flexural loading. The buckling-induced auxetic structure exhibits a compressive strength of 5.1 MPa, which is approximately 264% and 750% greater than that of cross-chiral and reentrant structures, respectively [403].

In their research, Zhao et al. [404] examined the mechanical behavior of reinforced concrete samples with five cellular structures (honeycomb, AH-V1, auxetic-struts, AH-V2, and reentrant auxetic) under in-plane quasi-static uniaxial compression [405]. The cellular structures were fabricated using PA6 (nylon 6, polyamide 6) as the molding material and then filled with cementitious mortar. Compression tests were conducted with an ultimate load of 100 kN. Results showed that honeycomb and reentrant auxetic structures reinforced with concrete had substantial energy absorption under uniaxial loading. In contrast, auxetic-strut structures exhibited performance inconsistencies due to stress concentrations at the corners of the vertical rods, leading to material failure and structural damage. The experiments revealed performance variations in reinforced concrete specimens, with notable improvements in energy absorption capacity and ductility, attributed to different deformation modes [404]. Figure 28 illustrates the cellular structures made from 3D-printed PA6 (A) and the concrete specimens at the stage when the mold is prepared for removal (B). In Figure 29, part A shows the force-displacement curves for various specimens, while part B displays the corresponding energy-displacement curves.

Chen et al. [406] conducted an extensive study on the compressive behavior of ultra-high-performance concrete (UHPC) reinforced with a 3D-printed triangular (T-UHPC), reentrant honeycomb (H-UHPC), and octet (O-UHPC) lattices, along with steel fiber-reinforced UHPC (S-UHPC) (Figure 30). Comparisons with plain UHPC and S-UHPC revealed H-UHPC's static compressive strength was 14.6–19.4% higher than O-UHPC and T-UHPC. At higher strain rates, H-UHPC showed peak compressive strength (262.7 MPa), improved flexibility, and superior energy absorption, highlighting reentrant honeycomb lattices as optimal for creating auxetic 3D-reinforced UHPC [406].

Meng et al. [407] investigated cementitious composites with 3D-printed auxetic lattices, which display negative Poisson ratios. Using X-ray CT, they found that auxetic lattices effectively constrain crack growth and dissipate energy, resulting in 1.7 times higher densification energy compared to conventional materials. This research enhances the understanding of auxetic lattice-reinforced composites for improved load-bearing and energy dissipation [407]. Edmund et al. [408] 3D printed reentrant chiral auxetic (RCA) meshes with PLA and TPU filaments, embedding them in low- and high-strength mortars to create ACC samples. The highest tensile strength (11 MPa) and ductility were achieved with TPU-RCA meshes. PLA-RCA meshes exhibited the highest shear bond strength (0.44 MPa). The study shows that ACC can enhance masonry and cementitious structures [408].

2.7.4. Lattice concrete moulds

LSs are increasingly used as concrete molds and in construction to fulfill structural and functional requirements [409–416]. To enable multiple healing cycles and optimize healing efficiency in vascular self-healing concrete, Wan et al. [417] designed an octet-structure lattice as a vascular network, effectively delivering healing agents to cracks. Redundancy ensures access through multiple pathways, enhancing ductility by increasing crack tortuosity. To study layer height and printing orientation effects, four vascular network configurations were made using ABS filament. In instances where specimens exhibited fractures during the 4-point flexural experiments, epoxy resin was utilized as the healing agent, attributed to its effective healing capabilities. Figure 31 illustrates the vascular network schematic (A), the manual healing procedure schematic (B), the 4-point bending experimental setup (C), and the comparison of the sample's flexural strength (D).

The results show that self-healing concrete with vascular systems has lower initial flexural strengths than control samples. This reduction is influenced by printing parameters: horizontally oriented vascular networks have higher flexural strength compared to vertically oriented ones. Smaller printing layer heights result in less reduction in initial flexural strength compared to larger layer heights. Regarding water-tightness recovery, all vascular-based self-healing samples achieved full (100%) recovery, indicating that printing direction and layer height do not significantly affect water-tightness recovery [417].

Nguyen et al. [418] introduced an innovative variant of lightweight cellular foamed concrete (FC) based on gyroid, primitive, and baseline lattice models. PLA filaments were used to produce the cellular molds. Foamed concrete was poured into the molds. Three samples from each batch of foamed concrete were tested using a 50 kN testing machine to evaluate their mechanical properties. The 3D-printed mold design significantly impacted the microstructure and compressive strength of foamed concrete, with TPMS structures showing much higher strength than standard strut-based lattices. Figure 32 shows the lattice types (A), PLA mold fabrication methods, and concrete structures (B). Figure 33 presents the performance of bio-inspired foamed concrete, highlighting (A) compression performance and (B) load-displacement curves for both molds and foamed concrete (density 800 kg/m^3).

Nguyen-Van et al. [419] combined primitive, gyroid, and cubic blocks reaching a 50% volume fraction. Lightweight cement mortar samples were made using 3D-printed PLA molds and tested under uniaxial compression. Compression tests on the cement cubes were paired with tensile behavior analysis using a damage plasticity model. Finite element (FE) analysis predicted mechanical performance, including stress-strain curves, stress distributions, and damage behaviors, with

Figure 28. (A) The cellular structures made from 3D-printed PA6 and (B) the concrete specimens at the stage when the mold is prepared for removal [404].

compressive test results validated by the FE model. Figure 34(A) illustrates the unit cell types, (B) the gyroid and lattice cellular mold case designs for cement fillings, (C) the 3D printed mold structures (primitive (a), lattice (b), and gyroid (c)), and (D) the findings associated with the application of fresh cement mortar into casting molds.

FDM was used to create PLA molds, with three molds for each design. Finite element analysis showed that TPMS cellular structures had more uniform stress distributions under uniaxial compression compared to lattice blocks. The gyroid specimen also had consistent stress distributions due to its continuous curvature. Stress-strain curves indicated that the primitive block had the ultimate compressive strength, and then the gyroid. The primitive structure's superior performance suggests its use in lightweight bricks, coastal protection blocks, noise barriers, and decorative wall features [419].

Nguyen-Van et al. [420] examined the mechanical behavior of a three-dimensional Menger-Sponge (MS) cube and six other fractal-like designs with different hollow shapes. Using the finite element method, the mechanical responses under uniaxial compression were predicted and validated with previous experimental data. Comparing TPMS-Primitive and second-order MS cementitious structures, as well as other fractal structures, showed similar mechanical responses for MS and Primitive blocks. However, fractal-square (FS) structures exhibited superior performance, especially in the first and second fractal orders [420]. Song et al. [421] proposed a new type of 3D core-framework FCC-lattice cementitious composite, made from printed polymers combined with cement mortar. This innovative design aims to create energy-efficient building systems by focusing on thermal conductivity, mechanical properties, and the need

for lightweight materials. Their analysis showed that while the average compressive strength of these composites (CS-LCCs) is lower than that of cubic cement mortar samples, their specific strength is comparable. Additionally, the polymeric framework significantly enhances the ductility of the CS-LCCs [421].

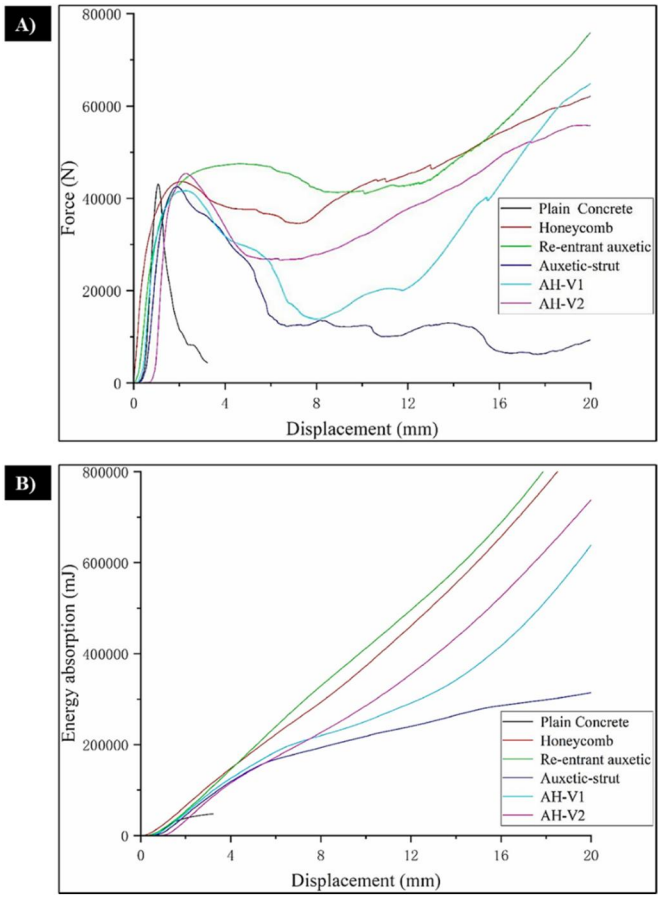

Figure 29. (A) The force-displacement curves of the specimens and (B) the energy-displacement curves corresponding to these specimens [404].

2.7.5. Composites and Metals

A significant benefit of using composites in LSs is the ability to optimize characteristics along the mainly axially loaded parts by adjusting the material anisotropy. Thus, composite LSs exhibit material-geometry effectiveness, where the geometry guides the forces to coincide with the principal fiber direction of the material [31]. 3D printing has revolutionized the creation of complex continuous fiber-reinforced composite LSs (CFRCLSs). However, the accuracy of geometry and mechanical performance is constrained by the absence of effective methods for crafting critical features, specifically joints [422]. 3D printed carbon-fiber reinforced composite LSs have been used frequently [423–425]. Glass fiber/PA12 composite is also used in producing LSs [426]. Peng et al. [427] employed short carbon fiber-reinforced polyamide 6 (CF/PA6) for the fabrication of their honeycomb structure [427]. Metals used in 3-D printing are becoming more popular in industries like healthcare, automotive, manufacturing, and aerospace [428]. Metal materials have superior physical qualities, making them suitable for sophisticated manufacturing, such as printing human organs, LSs, and aeronautical components. Aluminum [429], cobalt, nickel, stainless steel, inconel, and titanium alloys are examples of these materials [38, 428, 430–437].

Tzortzinis et al. [438] proposed a novel method for reinforcing concrete and mortar with steel auxetic truss lattices. Numerical analysis and experiments using 3D-printed steel lattices embedded in mortar under axial compression revealed enhanced confinement, increased strength, and exceptional ductility, with residual strength persisting beyond 20% strain. Computational modeling validated these

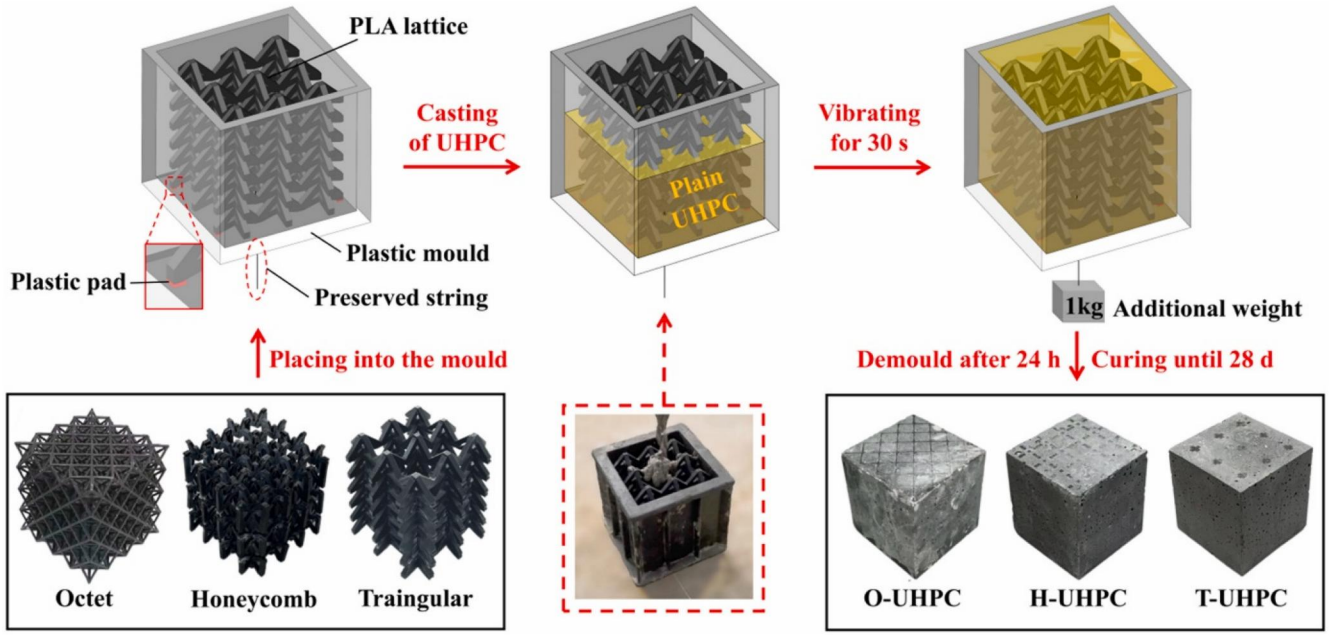

Figure 30. Diagrammatic representation of the preparation process for lattice-reinforced UHPC specimens [406].

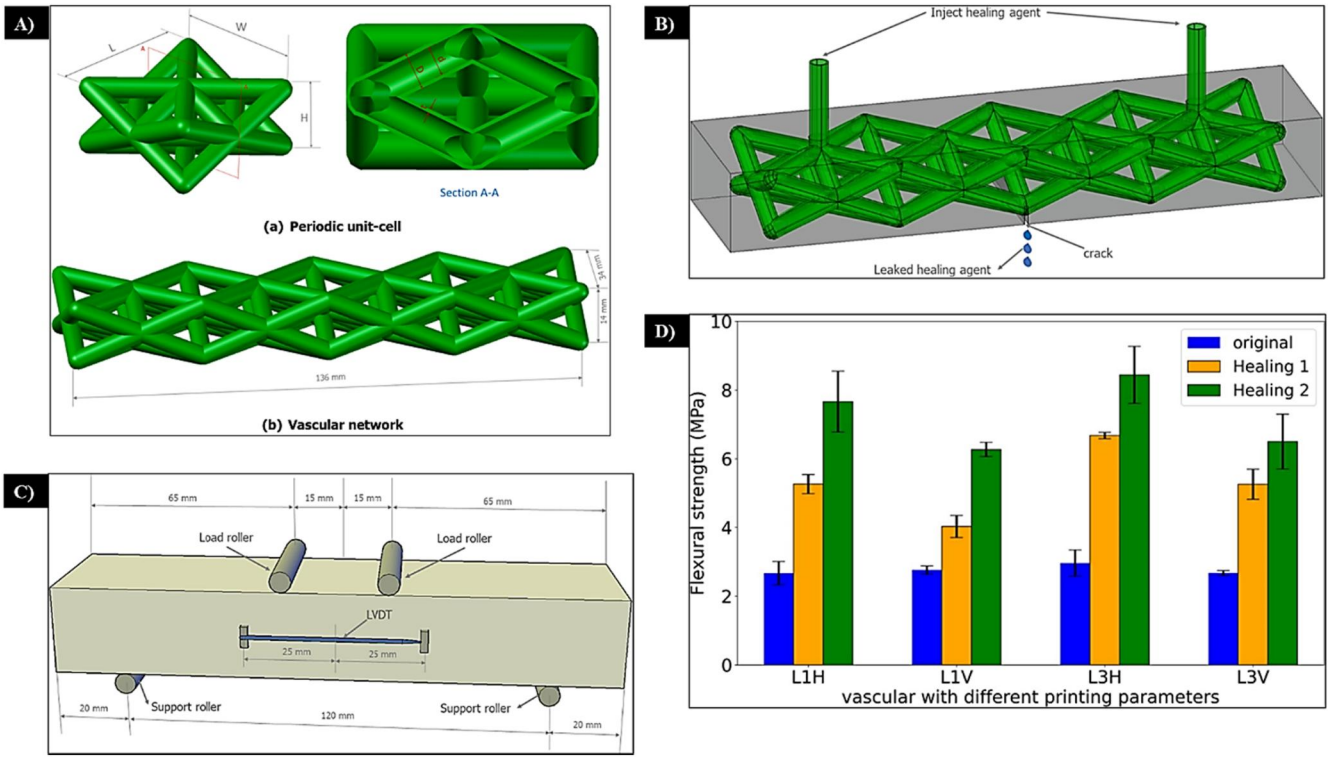

Figure 31. The vascular network schematic (A), the manual healing procedure schematic (B), the 4-point bending experimental setup (C), and the comparison of the sample's flexural strength (D) [417].

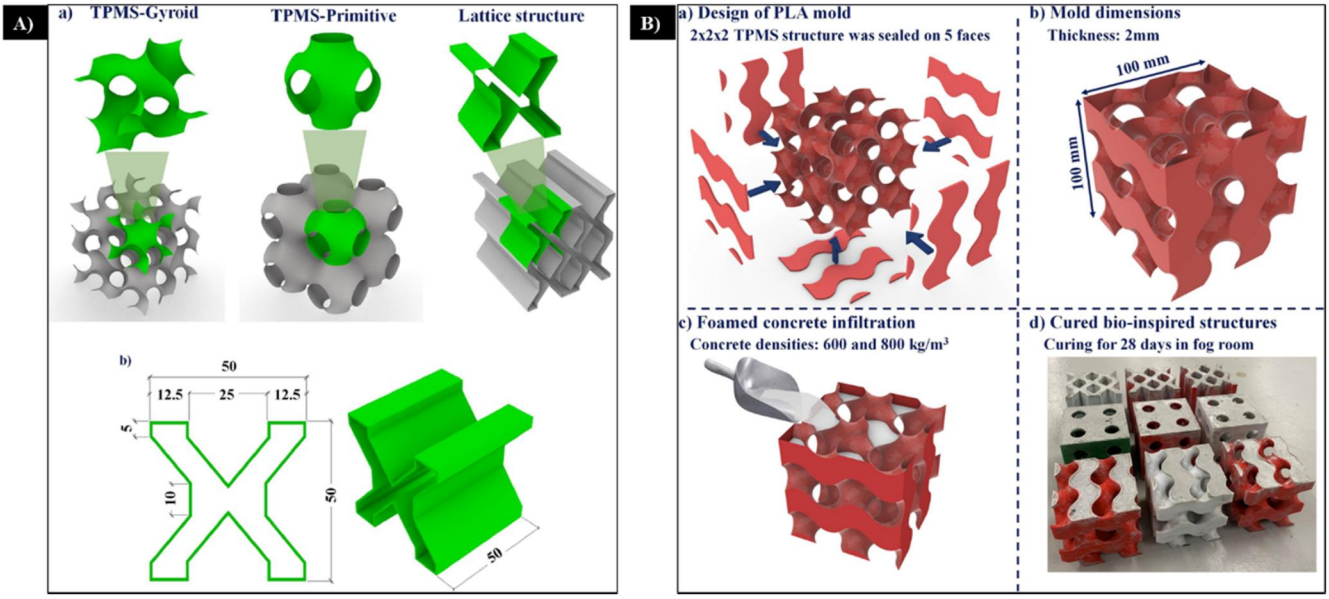

Figure 32. (A) The lattice structure types and (B) the fabrication methods of the PLA molds and the concrete structures [418].

findings, highlighting the potential of auxetic lattices for strengthening structures to withstand extreme loads, such as during earthquakes. The results in Figure 35 highlight the auxetic lattice's superior strength and ductility. While the conventional passive configuration enhances the mortar's peak load by 70%, the auxetic lattice achieves a significantly higher increase of 140% [438].

Luo et al. [439] introduced a concrete-filled auxetic stainless steel tube (CFASST) composite to enhance concrete confinement through auxetic tubular designs. Experimental and numerical analyses assessed axial compressive behavior, including strain response, load-displacement patterns, and failure mechanisms. Parametric studies explored the influence of tube thickness and Poisson's ratio. Findings revealed that CFASST structures display distinctive deformation patterns and superior confinement properties. Figure 36 presents comparisons of numerical and experimental results, including failure modes and load-displacement curves, showing strong agreement between test data and FE analysis.

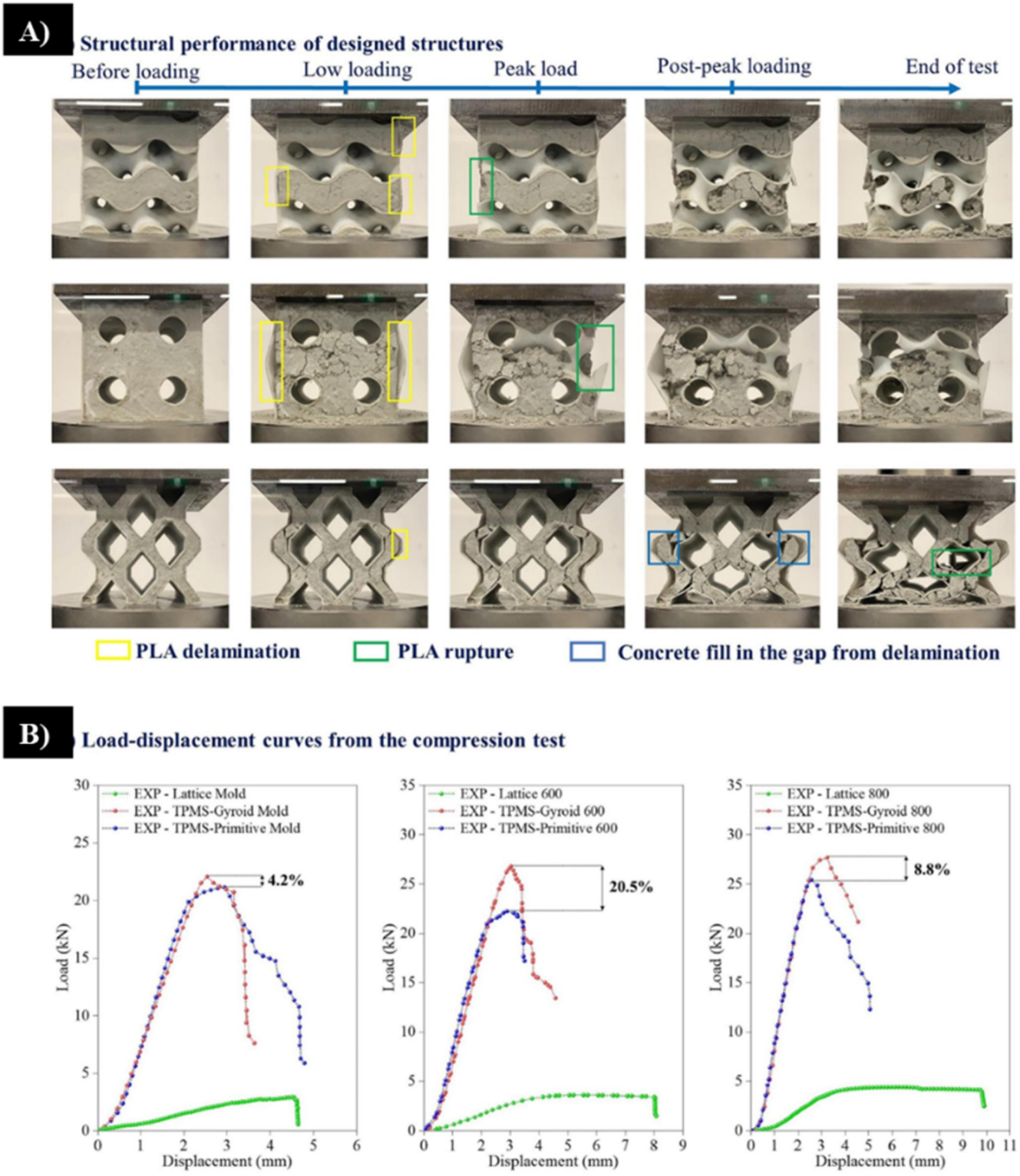

Figure 33. The evaluation of performance for bio-inspired foamed concrete structures is presented, which includes (A) an analysis of structural behavior at various stages of compression loading and (B) the load-displacement curves corresponding to the molds and the foamed concrete structures, where the density of the foamed concrete is 800 kg/m^3 [418].

Table 7 summarizes various lattice types along with their respective examples used in the literature.

2.7.6. Cellular lattice concrete structures

Concrete-based large-scale LSs have been realized in a variety of methods, as shown in [440], with some degree of success. These consist of extensive lattices constructed by casting concrete into intricate fabric formwork produced through CNC machining, substantial 3D printed clay formworks, or molds constructed from 3D printed sand. It was determined that while producing extensive concrete LSs is challenging, several technologically feasible approaches exist. Extrusion-based 3D concrete printing [441, 442] is excellent

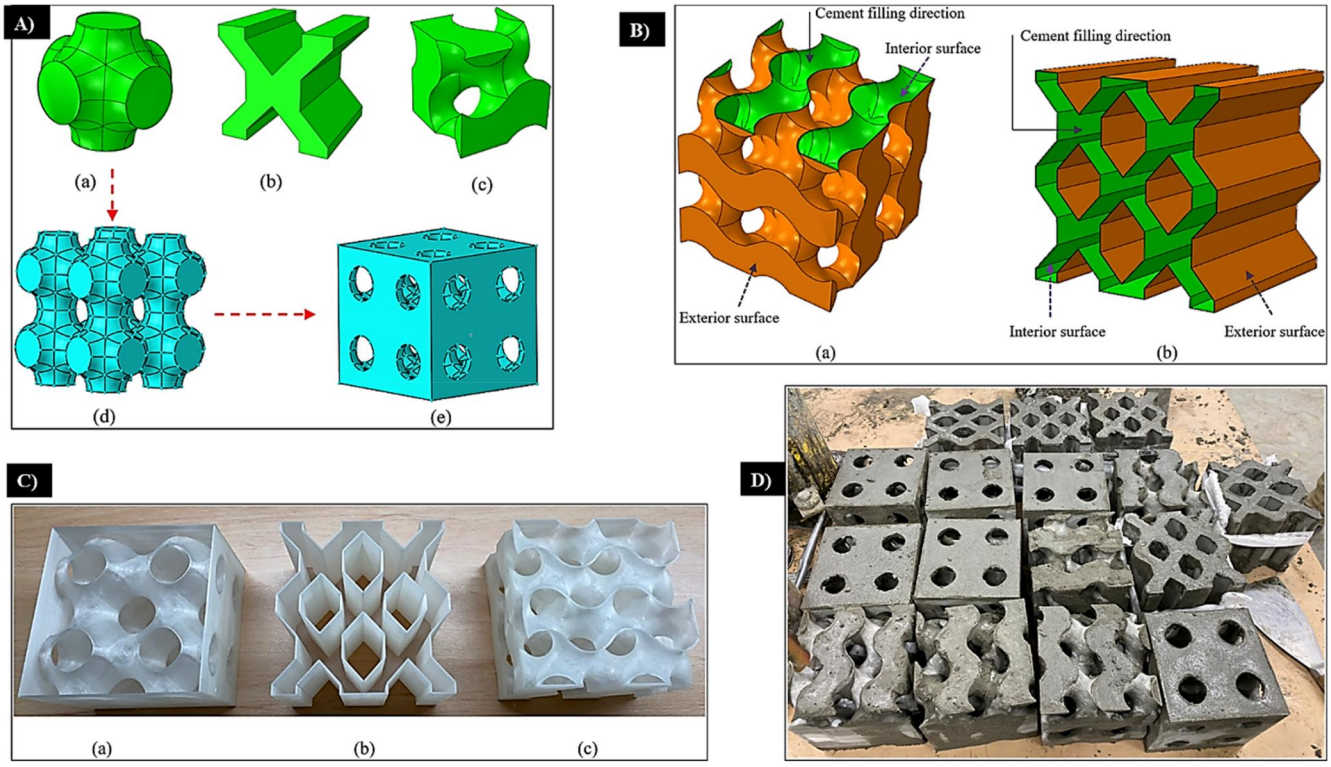

Figure 34. The unit cell types, (B) the gyroid and lattice cellular mold case designs for cement fillings, (C) the 3D printed mold structures (primitive (a), lattice (b), and gyroid (c)), and (D) the findings associated with the application of fresh cement mortar into casting molds [419].

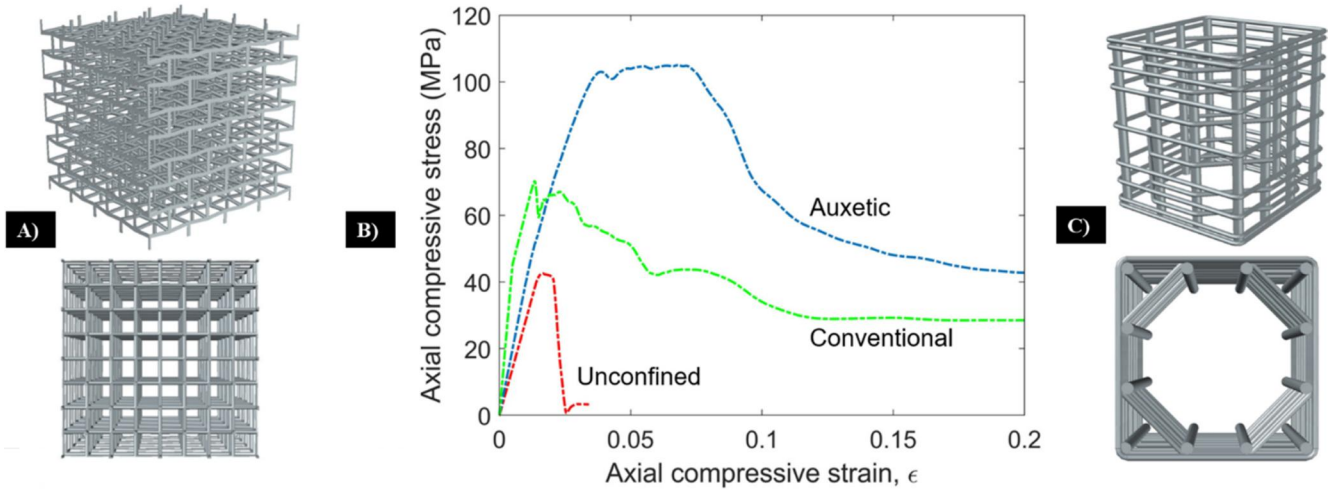

Figure 35. Stress-strain curves of unconfined (red), conventionally confined (green), and auxetic confined (blue) members highlight the superior strength and ductility of auxetic lattice confinement [438].

for creating basic 2D cellular structures. In addition to extrusion-based 3DCP [443], molds made of 3D-printed polymers could also be used to produce 3D-casted LSs [419, 444, 445].

The process of AM involving cementitious materials [446], specifically the variant characterized by material deposition through extrusion, commonly referred to as 3DCP [447, 448], is experiencing a swift rise in acceptance within the construction sector [449, 450]. The advent of 3DCP [451] technology can be traced back approximately twenty years [452–455]. Since its inception, numerous innovative projects and case studies have emerged, consistently demonstrating the capabilities of digital fabrication utilizing concrete [456]. The use of 3D printing technology for concrete is gaining recognition as a viable method for creating innovative structural components, offering several advantages. However, its effectiveness depends on a set of temporal parameters that can significantly affect the long-term performance and durability of printed elements, especially considering their exposure to external environmental conditions [457]. The application of 3DPC [458] offers the potential to boost construction efficiency, lower labor and material costs, and provide enhanced design flexibility by removing the need for traditional formwork [357, 459–463]. However, a key challenge to the widespread adoption of 3DPC is the variability in the printing materials.

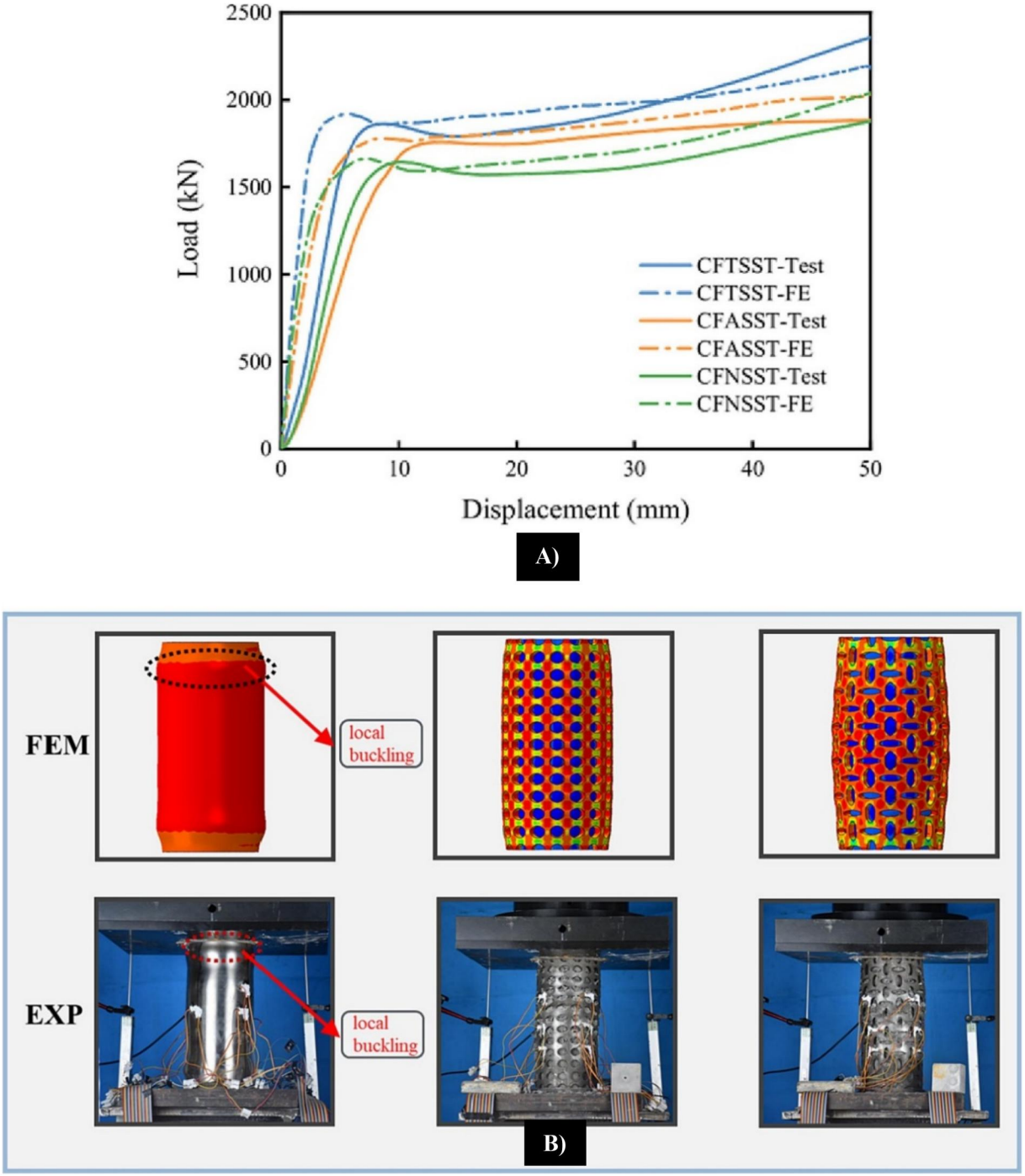

Figure 36. Comparisons of experimental and numerical results: A) displacement-load curves and B) modes of failure [439].

Significant differences in composition and performance metrics between 3DPC and conventional concrete present obstacles to its broader use in the construction industry [463].

To gain a comprehensive understanding of the ongoing advancements in 3D printing technology within the construction sector [464], numerous reviews have been conducted [102, 457, 463, 465–478]. Tiwari et al. [479] focused on developing cellular lattice concrete structures via 3D printing, using a powder bed technique with selective cement hydration. Fine sand, Ordinary Portland Cement, and water were used, without any admixtures. The printing method was a cost-effective syringe-based water jetting system applied to a cement and sand mixture. Two types of cellular concrete blocks were produced: gyroid structures and interconnected spherical voids, each with 15 cm edges. Uniaxial compression tests were performed to understand the strength characteristics of the 3D-printed specimens (Figure 37). Key insights include that the solid cubes exhibit greater strength than cellular lattices; solid cubes loaded perpendicular to the printed layers are stronger than those loaded parallel; strain at failure for perpendicular loading ranges from 0.005 to 0.018; dry specimens are significantly stronger than wet ones, sometimes by a factor of two or more. The study found that altering specimen density could

Table 7. Classification of LSs used in concrete reinforcement.

Lattice type	Examples
Triply periodic minimal surfaces (TPMS) lattices	Fischer-Koch S, Diamond, IWP, and Gyroid lattices
	TPMS-Primitive scaffolds
	Gyroid, primitive, and cubic blocks
	Gyroid structures with CFRP rods
Octet lattices	Octet lattice reinforcements
	Octet-Truss Engineered Concrete (OTEC)
	Octet lattice for cementitious composites
Reentrant and auxetic lattices	Reentrant, Rotating-Square (RS), Missing-Rib (MR), Chiral (CR) auxetic lattices
	Reentrant chiral auxetic (RCA) meshes
	Reentrant honeycomb lattice for UHPC
	Auxetic-struts and reentrant auxetic structures
	Auxetic cementitious composites
	Concrete-filled auxetic stainless steel tubes (CFASST)
	Steel auxetic truss lattices in mortar
Polymer and metal lattices	3D-printed polymer lattices (3D-PPL) using transparent resin (TR), ordinary resin (OR), and nylon (NY)
	PA6 polymer lattice reinforcements
	3D-printed PA6 spiral and skin LSs
	Selective laser sintered Polyamide 6 (PA6) lattices
	Short carbon fiber-reinforced polyamide 6 (CF/PA6) honeycomb structures
Topology-optimized and functionally graded lattices	Functionally graded LSs in cementitious composites
	Topology-optimized LSs in cement composites
LSs for self-healing and lightweight concrete	Vascular network lattices for self-healing concrete
	Menger-Sponge (MS) LSs
	Lightweight cement mortar reinforced with cellular lattices
	3D core-framework FCC-lattice cementitious composite

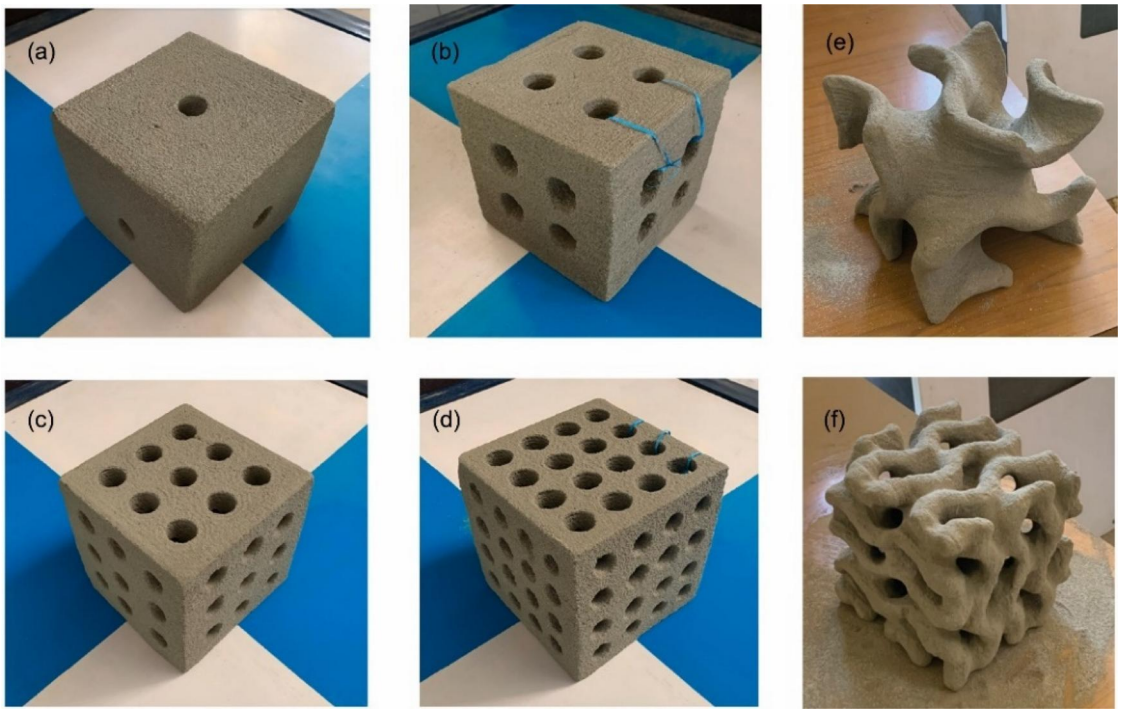

Figure 37. The printed specimens [479].

program strength, with a 30% density reduction leading to a 75% strength decrease. Additionally, leaving 3DPC specimens in the atmosphere after 28 days of curing increased their strength by 2 to 3 times due to carbonation [479].

Dey et al. [480] examined the bending performance of concrete beams that were 3D-printed with four infill patterns: triangular, lattice, sinusoidal, and lattice-triangular. Tests were conducted in vertical and transverse loading directions. All beams measured 290 mm in width, 200 mm in height, and 890 mm in length, classified as L-Beam, T-Beam, LT-Beam, and S-Beam (Figure 38(B)). Fabrication used an extrusion-based concrete printer (Figure 38(A)). The mortar mix included natural river sand and a cement-based binder (1:1.5 ratio), with Ordinary Portland Cement (OPC 43-grade) and densified Silica Fume (SF). A viscosity-modifying admixture (VMA) and a superplasticizer (SP) were added. Chopped polyvinyl alcohol (PVA) fibers (12 mm long, 0.04-0.06 mm diameter) provided reinforcement.

The authors found that L-Beams had 17.7% higher flexural deformation resistance under vertical loading, while T-Beams outperformed under transverse loading, achieving a 500% improvement in flexural resistance. Topology-optimized 3D-printed beams improved bending performance by 30%, with the optimal infill at 25% of the triangular infill

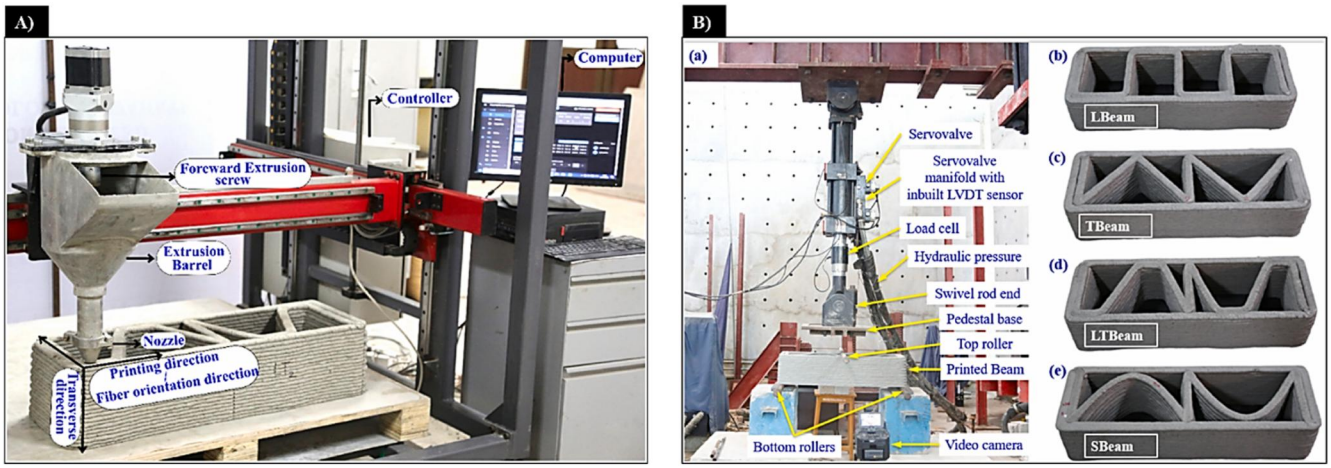

Figure 38. (A) The printing process and (B) the experimental setup with the printed specimens [480].

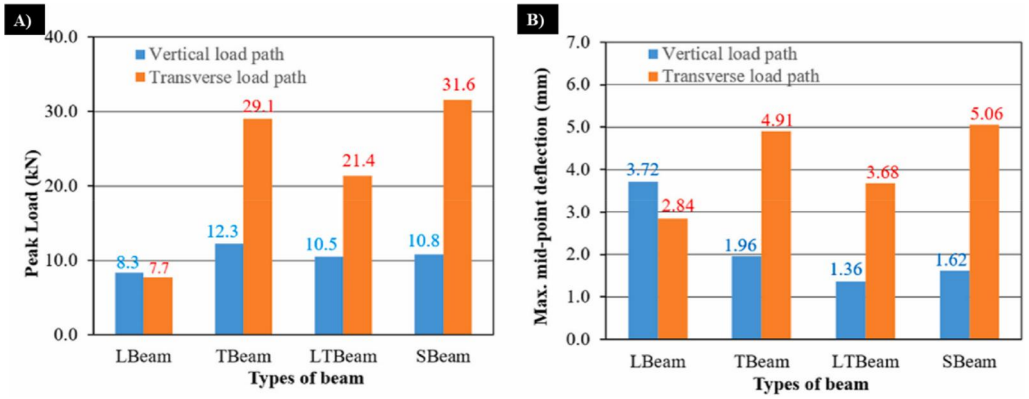

Figure 39. The maximum numerical bending load (A) the midpoint displacement (B) beams under both transverse and vertical loading conditions. [480].

width. Figure 39 shows the maximum numerical bending load (A) and midpoint displacement of the beams (B) [480].

Wang et al. [445] developed five concrete mixtures with different rates of lightweight ceramsite sand for 3D printing. To reduce shrinkage and micro-cracks, ceramsite sands were treated with polyvinyl alcohol. The optimized mixture was chosen for continuous printing. Cubic and beam elements with four internal hollow structures - cellular, truss-like, square lattice, and triangular grid - were 3D printed. Compressive tests showed the rectangular lattice had the highest strength, while truss-shaped beams had the best flexural performance [445]. Ye et al. [481] created six hollow beams without steel reinforcement and tested them using a four-point loading method. The outcomes showed that these beams, despite lacking steel, exhibited multiple cracks, flexural hardening, and ductile failure. Their flexural strength ranged from 6.06 MPa to 7.86 MPa. The authors concluded that using ultra-high-performance concrete (UHDC) in hollow structures is a revolutionary idea for 3DCP without needing steel reinforcement [481].

A comparative study was conducted by AlZahrani et al. [482] on the thermal characteristics of various infill structures in 3DPC walls, aiming to enhance thermal efficiency and reduce energy consumption without increasing material costs. A computational model analyzed the thermal behavior of different infill designs, keeping the concrete formulation and concrete-to-void ratio constant. The study compared the thermal performance of 3DPC walls with traditional materials like clay and concrete bricks. Results showed that infill geometry significantly influenced thermal conductivity, which ranged from 0.122 to 0.17 W/m.K. The authors concluded that replacing conventional materials with optimized infill structures could reduce annual energy costs by at least $\$1/m^2$, highlighting the importance of selecting the right infill design to lower energy consumption in buildings [482].

Nemova et al. [483] investigated the development of energy-efficient 3D-printable walls that can be applied globally, adhering to the criteria of energy efficiency and sustainability. The study employed numerical analysis and experimental investigations, utilizing bench tests with software tools and advanced precision equipment to evaluate the thermal behavior of 3DPC envelopes. Various designs, material arrangements, and insulation sorts were examined. The results indicated the successful creation of a novel energy-efficient ventilated 3DPC envelope characterized by a low thermal conductivity coefficient, tailored to specific climatic zones [483]. A study was performed by Suntharalingam et al. [484] to assess the fire performance of 20 distinct configurations of 3DPC walls, using confirmed finite element models under standard fire conditions. The findings indicated that 3DPC non-load-bearing cavity walls possess significant resistance to standard fire loads, with the

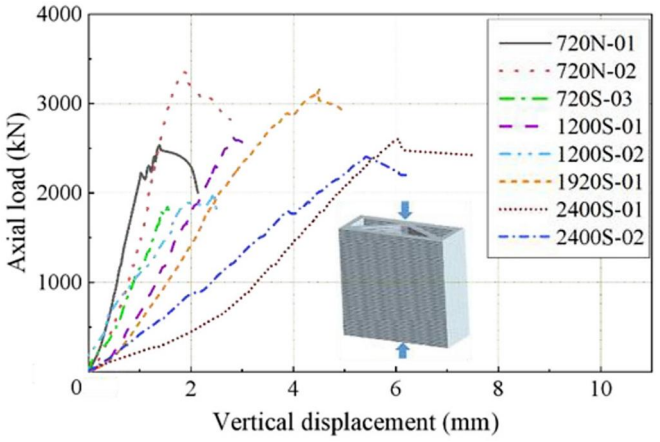

Figure 40. Load-displacement curves of the wall specimens [486].

potential for further enhancement using Rockwool insulation. The results demonstrated that a parallel increase in wall thickness correlates with a marked improvement in fire performance [484].

Ye et al. [485] developed engineered cementitious composites (ECC) lightweight slabs, which incorporated rectangular hollow sections (RS) and honeycomb-like (HS). Four-point flexural tests and FEA assessed their flexural behavior. The ECC slabs showed ductile failure modes without any addition of steel reinforcements. The flexural strength-to-mass ratio for HS and RS slabs was about 0.049 MPa/kg, like solid slabs. Numerical models were validated, and bond strength above 1.5 MPa ensures stable flexural performance in HS slabs [485]. Han et al. [486] analyzed the structural and failure patterns of large-scale 3DPC walls under axial compression. Polypropylene (PP) microfibres were used to improve buildability. Eight wall specimens with different height-to-thickness ratios were tested. Two lacked horizontal steel reinforcement, while six included it. All walls were 240 mm thick, with heights of 720, 1200, 1920, and 2400 mm, resulting in height-to-thickness ratios of 3, 5, 8, and 10. Figure 40 shows the axial compression load versus vertical displacement curves, which peaked and then declined steeply, indicating brittle failure. Cracking loads were below 1250 kN, with a maximum bearing capacity of 3352.4 kN. The ultimate bearing capacity initially increased with the height-to-thickness ratio, but then decreased [486].

Cuevas et al. [487] created a 3D-printable wall structure, which included insulating properties. A lightweight composite was formulated and used to 3D print wall structures with optimal load-bearing capabilities. A normal-weight mixture was also printed as a control. Both mixtures were suitable for printing, resulting in elements sized 30 cm (width) × 90 cm (length) × 45 cm (height). Seven wall samples were simulated to evaluate both the thermal and mechanical behaviors, using both a reference mixture as well as a lightweight mixture with expanded thermoplastic microspheres (ETM) for better insulating goals. The printed walls underwent compressive strength tests. The study found that inter-filament weaknesses and geometric flaws were the main causes of failure in printed envelopes [487]. Yang et al. [488] performed a study aimed at optimizing the spatial arrangement of supporting filaments. Their research is dedicated to evaluating the print quality of 3D concrete walls characterized by hollow sections, with a specific focus on the areas where supporting filaments intersect with the wall. Their study presents a range of strategies for the arrangement of these filaments, as well as methods for ensuring the quality of surface finishes at the connection points [488].

2.8. Critical review of Materials and applications of LSs and recommendations

LSs like polymer, composite, metal, and cellular lattices are revolutionizing digital construction with maximized structural efficiency, reduced material usage, and customized reinforcement patterns. The Materials and Applications of LSs section provides a broad overview of the materials employed in LSs and their applications for additive manufacturing and civil engineering. It properly categorizes LS materials based on their structural behavior, mechanical properties, and 3D printing technology compatibility, including SLS, MJF, and FDM. It also includes a high amount of experimental and computational research, including DIC, AE), FEM, and numerical analysis, to examine LS performance in structural applications. LSs are brought to prominence for their impacts on reinforced concrete, digital construction, energy-saving designs, and self-healing structures, having the potential to enhance ductility, strength-to-weight ratios, and failure mechanisms in cementitious composites. While the review is informative about LS materials and mechanical properties, certain areas need further research to take full advantage of their efficacy and applicability in practice.

One of the main challenges is the lack of long-term durability tests since most studies focus on initial mechanical improvements without considering moisture resistance, fatigue behavior, freeze-thaw resistance, or chemical degradation in real environments. The interplay between polymer LSs and cementitious materials remains an issue since poor bonding can reduce compressive and flexural strength. Research needs to be directed toward optimizing lattice geometry, surface finish, and hybrid reinforcement for enhanced stress transfer and mechanical integrity. Standard testing protocols, such as DIC and AE, also need to be developed to ensure consistency of performance. Auxetic polymer lattices are highly promising for increasing ductility and resiliency, but need resolution of bonding, reinforcement ratios, and production variability to facilitate large-scale applications. At the same time, lattice concrete molds offer a fresh approach to shaping and reinforcing concrete with reduced material consumption. Nevertheless, shortcomings in early strength, inter-layer adhesion, and print orientation could compromise their strength-carrying capacity, which necessitates investigations into lattice infill patterns, integration of reinforcement, and adaptive print approaches to make them more mechanically efficient. Furthermore, test performances for durability, exposure, and longevity in harsh environments are relevant for confirming the quality

of such molds in regular use for years. Lastly, the eco-friendliness of molds based on polymer invites the need to address the problem again through ongoing investigation into its life cycle assessment (LCA), reusability, or greenery alternatives.

Aside from polymer lattices, composite and metal LSs are advantageous when it comes to strength-to-weight ratios and optimized mechanical properties and are used in manufacturing and building. Carbon fiber-reinforced composite (CFRPs) provides additional anisotropic strength, and metal lattices made of aluminum, titanium, and stainless steel are extremely long-lasting and shock-resistant. However, geometric precision, material compatibility, and joint production remain the most significant challenges, especially in 3D-printed composite lattices, which are prone to fiber orientation and bonding problems affecting structural integrity. There must be studies on joint design optimization, interface adhesion techniques, and hybrid composite-metal reinforcement strategies to attain optimal performance. Besides, auxetic reinforcement methods in metal lattices have been discovered to increase strength and ductility, but their use is hindered by the complexity of manufacturing, high expense, and limited long-term performance data. Future studies should concentrate on precision manufacturing processes, topology optimization techniques, and high-performance coatings or treatments to ensure mechanical reliability and economic feasibility.

Cell lattice concrete structures are a game-changer in 3DCP, enabling complex architectural forms, reduced use of material, and better thermal performance. However, variability of printing material, mechanical response, and environmental performance provides a robust barrier to large-scale implementation. Investigations should focus on standardization of material composition, optimal printing parameter selection, and incorporation of high-performance additives or fibers to improve structural uniformity and reliability. The other primary challenge is the effects of moisture, thermal cycling, and carbonation on the long-term durability of 3D-printed concrete, which is an under-researched area. The fire resistance, seismic response, and dynamic loading behavior of the 3D-printed LSs also need to be determined in future studies to comply with modern building safety standards.

Apart from material and structural concerns, cross-disciplinary research is needed to integrate machine learning, real-time structural health monitoring, and adaptive manufacturing techniques in lattice-based construction. Predictive modeling using finite element analysis and AI-optimized design can accelerate material selection, defect detection, and performance enhancement. Furthermore, the addition of self-healing mechanisms, bio-inspired designs, and smart materials can lead to highly adaptive, resilient LSs. Sustainability remains a critical concern, requiring further research into biodegradable polymers, low-carbon cement alternatives, and fully recyclable metal lattices to meet global environmental objectives.

With rapid digital fabrication, LSs possess vast potential to transform the industry, but challenges of material compatibility, durability, accuracy of fabrication, and scalability of application must be addressed. Bridging these fundamental research gaps will make LSs available for full utilization and result in stronger, more efficient, and more sustainable construction solutions.

2.9. Enhancing LSs

To improve AM LSs, it is essential to employ advanced techniques like topology optimization [489], which strategically arranges material for optimal strength with minimal weight. Surface treatments, such as polishing and coatings, are vital for enhancing mechanical properties and extending the lifespan of these structures. The addition of nanomaterials further increases strength and thermal stability, while graphene coatings [490] enhance conductivity and overall robustness. The integration of these methods results in highly optimized, lightweight, and multifunctional LSs, ensuring enhanced performance in various fields, including construction, automotive, and medical devices.

Wang et al. [491] developed a new hierarchical lattice metamaterial by modifying a face-centered cubic (FCC) cell design. This structure features two key innovations: reinforced double diagonal supports and hierarchically arranged circular elements. These modifications were designed to deliver three main benefits: enhanced strength, improved energy absorption, and predictable deformation behavior. By altering the conventional FCC lattice metamaterials, they introduced a unique lattice metamaterial that was inspired by the structural properties of glass sponge skeletons. Four samples were assessed under quasi-static compression. The authors demonstrated the superior mechanical performance of novel MFCC and MHCFCC lattice metamaterial architectures over conventional FCC and Octet structures, exhibiting enhanced specific strength, energy absorption efficiency, and deformation characteristics through strategic structural modifications [491].

Park et al. [290] developed an optimal technique for designing LSs and created a database to identify unit cell topologies. Using linear static FEA, nonlinear FEA, and experimental testing, eleven LSs ($20 \times 20 \times 20$ mm) were evaluated. The best axial compressive strength at the same density was shown by simple cubic, octahedron, truncated cube, and truncated octahedron designs in a $3 \times 3 \times 3$ array. Correlations between unit cell types, lattice topologies, densities, array patterns, and mechanical properties were identified. Yield forces for simple cubic structures at densities of 0.1, 0.2, and 0.3 were 3070 N, 8400 N, and 14,470 N, respectively, with increases of 174% from 0.1 to 0.2 and 371% from 0.1 to 0.3. At a density of 0.1, yield forces for $1 \times 1 \times 1$, $2 \times 2 \times 2$, $3 \times 3 \times 3$, and $4 \times 4 \times 4$ structures were 3070, 3715, 4890, and 4860 N. The yield force of LSs significantly increased with higher density, given the same unit cell type and layout [290].

Mubarak et al. [492] used the sol-gel method to produce silver-adorned TiO2 semiconducting nanoparticles. These nanofillers were incorporated into photo resin to enhance the mechanical and thermal properties of 3D printed products *via* stereolithography. The Ag-TiO2 nanoparticles (Ag-

Table 8. An overview of the methods performed to improve the mechanical behavior of LSs.

Improvement type	Method	Result(s)	Author(s)/Ref
Topology optimization	Multi-material (geometry projection) topology optimization	The method effectively generates multi-material lattices that maximize bulk and shear moduli while minimizing the effective Poisson ratio.	Kazemi et al. [495]
	Genetic algorithm topology optimization	Numerical examples confirmed the accuracy and efficiency of the two-stage topology optimization method, producing diverse, lightweight, and effective LSs.	Feng et al. [496]
	Lightweight design method	Comparisons of LSs made from 316 L stainless steel show that topology-optimized designs outperform most others, validating the use of topology optimization for selecting lattice units.	Xiao et al. [497]
Surface treatments	Chemical–electrochemical surface treatment	A 90% increase in the fatigue strength-to-modulus ratio.	Oosterbeek et al. [498]
	Plasma electrolytic polishing	Comparisons before and after treatment demonstrate that smooth and specular outer surfaces can be achieved.	Wahl et al. [499]
	Chemical post-treatment	There has been a notable reduction in surface defects (which have a negative influence on mechanical behavior) resulting from the manufacturing process.	Soro et al. [500]
Nanomaterials	Silica nanoparticle	The presence of fillers within the matrix has contributed to greater composite rigidity, thereby restricting the movement of polymer molecules and achieving a substantial increase in flexural strength of 16.2963%.	Mohan et al. [501]
Graphene	Coating technique	Increasing GO content, reducing the polymer template's relative density, and decreasing the unit cell size typically result in enhanced mechanical properties of gyroid graphene lattices.	Taher et al. [502]

TNP) were synthesized and characterized through XRD, XPS, Raman, and FESEM, with their morphologies examined using TEM analysis. Incorporating 1.0% w/w Ag-TNP into the SLR (stereolithography resin) matrix led to a 60.8% increase in tensile strength and a 71.8% increase in flexural strength of the SLR/Ag-TNP nanocomposites. Similarly, SLR/Ag-TNP nanocomposites were shown to have greater thermal conductivity and thermal stability, which is equivalent to pristine SLR [492]. Markandan and Lai [493] used stereolithography to create 3D-printed graphene-polymer composite structures and studied their mechanical characteristics. It was demonstrated that the anisotropic mechanical characteristics of the graphene-polymer composite structures produced in this manner could be successfully enhanced by heat treatment, namely, post-print baking, which increased the composite materials' modulus and strength. According to their research's conclusions, graphene-polymer composites produced three-dimensionally using the SLA process have the potential to become a top material for uses needing a high degree of particular stiffness and strength [493].

Geng et al. [494] were interested in investigating the use of biomimetically designed LSs for functional nickel plating to accomplish improved energy absorption, stiffness, and strength properties. The research demonstrates that metal coating significantly enhances the mechanical characteristics and energy absorption capability of micro-lattices. The authors concluded that the composite electroplating enhances the bioinspired hierarchical circular lattice (HCirC) structure's specific strength, stiffness, and energy absorption by 546.9%, 120.7%, and 2113.8%, primarily due to the shell-core structure and biomimetic structural design-based functional nickel plating [494]. Table 8 shows an overview of methods utilized to improve the mechanical behavior of LSs.

3. Future scopes and research gaps

The review highlights several key findings, including the significant improvements in the mechanical properties of cementitious composites with the incorporation of 3D-printed LSs, such as enhanced ductility, reduced weight, and increased energy absorption capacity. The versatility of materials and 3D printing techniques also provides opportunities for tailoring LSs to specific needs, further optimizing the performance of these composites. However, several research gaps remain, particularly the lack of standardized testing protocols to compare results across studies, the need to assess the long-term durability and real-world performance of lattice-reinforced cementitious materials, and challenges in scaling these solutions for large-scale applications. Future research should focus on developing standardized evaluation methods, exploring hybrid materials to enhance mechanical properties, addressing the environmental and sustainability impacts of 3D printing, and transitioning from small-scale studies to practical, large-scale infrastructure applications. Such efforts will open new possibilities for 3D-printed LSs in infrastructure reinforcement, disaster-resilient buildings, and sustainable construction practices, positioning these materials as promising solutions for future civil engineering projects.

4. Summary and conclusions

This paper presents a comprehensive review of current literature on incorporating 3D-printed LSs within cementitious composites and the application of 3D-printed concrete utilizing lattice models. The paper is structured into four sections, each presenting a focused analysis of the relevant topics. A summary of each section and the key conclusions derived are provided below:

1. Section 1 outlines a general introduction of the main topic and the motivation behind the investigation of 3D-printed LSs incorporated into cementitious composites.
2. Section 2 provides a comprehensive categorization of additively manufactured LSs based on various parameters, including 2D versus 3D structures, random

configurations, and cellular designs. It discusses the significance of these structures and their key mechanical characteristics, such as being lightweight, having high specific strength, and effective heat dissipation. Examples of LSs include 2D cellular structures (honeycomb structures [31, 135–143], hierarchical two-dimensional [144–152], and auxetic [153–161], etc.), 3D LSs (plate-structured, shell-structured, truss-structured, and hierarchical-structured elements [178–188]), random structures (triangle-shaped and Voronoi-shaped), and cellular structures (periodic structures). The section also delves into the materials employed in LSs, focusing on polymers (e.g., PEEK, PLA, ABS, TPU, nylon, PC, etc.), concrete, and composites, outlining their mechanical characteristics and 3D printing methods. Additionally, the section discusses the mechanical characteristics of LSs and the main factors influencing these properties, such as:

- Bending-dominated structures are linked with lower relative densities, whereas higher densities are typically linked to stretch-dominated structures [29, 268]. Ling et al. [270] concluded that the mechanical performance of printed octet structures is affected by both the material's inherent properties and the structure's relative density. Structures with greater density showed enhanced compressive and yield strengths [270]. Additionally, another study found that increasing the relative density of structures led to improvements in both Young's modulus and energy absorption capabilities [271].
- Volume fraction is a crucial factor influencing the mechanical characteristics of LSs, including stiffness, strength, and weight. It is concluded that the structure's mechanical characteristics, including compressive modulus and ultimate yield strength, improved as the volume percentage increased [282].
- Design parameters include strut thickness, length, and unit cell geometry, which dictate the mechanical behavior. By mapping the equivalent stress to the strut wall thickness, the optimization of strut design is achieved [289]. Moreover, the variant strut length body-centered cubic lattice structure (BCC LS), including a strut angle of 40°, yields the ultimate specific strain energy absorption and specific stiffness while minimizing weight [291]. Results indicated that the alterations to strut-based LSs, driven by variations in strut orientation and length, significantly influence these structures' mechanical behavior [294].
- Stretch-dominated structures (diagonal LS) tend to have higher stiffness, while bending-dominated (octet LS) structures can be more flexible [266].
- The concept of novel or hybrid LSs is introduced, showcasing designs that combine different lattice types or incorporate advanced materials. Procedures for enhancing the mechanical and physical characteristics of such structures are outlined, including topology Optimization (by creating efficient load-bearing designs). Nanotechnology methods, such as integrating graphene to improve strength and conductivity, and coatings to increase durability and resistance to environmental factors. This section highlights the versatility of LSs for a range of applications, such as in aerospace component designs, medical implants, and structural elements in civil engineering, illustrating their flexibility and performance benefits.

This section also analyses the mechanical properties of 3D-printed LSs as reinforcement in cement-based composites. It highlights how these structures improve mechanical performance and ductility and reduce weight. The section also discusses the use of 3D-printed lattice molds for complex concrete designs and the advantages of 3D printing in optimizing material use while maintaining structural integrity. Key conclusions include:

- LSs and gradation designs have a substantial influence on the bending behavior of cement-based composites [342].
- Raising the PLA reinforcement proportion from 19.2 to 33.7% caused a 38% boost in the average peak load [28].
- 3D-printed lattices play a role in enhancing the compressive strength of cement-based materials and offer a novel approach to increasing their compressive strength [351].
- Reinforcing cementitious composites with 3D-printed LSs altered their failure behavior from brittle to ductile [21].
- Increasing the volume ratios of lattice reinforcement could improve the energy absorption, flexural strength, and ductility of composite beams reinforced with LSs [385].
- Tensile and shear cracks were primarily observed in polymer 3D-printed lattice-reinforced (CBC) samples, demonstrating 3D-PPL's potential to greatly improve CBC's bending performance and offering a novel method for enhancing its structural resilience [386].
- The mechanical characteristics of concrete have been notably improved with the incorporation of a lattice structure, with the rhombicuboctahedron (RO) lattice significantly increasing the maximum load-bearing capacity of concrete samples [22].
- Due to its strain-hardening behavior under uniaxial compression, the ACC shows a much greater energy absorption capacity compared to both conventional cementitious mortar and the polymeric auxetic TPU frame [401].
- The TPMS structure exhibited significantly higher compressive strength than the standard strut-based lattice. The configuration of the 3D-printed mold greatly affects the microstructure of infilled foamed concrete, impacting its compressive strength [418].
- Cubes loaded perpendicular to the 3D-printed layers of cellular lattice concrete structures exhibit significantly higher strength than those loaded parallel to the layers [479].
- When subjected to transverse loading, the 3D-printed concrete TBeam significantly surpasses the LBeam, showing a remarkable increase in peak load and a rise in maximum midpoint displacement, which corresponds to an approximate 500% enhancement in flexural deformation resistance capacity [480].

5. Review and recommendations

The extensive studies reviewed in this document highlight significant advancements in mechanical testing, hybrid innovations, materials, and applications of LSs. Based on these findings, several key recommendations are proposed to further enhance the development and application of AM LSs in cementitious composites:

- Develop standard testing protocols for AM lattice-reinforced cementitious composites to ensure uniformity in compressive strength, flexural resistance, and durability tests.
- Develop benchmark datasets to compare different lattice geometries, reinforcement strategies, and material blends under various loading conditions.
- Study hybrid LSs with bending- and stretch-dominated properties for improved strength, ductility, and energy absorption.
- Further study graded density and functionally graded LSs for better-localized stress distribution and mechanical performance.
- Study nano-reinforcements (e.g., nano-silica, carbon nanotubes) for better bonding efficiency, mechanical properties, and durability.
- Develop adaptive control and real-time monitoring systems to avoid delamination, printing defects, and porosity of AM LSs.
- Improve multi-material LSs of polymers, metals, and composites for certain mechanical and functional properties.
- Improve surface treatments and coatings to improve interface adhesion between cementitious materials and 3D-printed LSs.
- Perform systematic research on fatigue behavior, creep, and cyclic and dynamic loading performance.
- Examine the impact of moisture, freeze-thaw, chemical attack, and thermal cycling on long-term mechanical integrity.
- Test fire resistance, seismic performance, and environmental degradation to meet building safety requirements.
- Integrate machine learning and finite element analysis for failure analysis, stress distribution prediction, and performance optimization.
- Develop AI-driven topology optimization algorithms to optimize LSs for weight savings and enhanced strength.
- Utilize large-scale structural verification through real-world load testing, seismic evaluation, and long-term monitoring.
- Create low-cost and autonomous 3D printing technologies to facilitate prefabricated and modular LS-based construction.
- Create self-healing and self-sensing LSs to improve damage detection, real-time monitoring, and longer service life.
- Conduct lifecycle assessments (LCA) to compare the environmental footprint, recyclability, and potential waste reduction of LS-reinforced cementitious composites.
- Develop biodegradable and recycled materials for green 3D printing and eco-friendly lattice manufacture.
- Efficient lattice material designs engineered to minimize resource utilization while maintaining structural integrity.
- Foster cross-disciplinary collaboration between material scientists, structural engineers, and computational experts to develop LS-reinforced composite technology.
- Encourage pilot projects and commercial partnerships to bridge the gap between academic research and industrial application.
- Initiate cross-disciplinary fusion of digital fabrication, structural engineering, and AI-based design strategies to maximize construction efficiency and material performance.

Through addressing these research requirements, additively manufactured LSs can be optimized for greener, stronger, and more robust applications in digital construction, advanced manufacturing, and civil engineering.

Acknowledgement

The authors gratefully acknowledge the support provided by the Australian Government Research Training Program (RTP) Scholarship.

Author contributions

CRediT: **Hamza El Etri**: Conceptualization, Data curation, Formal analysis, Investigation, Methodology, Resources, Software, Validation, Visualization, Writing – original draft, Writing – review & editing; **Tohid Ghanbari-Ghazijahani**: Conceptualization, Data curation, Formal analysis, Funding acquisition, Investigation, Methodology, Project administration, Resources, Software, Supervision, Validation, Visualization, Writing – original draft, Writing – review & editing; **Rouzbeh Abbassi**: Conceptualization, Funding acquisition, Investigation, Supervision, Writing – original draft, Writing – review & editing; **Erik Schlangen**: Conceptualization, Investigation, Supervision, Writing – original draft, Writing – review & editing.

Disclosure statement

No potential conflict of interest was reported by the author(s).

References

[1] B.K. Nagesha, V. Dhinakaran, M. Varsha Shree, K.P. Manoj Kumar, D. Chalawadi, and T. Sathish, Review on characterization and impacts of the lattice structure in additive manufacturing, Mater. Today Proc., vol. 21, pp. 916–919, 2020. DOI: 10.1016/j.matpr.2019.08.158.

[2] I. Karakurt and L. Lin, 3D printing technologies: techniques, materials, and post-processing, Curr. Opin. Chem. Eng., vol. 28, pp. 134–143, 2020. DOI: 10.1016/j.coche.2020.04.001.

[3] A.A. Elhadad, A. Rosa-Sainz, R. Cañete, E. Peralta, B. Begines, M. Balbuena, A. Alcudia, and Y. Torres, Applications and multidisciplinary perspective on 3D printing techniques: recent developments and future trends, Mater. Sci. Eng. R Rep., vol. 156, pp. 100760, 2023. DOI: 10.1016/j.mser.2023.100760.

[4] D. Srinivasan, M. Meignanamoorthy, M. Ravichandran, V. Mohanavel, S.V. Alagarsamy, C. Chanakyan, S. Sakthivelu, A. Karthick, T.R. Prabhu, and S. Rajkumar, 3D printing manufacturing techniques, materials, and applications: an overview,

Adv. Mater. Sci. Eng., vol. 2021, no. 1, 2021. DOI: 10.1155/2021/5756563.
[5] B. Wittbrodt and J.M. Pearce, The effects of PLA color on material properties of 3-D printed components, Addit. Manuf., vol. 8, pp. 110–116, 2015. DOI: 10.1016/j.addma.2015.09.006.
[6] M. Samykano, S.K. Selvamani, K. Kadirgama, W.K. Ngui, G. Kanagaraj, and K. Sudhakar, Mechanical property of FDM printed ABS: influence of printing parameters, Int. J. Adv. Manuf. Technol., vol. 102, no. 9–12, pp. 2779–2796, 2019. DOI: 10.1007/S00170-019-03313-0/METRICS.
[7] S. Guessasma, S. Belhabib, and H. Nouri, Effect of printing temperature on microstructure, thermal behavior and tensile properties of 3D printed nylon using fused deposition modeling, J. Appl. Polym. Sci., vol. 138, no. 14, pp. 50162, 2021. DOI: 10.1002/app.50162.
[8] B. Wang, Z. Zhang, Z. Pei, J. Qiu, and S. Wang, Current progress on the 3D printing of thermosets, Adv. Compos. Hybrid Mater., vol. 3, no. 4, pp. 462–472, 2020. DOI: 10.1007/S42114-020-00183-Z/FIGURES/9.
[9] K. Kim, J. Park, J-h Suh, M. Kim, Y. Jeong, and I. Park, 3D printing of multiaxial force sensors using carbon nanotube (CNT)/thermoplastic polyurethane (TPU) filaments, Sens. Actuat. A Phys., vol. 263, pp. 493–500, 2017. DOI: 10.1016/j.sna.2017.07.020.
[10] P. Awasthi and S.S. Banerjee, Fused deposition modeling of thermoplastic elastomeric materials: challenges and opportunities, Addit. Manuf., vol. 46, pp. 102177, 2021. DOI: 10.1016/j.addma.2021.102177.
[11] C. Zhang, Y. Li, W. Kang, X. Liu, and Q. Wang, Current advances and future perspectives of additive manufacturing for functional polymeric materials and devices, SusMat., vol. 1, no. 1, pp. 127–147, 2021. DOI: 10.1002/sus2.11.
[12] Y. Lyu, Y. Chen, L. Lin, A.K. Schlarb, Y. Li, and X. Shi, Architecture of covalent bonds between filament layers to enhance performance of 3D printing biodegradable polymer blends, Polym. Test., vol. 106, pp. 107456, 2022. DOI: 10.1016/j.polymertesting.2021.107456.
[13] Z.C. Kennedy and J.F. Christ, Printing polymer blends through in situ active mixing during fused filament fabrication, Addit. Manuf., vol. 36, pp. 101233, 2020. DOI: 10.1016/j.addma.2020.101233.
[14] S.C. Ligon, R. Liska, J. Stampfl, M. Gurr, and R. Mülhaupt, Polymers for 3D printing and customized additive manufacturing, Chem. Rev., vol. 117, no. 15, pp. 10212–10290, 2017. DOI: 10.1021/acs.chemrev.7b00074.
[15] G.P. Borikar, A.R. Patil, and S.B. Kolekar, Additively manufactured lattice structures and materials: present progress and future scope, Korean Soc. Prec. Eng., vol. 24, pp. 2133–2180, 2023. DOI: 10.1007/s12541-023-00848-x.
[16] Y. Li, D. Jiang, R. Zhao, X. Wang, L. Wang, and L.-C. Zhang, High mechanical performance of lattice structures fabricated by additive manufacturing, Met., vol. 14, no. 10, pp. 1165, 2024. DOI: 10.3390/met14101165.
[17] H. Yin, W. Zhang, L. Zhu, F. Meng, J. Liu, and G. Wen, Review on lattice structures for energy absorption properties, Compos. Struct., vol. 304, pp. 116397, 2023. DOI: 10.1016/j.compstruct.2022.116397.
[18] R. Liu, W. Chen, and J. Zhao, A review on factors affecting the mechanical properties of additively-manufactured lattice structures, J. Mater. Eng. Perform., vol. 33, no. 10, pp. 4685–4711, 2024. DOI: 10.1007/s11665-023-08423-1.
[19] C. Pan, Y. Han, and J. Lu, Design and optimization of lattice structures: a review, Appl Sci., vol. 10, no. 18, pp. 6374, 2020. DOI: 10.3390/app10186374.
[20] M.I. Chibinyani, T.C. Dzogbewu, M. Maringa, and A. Muiruri, Lattice structures built with different polygon hollow shapes: a review on their analytical modelling and engineering applications, Appl Sci., vol. 14, no. 4, pp. 1582, 2024. DOI: 10.3390/app14041582.
[21] Y. Xu, H. Zhang, Y. Gan, and B. Šavija, Cementitious composites reinforced with 3D printed functionally graded polymeric lattice structures: experiments and modelling, Addit. Manuf., vol. 39, pp. 101887, 2021. DOI: 10.1016/j.addma.2021.101887.
[22] J. Liu, H. Kanwal, C. Tang, and W. Hao, Study on flexural properties of 3D printed lattice-reinforced concrete structures using acoustic emission and digital image correlation, Constr. Build. Mater., vol. 333, pp. 127418, 2022. DOI: 10.1016/j.conbuildmat.2022.127418.
[23] C. Tang, J. Liu, J. Qiao, Y. Wei, C. Shi, and W. Hao, The preparation and axial compressive properties of 3D-printed polymer lattice-reinforced cementitious composite columns, J. Build. Eng., vol. 97, pp. 110770, 2024., DOI: 10.1016/j.jobe.2024.110770.
[24] Y. Xu, and B. Šavija, Development of strain hardening cementitious composite (SHCC) reinforced with 3D printed polymeric reinforcement: mechanical properties, Compos. Part B Eng., vol. 174, pp. 107011, 2019. DOI: 10.1016/j.compositesb.2019.107011.
[25] Y. Xu, Z. Wan, and B. Šavija, Elevating mechanical performance of cementitious composites with surface-modified 3D-printed polymeric reinforcements, Dev. Built. Environ., vol. 19, pp. 100522, 2024. DOI: 10.1016/j.dibe.2024.100522.
[26] W. Wu, J. Qiao, Y. Wei, W. Hao, and C. Tang, Numerical simulation of compressive mechanical properties of 3D printed lattice-reinforced cement-based composites based on ABAQUS, Materials, vol. 17, no. 10, 2024. DOI: 10.3390/ma17102370.
[27] R. Guamán-Rivera, A. Martínez-Rocamora, R. García-Alvarado, C. Muñoz-Sanguinetti, L.F. González-Böhme, and F. Auat-Cheein, Recent developments and challenges of 3D-printed construction: a review of research fronts, Build., vol. 12, no. 2, pp. 229, 2022. DOI: 10.3390/buildings12020229.
[28] B. Salazar, P. Aghdasi, I.D. Williams, C.P. Ostertag, and H.K. Taylor, Polymer lattice-reinforcement for enhancing ductility of concrete, Mater. Des., vol. 196, pp. 109184, 2020. DOI: 10.1016/j.matdes.2020.109184.
[29] N. Khan and A. Riccio, A systematic review of design for additive manufacturing of aerospace lattice structures: current trends and future directions, Prog. Aerosp. Sci., vol. 149, pp. 101021, 2024. DOI: 10.1016/j.paerosci.2024.101021.'
[30] M. Helou and S. Kara, Design, analysis and manufacturing of lattice structures: an overview, Int. J. Comput. Integr. Manuf., vol. 31, no. 3, pp. 243–261, 2018. DOI: 10.1080/0951192X.2017.1407456.
[31] C.J. Hunt, F. Morabito, C. Grace, Y. Zhao, and B.K.S. Woods, A review of composite lattice structures, Compos. Struct., vol. 284, pp. 115120, 2022. DOI: 10.1016/j.compstruct.2021.115120.
[32] I. Echeta, X. Feng, B. Dutton, R. Leach, and S. Piano, Review of defects in lattice structures manufactured by powder bed fusion, Int. J. Adv. Manuf. Technol., vol. 106, no. 5–6, pp. 2649–2668, 2020. DOI: 10.1007/s00170-019-04753-4.
[33] E.O. Momoh, A. Jayasinghe, M. Hajsadeghi, R. Vinai, K.E. Evans, P. Kripakaran, and J. Orr, A state-of-the-art review on the application of auxetic materials in cementitious composites, Thin-Walled Struct., vol. 196, pp. 111447, 2024. DOI: 10.1016/j.tws.2023.111447.
[34] C.V. Amaechi, E.F. Adefuye, I.M. Kgosiemang, B. Huang, and E.C. Amaechi, Scientometric review for research patterns on additive manufacturing of lattice structures, Materials, vol. 15, no. 15, pp. 5323, 2022. DOI: 10.3390/MA15155323.
[35] T. Maconachie, M. Leary, B. Lozanovski, X. Zhang, M. Qian, O. Faruque, and M. Brandt, SLM lattice structures: properties, performance, applications and challenges, Mater. Des., vol. 183, pp. 108137, 2019. DOI: 10.1016/j.matdes.2019.108137.
[36] A. Kantaros and D. Piromalis, Fabricating lattice structures via 3D printing: the case of porous bio-engineered scaffolds, Appl. Mech. vol. 2, no. 2, pp. 289–302, 2021. DOI: 10.3390/applmech2020018.

[37] M. Majeed, H.M. Khan, G. Wheatley, and R. Situ, Influence of post-processing on additively manufactured lattice structures, J. Braz. Soc. Mech. Sci. Eng., vol. 44, no. 9, pp. 1–28, 2022. DOI: 10.1007/s40430-022-03703-8.

[38] T. DebRoy, H.L. Wei, J.S. Zuback, T. Mukherjee, J.W. Elmer, J.O. Milewski, A.M. Beese, A. Wilson-Heid, A. De, and W. Zhang, Additive manufacturing of metallic components – process, structure and properties, Prog. Mater. Sci., vol. 92, pp. 112–224, 2018. DOI: 10.1016/j.pmatsci.2017.10.001.

[39] S. Amin Yavari, S.M. Ahmadi, J. van der Stok, R. Wauthle, A.C. Riemslag, M. Janssen, J. Schrooten, H. Weinans, and A.A. Zadpoor, Effects of bio-functionalizing surface treatments on the mechanical behavior of open porous titanium biomaterials, J. Mech. Behav. Biomed. Mater., vol. 36, pp. 109–119, 2014. DOI: 10.1016/J.JMBBM.2014.04.010.

[40] M. Askari, D.A. Hutchins, P.J. Thomas, L. Astolfi, R.L. Watson, M. Abdi, M. Ricci, S. Laureti, L. Nie, S. Freear, R. Wildman, C. Tuck, M. Clarke, E. Woods, and A.T. Clare, Additive manufacturing of metamaterials: a review, Addit. Manuf., vol. 36, pp. 101562, 2020. DOI: 10.1016/j.addma.2020.101562.

[41] T.D. Ngo, A. Kashani, G. Imbalzano, K.T.Q. Nguyen, and D. Hui, Additive manufacturing (3D printing): a review of materials, methods, applications and challenges, Compos Part B Eng., vol. 143, pp. 172–196, 2018. DOI: 10.1016/j.compositesb.2018.02.012.

[42] M.K. Thompson, G. Moroni, T. Vaneker, G. Fadel, R.I. Campbell, I. Gibson, A. Bernard, J. Schulz, P. Graf, B. Ahuja, and F. Martina, Design for additive manufacturing: trends, opportunities, considerations, and constraints, CIRP Ann., vol. 65, no. 2, pp. 737–760, 2016. DOI: 10.1016/j.cirp.2016.05.004.

[43] S.D. Nat, and S. Nilufar, An overview of additive manufacturing of polymers and associated composites, Polymers, vol. 12, no. 11, pp. 2719, 2020. DOI: 10.3390/POLYM12112719.

[44] A. Kostadinov, L. Yan, A.Q.A. Teo, and G. O'Neill, Slanted and cluttered: solving deficiencies in SLM-manufactured lattice geometries, Mater. Des., vol. 211, pp. 110130, 2021. DOI: 10.1016/j.matdes.2021.110130.

[45] A. Elkaseer, K.J. Chen, J.C. Janhsen, O. Refle, V. Hagenmeyer, and S.G. Scholz, Material jetting for advanced applications: a state-of-the-art review, gaps and future directions, Addit. Manuf., vol. 60, pp. 103270, 2022. DOI: 10.1016/j.addma.2022.103270.

[46] E. Salcedo, D. Baek, A. Berndt, and J.E. Ryu, Simulation and validation of three dimension functionally graded materials by material jetting, Addit. Manuf., vol. 22, pp. 351–359, 2018. DOI: 10.1016/j.addma.2018.05.027.

[47] M. Dinovitzer, X. Chen, J. Laliberte, X. Huang, and H. Frei, Effect of wire and arc additive manufacturing (WAAM) process parameters on bead geometry and microstructure, Addit. Manuf., vol. 26, pp. 138–146, 2019. DOI: 10.1016/j.addma.2018.12.013.

[48] B. Wu, Z. Pan, D. Ding, D. Cuiuri, H. Li, J. Xu, and J. Norrish, A review of the wire arc additive manufacturing of metals: properties, defects and quality improvement, J Manuf Process., vol. 35, pp. 127–139, 2018. DOI: 10.1016/j.jmapro.2018.08.001.

[49] L. Nobre, D. Barros, J. Bessa, F. Cunha, M. Machado, J.P. Mendonça, J. Luís, M. Oliveira, P. Machado, C. Fernandes, and R. Fangueiro, Enhancing mechanical performance in SLS-printed PA12-slate composites through amino-silane treatment of mineral waste, Int. J. Adv. Manuf. Technol., vol. 134, no. 5-6, pp. 2979–2992, 2024. DOI: 10.1007/S00170-024-13989-8/TABLES/3.

[50] S. Singh, D. Kaur, M. Singh, R. Balu, A. Mehta, and H. Vasudev, Challenges and issues in manufacturing of components using polymer-based selective laser sintering (SLS): a review, Int. J. Interact. Des. Manuf., vol. 2024, pp. 1–24, 2024. DOI: 10.1007/s12008-024-02049-w.

[51] X. Xu, P. Robles-Martinez, C.M. Madla, F. Joubert, A. Goyanes, A.W. Basit, and S. Gaisford, Stereolithography (SLA) 3D printing of an antihypertensive polyprintlet: case study of an unexpected photopolymer-drug reaction, Addit. Manuf., vol. 33, pp. 101071, 2020. DOI: 10.1016/j.addma.2020.101071.

[52] J. Wang, A. Goyanes, S. Gaisford, and A.W. Basit, Stereolithographic (SLA) 3D printing of oral modified-release dosage forms, Int. J. Pharm., vol. 503, no. 1–2, pp. 207–212, 2016. DOI: 10.1016/J.IJPHARM.2016.03.016.

[53] D. Xuan Luong, A.K. Subramanian, G.A. Lopez Silva, et al., Laminated object manufacturing of 3D-printed laser-induced graphene foams, Adv Mater., vol. 30, pp. 1707416, 2018. DOI: 10.1002/ADMA.201707416.

[54] B. Dermeik and N. Travitzky, Laminated object manufacturing of ceramic-based materials, Adv. Eng. Mater., vol. 22, no. 9, pp. 2000256, 2020. DOI: 10.1002/adem.202000256.

[55] A. Menghini, S. Maffia, A.G. Demir, A. Kanyilmaz, F. Berto, C.A. Castiglioni, and B. Previtali, Performance of laser metal deposition on hot-rolled stainless steel for hybrid steel structures, Constr. Build. Mater., vol. 443, pp. 137744, 2024. DOI: 10.1016/j.conbuildmat.2024.137744.

[56] A. Hatem, C. Schulz, T. Schlaefer, J.T. Boobhun, N. Stanford, and C. Hall, Influence of laser absorption by water- and gas-atomised powder feedstock on laser metal deposition of AISI 431 stainless steel, Addit. Manuf., vol. 47, pp. 102242, 2021. DOI: 10.1016/j.addma.2021.102242.

[57] Y. Li, Q. Mao, J. Yin, Y. Wang, J. Fu, and Y. Huang, Theoretical prediction and experimental validation of the digital light processing (DLP) working curve for photocurable materials, Addit. Manuf., vol. 37, pp. 101716, 2021. DOI: 10.1016/j.addma.2020.101716.

[58] R. Chaudhary, P. Fabbri, E. Leoni, F. Mazzanti, R. Akbari, and C. Antonini, Additive manufacturing by digital light processing: a review, Prog. Addit. Manuf., vol. 8, no. 2, pp. 331–351, 2023. DOI: 10.1007/s40964-022-00336-0.

[59] K.N. Kalashnikov, V.E. Rubtsov, N.L. Savchenko, T.A. Kalashnikova, K.S. Osipovich, A.A. Eliseev, and A.V. Chumaevskii, The effect of wire feed geometry on electron beam freeform 3D printing of complex-shaped samples from Ti-6Al-4V alloy, Int. J. Adv. Manuf. Technol., vol. 105, no. 7–8, pp. 3147–3156, 2019. DOI: 10.1007/S00170-019-04589-Y/TABLES/3.

[60] J. Xu, J. Zhu, J. Fan, Q. Zhou, Y. Peng, and S. Guo, Microstructure and mechanical properties of Ti–6Al–4V alloy fabricated using electron beam freeform fabrication, Vacuum., vol. 167, pp. 364–373, 2019. DOI: 10.1016/j.vacuum.2019.06.030.

[61] J.K. Algardh, T. Horn, H. West, R. Aman, A. Snis, H. Engqvist, J. Lausmaa, and O. Harrysson, Thickness dependency of mechanical properties for thin-walled titanium parts manufactured by Electron Beam Melting (EBM)®, Addit. Manuf., vol. 12, pp. 45–50, 2016. DOI: 10.1016/j.addma.2016.06.009.

[62] M.A.S.R. Saadi, A. Maguire, N.T. Pottackal, M.S.H. Thakur, M.M. Ikram, A.J. Hart, P.M. Ajayan, and M.M. Rahman, Direct ink writing: a 3D printing technology for diverse materials, Adv. Mater., vol. 34, no. 28, pp. 2108855, 2022. DOI: 10.1002/adma.202108855.

[63] J. Yan, S. Huang, Y.V. Lim, T. Xu, D. Kong, X. Li, H.Y. Yang, and Y. Wang, Direct-ink writing 3D printed energy storage devices: from material selectivity, design and optimization strategies to diverse applications, Mater. Today., vol. 54, pp. 110–152, 2022. DOI: 10.1016/j.mattod.2022.03.014.

[64] M. Heidari-Rarani, M. Rafiee-Afarani, and A.M. Zahedi, MR-A-CPB, U Mechanical characterization of FDM 3D printing of continuous carbon fiber reinforced PLA composites, Composites Part B Eng., vol. 175, pp. 107147, 2019. DOI: 10.1016/j.compositesb.2019.107147.

[65] S. Garzon-Hernandez, D. Garcia-Gonzalez, A. Jérusalem, and A. Arias, Design of FDM 3D printed polymers: an

experimental-modelling methodology for the prediction of mechanical properties, Mater. Des., vol. 188, pp. 108414, 2020. DOI: 10.1016/j.matdes.2019.108414.

[66] M. Khorasani, E. MacDonald, D. Downing, A. Ghasemi, M. Leary, J. Dash, E. Sharabian, A. Almalki, M. Brandt, and S. Bateman, Multi jet fusion (MJF) of polymeric components: a review of process, properties and opportunities, Addit. Manuf., vol. 91, pp. 104331, 2024. DOI: 10.1016/j.addma.2024.104331.

[67] X. Liu, W.S. Tey, J.Y.C. Choo, J. Chen, P. Tan, C. Cai, A. Ong, L. Zhao, and K. Zhou, Enhancing the mechanical strength of multi jet fusion–printed polyamide 12 and its glass fiber-reinforced composite via high-temperature annealing, Addit. Manuf., vol. 46, pp. 102205, 2021. DOI: 10.1016/j.addma.2021.102205.

[68] S.Y. Chin, V. Dikshit, B.M. Priyadarshini, and Y. Zhang, Powder-based 3D printing for the fabrication of device with micro and mesoscale features, Micromachines, vol. 11, no. 7, pp. 658, 2020. DOI: 10.3390/MI11070658.

[69] L.E. dos Santos Paes, M. Pereira, F.A. Xavier, W.L. Weingaertner, A.S.C.M. D'Oliveira, E.C. Costa, L.O. Vilarinho, and A. Scotti, Understanding the behavior of laser surface remelting after directed energy deposition additive manufacturing through comparing the use of iron and Inconel powders, J Manuf Process., vol. 70, pp. 494–507, 2021. DOI: 10.1016/j.jmapro.2021.08.061.

[70] F. Liravi, and M. Vlasea, Powder bed binder jetting additive manufacturing of silicone structures, Addit. Manuf., vol. 21, pp. 112–124, 2018. DOI: 10.1016/j.addma.2018.02.017.

[71] S.-Y. Chun, T. Kim, B. Ye, B. Jeong, M-j Lee, D.H. Lee, E.-S. Kim, H. Lee, and H.-D. Kim, Capillary pressure and saturation of pore-controlled granules for powder bed binder jetting, Appl. Surf. Sci., vol. 515, pp. 145979, 2020. DOI: 10.1016/j.apsusc.2020.145979.

[72] S. Aghajani, C. Wu, Q. Li, and J. Fang, Additively manufactured composite lattices: a state-of-the-art review on fabrications, architectures, constituent materials, mechanical properties, and future directions, Thin-Walled Struct., vol. 197, pp. 111539, 2024. DOI: 10.1016/j.tws.2023.111539.

[73] H. Dommati, S.S. Ray, J.C. Wang, and S.S. Chen, A comprehensive review of recent developments in 3D printing technique for ceramic membrane fabrication for water purification, RSC Adv., vol. 9, no. 29, pp. 16869–16883, 2019. DOI: 10.1039/C9RA00872A.

[74] A. Kafle, E. Luis, R. Silwal, H.M. Pan, P.L. Shrestha, and A.K. Bastola, 3D/4D printing of polymers: fused deposition modelling (FDM), selective laser sintering (SLS), and stereolithography (SLA), Polymers, vol. 13, no. 18, pp. 3101, 2021. DOI: 10.3390/POLYM13183101.

[75] K.R. Hossain, P. Jiang, X. Yao, X. Yang, D. Hu, and X. Wang, Ionic liquids for 3D printing: fabrication, properties, applications, J Ion Liq., vol. 3, no. 2, pp. 100066, 2023. DOI: 10.1016/j.jil.2023.100066.

[76] X. Wang, M. Jiang, Z. Zhou, J. Gou, and D. Hui, 3D printing of polymer matrix composites: a review and prospective, Compos Part B Eng., vol. 110, pp. 442–458, 2017. DOI: 10.1016/j.compositesb.2016.11.034.

[77] A. Raina, M.I.U. Haq, M. Javaid, S. Rab, and A. Haleem, 4D printing for automotive industry applications, J. Inst. Eng. India. Ser. D., vol. 102, no. 2, pp. 521–529, 2021. DOI: 10.1007/S40033-021-00284-Z/TABLES/1.

[78] O.A. Mohamed, S.H. Masood, and J.L. Bhowmik, Optimization of fused deposition modeling process parameters: a review of current research and future prospects, Adv. Manuf., vol. 3, no. 1, pp. 42–53, 2015. DOI: 10.1007/S40436-014-0097-7/TABLES/2.

[79] A. Jandyal, I. Chaturvedi, I. Wazir, A. Raina, and M.I. Ul Haq, 3D printing – A review of processes, materials and applications in industry 4.0, Sustain Oper Comput., vol. 3, pp. 33–42, 2022. DOI: 10.1016/j.susoc.2021.09.004.

[80] D. Li, Y. Li, D. Wu, Z. Xu, and D. Guo, Investigation on compression properties of perforated face-centered-cubic plate-lattice structures, Mech. Adv. Mater. Struct., vol. 0, pp. 1–16, 2025. DOI: 10.1080/15376494.2024.2447055.

[81] B.M. Tymrak, M. Kreiger, and J.M. Pearce, Mechanical properties of components fabricated with open-source 3-D printers under realistic environmental conditions, Mater. Des., vol. 58, pp. 242–246, 2014. DOI: 10.1016/j.matdes.2014.02.038.

[82] P. Tran, T.D. Ngo, A. Ghazlan, and D. Hui, Bimaterial 3D printing and numerical analysis of bio-inspired composite structures under in-plane and transverse loadings, Compos Part B Eng., vol. 108, pp. 210–223, 2017. DOI: 10.1016/j.compositesb.2016.09.083.

[83] H. Peng, B. Han, T. Tong, et al., 3D printing of textile-based structures by Fused Deposition Modelling (FDM) with different polymer materials. IOP Conf. Ser. Mater. Sci. Eng., DOI: 10.1088/1757-899X/62/1/012018.

[84] C.R. Garcia, J. Correa, D. Espalin, J.H. Barton, R.C. Rumpf, R. Wicker, and V. Gonzalez, 3D printing of anisotropic metamaterials, PIER. Letters., vol. 34, pp. 75–82, 2012. DOI: 10.2528/PIERL12070311.

[85] B. Caulfield, P.E. McHugh, and S. Lohfeld, Dependence of mechanical properties of polyamide components on build parameters in the SLS process, J. Mater. Process. Technol., vol. 182, no. 1–3, pp. 477–488, 2007. DOI: 10.1016/j.jmatprotec.2006.09.007.

[86] Q. Sun, G.M. Rizvi, C.T. Bellehumeur, and P. Gu, Effect of processing conditions on the bonding quality of FDM polymer filaments, Rapid Prototyp J., vol. 14, no. 2, pp. 72–80, 2008. DOI: 10.1108/13552540810862028/FULL/PDF.

[87] M. Ateeq, M. Shafique, A. Azam, and M. Rafiq, A review of 3D printing of the recycled carbon fiber reinforced polymer composites: processing, potential, and perspectives, J. Mater. Res. Technol., vol. 26, pp. 2291–2309, 2023. DOI: 10.1016/j.jmrt.2023.07.171.

[88] O. Sai Saran, A. Prudhvidhar Reddy, L. Chaturya, and M. Pavan Kumar, 3D printing of composite materials: a short review, Mater Today Proc., vol. 64, pp. 615–619, 2022. DOI: 10.1016/j.matpr.2022.05.144.

[89] X. Han, D. Yang, C. Yang, S. Spintzyk, L. Scheideler, P. Li, D. Li, J. Geis-Gerstorfer, and F. Rupp, Carbon fiber reinforced PEEK composites based on 3d-printing technology for orthopedic and dental applications, J. Clin. Med., vol. 8, no. 2, pp. 240, 2019. DOI: 10.3390/JCM8020240.

[90] C.M. Shemelya, A. Rivera, A.T. Perez, C. Rocha, M. Liang, X. Yu, C. Kief, D. Alexander, J. Stegeman, H. Xin, R.B. Wicker, E. MacDonald, and D.A. Roberson, Mechanical, electromagnetic, and X-ray shielding characterization of a 3d printable tungsten–polycarbonate polymer matrix composite for space-based applications, J. Elec. Mater., vol. 44, no. 8, pp. 2598–2607, 2015. DOI: 10.1007/S11664-015-3687-7/METRICS.

[91] S.C. Joshi and A.A. Sheikh, 3D printing in aerospace and its long-term sustainability, Virtual Phys. Prototyp., vol. 10, no. 4, pp. 175–185, 2015. DOI: 10.1080/17452759.2015.1111519.

[92] A. Uriondo, M. Esperon-Miguez, and S. Perinpanayagam, The present and future of additive manufacturing in the aerospace sector: a review of important aspects, Proc Inst Mech Eng Part G J Aerosp Eng., vol. 229, no. 11, pp. 2132–2147, 2015. DOI: 10.1177/0954410014568797.

[93] C. Dong, M. Petrovic, and I.J. Davies, Applications of 3D printing in medicine: a review, Ann 3D Print Med., vol. 14, pp. 100149, 2024. DOI: 10.1016/j.stlm.2024.100149.

[94] S.L. Sing, J. An, W.Y. Yeong, and F.E. Wiria, Laser and electron-beam powder-bed additive manufacturing of metallic implants: a review on processes, materials and designs, J. Orthop. Res., vol. 34, no. 3, pp. 369–385, 2016. DOI: 10.1002/JOR.23075.

[95] M.K. Włodarczyk-Biegun, and A. del Campo, 3D bioprinting of structural proteins, Biomaterials, vol. 134, pp. 180–201, 2017. DOI: 10.1016/J.BIOMATERIALS.2017.04.019.

[96] S.V. Murphy and A. Atala, 3D bioprinting of tissues and organs, Nat. Biotechnol., vol. 32, no. 8, pp. 773–785, 2014. DOI: 10.1038/NBT.2958.

[97] F.P.W. Melchels, M.A.N. Domingos, T.J. Klein, J. Malda, P.J. Bartolo, and D.W. Hutmacher, Additive manufacturing of tissues and organs, Prog. Polym. Sci., vol. 37, no. 8, pp. 1079–1104, 2012. DOI: 10.1016/j.progpolymsci.2011.11.007.

[98] S. Bauer, P. Schmuki, K. von der Mark, and J. Park, Engineering biocompatible implant surfaces: part I: materials and surfaces, Prog. Mater. Sci., vol. 58, no. 3, pp. 261–326, 2013. DOI: 10.1016/j.pmatsci.2012.09.001.

[99] M. Geetha, A.K. Singh, R. Asokamani, and A.K. Gogia, Ti based biomaterials, the ultimate choice for orthopaedic implants – a review, Prog. Mater. Sci., vol. 54, no. 3, pp. 397–425, 2009. DOI: 10.1016/j.pmatsci.2008.06.004.

[100] E.S. Bishop, S. Mostafa, M. Pakvasa, H.H. Luu, M.J. Lee, J.M. Wolf, G.A. Ameer, T.-C. He, and R.R. Reid, 3-D bioprinting technologies in tissue engineering and regenerative medicine: current and future trends, Genes Dis., vol. 4, no. 4, pp. 185–195, 2017. DOI: 10.1016/J.GENDIS.2017.10.002.

[101] P. Wu, J. Wang, and X. Wang, A critical review of the use of 3-D printing in the construction industry, Autom. Constr., vol. 68, pp. 21–31, 2016. DOI: 10.1016/j.autcon.2016.04.005.

[102] A. Siddika, M.A.A. Mamun, W. Ferdous, A.K. Saha, and R. Alyousef, 3D-printed concrete: applications, performance, and challenges, J Sustain Cem Mater., vol. 9, no. 3, pp. 127–164, 2020. DOI: 10.1080/21650373.2019.1705199.

[103] I. Hager, A. Golonka, and R. Putanowicz, 3D printing of buildings and building components as the future of sustainable construction?, Procedia Eng., vol. 151, pp. 292–299, 2016. DOI: 10.1016/J.PROENG.2016.7.357.

[104] L.Y. Chen, S.X. Liang, Y. Liu, and L.C. Zhang, Additive manufacturing of metallic lattice structures: unconstrained design, accurate fabrication, fascinated performances, and challenges, Mater Sci Eng R Rep., vol. 146, pp. 100648, 2021. DOI: 10.1016/j.mser.2021.100648.

[105] S.H. Gompana, and R. Koona, Study of adaptive multi-scale optimization of lattice structures : A novel framework for engineering applications, Mech. Adv. Mater. Struct., vol. 0, pp. 1–18, 2025. DOI: 10.1080/15376494.2025.2463695.

[106] F. Zhu, G. Lu, D. Ruan, and Z. Wang, Plastic deformation, failure and energy absorption of sandwich structures with metallic cellular cores, Int J Prot Struct., vol. 1, no. 4, pp. 507–541, 2010. DOI: 10.1260/2041-4196.1.4.507.

[107] M. Al Khalil, N. Lebaal, F. Demoly, and S. Roth, Bio-inspired-based structures optimization for additive manufacturing using metaheuristic Kriging, Mech. Adv. Mater. Struct., vol. 31, no. 21, pp. 5290–5299, 2024. DOI: 10.1080/15376494.2023.2214915.

[108] C. Yan, L. Hao, A. Hussein, S.L. Bubb, P. Young, and D. Raymont, Evaluation of light-weight AlSi10Mg periodic cellular lattice structures fabricated via direct metal laser sintering, J Mater Process Technol 2014•Elsevier., vol. 214, no. 4, pp. 856–864, 2014. DOI: 10.1016/j.jmatprotec.2013.12.004.

[109] R. Ashby, The properties of foams and lattices, Philosophical Trans R Soc A., vol. 364, pp. 15–30, 2006. DOI: 10.1098/rsta.2005.1678.

[110] L.J. Gibson. Undefined modelling the mechanical behavior of cellular materials, Materials Sci Eng A, vol. 110, pp. 1–36, 1989.

[111] G. Kooistra, V. Deshpande, and H.W.-A. Materialia, Compressive behavior of age hardenable tetrahedral lattice truss structures made from aluminium, Acta Mater., vol. 52, pp. 4229–4237, 2004.

[112] D. Queheillalt, Y. Murty, and H.W.-S. Materialia, Mechanical properties of an extruded pyramidal lattice truss sandwich structure, Scripta Mater, vol. 58, no. 1, pp. 76–79, 2008.

[113] H. Fan, F. Sun, L. Yang, F. Jin, and D. Zhao, Interlocked hierarchical lattice materials reinforced by woven textile sandwich composites, Composit. Sci. Technol., vol. 87, pp. 142–148, 2013. DOI: 10.1016/j.compscitech.2013.07.028.

[114] H.-L. Fan, T. Zeng, D.-N. Fang, and W. Yang, Mechanics of advanced fiber reinforced lattice composites, Acta Mech. Sin., vol. 26, no. 6, pp. 825–835, 2010. DOI: 10.1007/s10409-010-0390-z.

[115] W. Li, F. Sun, P. Wang, H. Fan, and D. Fang, A novel carbon fiber reinforced lattice truss sandwich cylinder: fabrication and experiments, Compos. Part A Appl. Sci. Manuf. vol. 81, pp. 313–322, 2016. DOI: 10.1016/j.compositesa.2015.11.034.

[116] H. Fan, F. Meng, and W.Y.-C. Structures, U sandwich panels with Kagome lattice cores reinforced by carbon fibers, Composite Struct., vol. 81, no. 4, pp. 533–539, 2007. DOI: 10.1016/j.compstruct.2006.09.011.

[117] R.G. Silva, C.S. Estay, G.M. Pavez, et al., Influence of geometric and manufacturing parameters on the compressive behavior of 3D printed polymer lattice structures, Mater., vol. 14, pp. 1462, 2021. DOI: 10.3390/MA14061462.

[118] G. Dong, Y. Tang, and Y.F. Zhao, A survey of modeling of lattice structures fabricated by additive manufacturing, J Mech Des., vol. 139, no. 10, 2017. DOI: 10.1115/1.4037305/367020.

[119] C. Tang, J. Liu, Y. Yang, Y. Liu, S. Jiang, and W. Hao, Effect of process parameters on mechanical properties of 3D printed PLA lattice structures, Compos Part C Open Access., vol. 3, pp. 100076, 2020. DOI: 10.1016/j.jcomc.2020.100076.

[120] J. León-Becerra, O.A. González-Estrada, and J. Quiroga, Effect of relative density in in-plane mechanical properties of common 3D-printed polylactic acid lattice structures, ACS Omega., vol. 6, no. 44, pp. 29830–29838, 2021. DOI: 10.1021/ACSOMEGA.1C04295/ASSET/IMAGES/LARGE/AO1C04295_0013.JPEG.

[121] R. Guerra Silva, C. Salinas Estay, G. Morales Pavez, M.J. Torres, and J. Zahr Viñuela, Assessment of analytical relationships for mechanical properties of truncated octahedron and diamond lattice structures, Mater. Today Commun., vol. 29, pp. 102756, 2021. DOI: 10.1016/j.mtcomm.2021.102756.

[122] D.W. Abueidda, M. Elhebeary, C.-S.(. Shiang, S. Pang, R.K. Abu Al-Rub, and I.M. Jasiuk, Mechanical properties of 3D printed polymeric Gyroid cellular structures: experimental and finite element study, Mater. Des., vol. 165, pp. 107597, 2019. DOI: 10.1016/j.matdes.2019.107597.

[123] N. Ahmed, I. Barsoum, and R.K. Abu Al-Rub, Numerical investigation on the effect of residual stresses on the effective mechanical properties of 3D-printed TPMS lattices, Met., vol. 12, no. 8, pp. 1344, 2022. DOI: 10.3390/met12081344.

[124] S. Ma, Q. Tang, Y. Liu, and Q. Feng, Prediction of mechanical properties of three-dimensional printed lattice structures through machine learning, J. Comput. Inf. Sci. Eng., vol. 22, no. 3, pp. 031008, 2022. DOI: 10.1115/1.4053077/1128853.

[125] S. Lee, Z. Zhang, and G.X. Gu, Generative machine learning algorithm for lattice structures with superior mechanical properties, Mater. Horiz., vol. 9, no. 3, pp. 952–960, 2022. DOI: 10.1039/D1MH01792F.

[126] B.V. Siva Reddy, A.M. Shaik, C.C. Sastry, J. Krishnaiah, C.A. Bhise, and B. Ramakrishna, Machine learning approaches for predicting mechanical properties in additive manufactured lattice structures, Mater. Today Commun., vol. 40, pp. 109937, 2024. DOI: 10.1016/j.mtcomm.2024.109937.

[127] M. Ali, U. Sajjad, I. Hussain, N. Abbas, H.M. Ali, W.-M. Yan, and C.-C. Wang, On the assessment of the mechanical properties of additively manufactured lattice structures, Eng Anal Bound Elem., vol. 142, pp. 93–116, 2022. DOI: 10.1016/j.enganabound.2022.05.019.

[128] M. Carraturo, G. Alaimo, S. Marconi, E. Negrello, E. Sgambitterra, C. Maletta, A. Reali, and F. Auricchio, Experimental and numerical evaluation of mechanical properties of 3D-printed stainless steel 316L lattice structures, J. Mater. Eng. Perform., vol. 30, no. 7, pp. 5247–5251, 2021. DOI: 10.1007/S11665-021-05737-W/FIGURES/6.

[129] X. Cao, S. Duan, J. Liang, W. Wen, and D. Fang, Mechanical properties of an improved 3D-printed rhombic dodecahedron stainless steel lattice structure of variable cross section, Int. J. Mech. Sci., vol. 145, pp. 53–63, 2018. DOI: 10.1016/j.ijmecsci.2018.07.006.

[130] B. Hanks, J. Berthel, M. Frecker, and T.W. Simpson, Mechanical properties of additively manufactured metal lattice structures: data review and design interface, Addit. Manuf., vol. 35, pp. 101301, 2020. DOI: 10.1016/j.addma.2020.101301.

[131] A. Ruzanna Aziz, J. Zhou, D. Thorne, et al., Geometrical scaling effects in the mechanical properties of 3D-printed body-centered cubic (BCC) lattice structures, Polym., vol. 13, pp. 3967, 2021. DOI: 10.3390/POLYM13223967.

[132] F. Teng, Y. Sun, S. Guo, B. Gao, and G. Yu, Topological and mechanical properties of different lattice structures based on additive manufacturing, Micromachines., vol. 13, no. 7, pp. 1017, 2022. DOI: 10.3390/MI13071017.

[133] M. Sadeghzade, H. Gharehbaghi, and A. Farrokhabadi, Experimental and analytical studies of mechanical properties of additively manufactured lattice structure based on octagonal bipyramid cubic unit cell, Addit. Manuf., vol. 48, pp. 102403, 2021. DOI: 10.1016/j.addma.2021.102403.

[134] B. Panda, M. Leite, B.B. Biswal, X. Niu, and A. Garg, Experimental and numerical modelling of mechanical properties of 3D printed honeycomb structures, Measurement., vol. 116, pp. 495–506, 2018. DOI: 10.1016/j.measurement.2017.11.037.

[135] Q. Zhang, X. Yang, P. Li, G. Huang, S. Feng, C. Shen, B. Han, X. Zhang, F. Jin, F. Xu, and T.J. Lu, Bioinspired engineering of honeycomb structure – using nature to inspire human innovation, Prog. Mater. Sci., vol. 74, pp. 332–400, 2015. DOI: 10.1016/j.pmatsci.2015.05.001.

[136] Z. Wang, Recent advances in novel metallic honeycomb structure, Compos. Part B Eng., vol. 166, pp. 731–741, 2019. DOI: 10.1016/j.compositesb.2019.02.011.

[137] C. Qi, F. Jiang, and S. Yang, Advanced honeycomb designs for improving mechanical properties: a review, Compos. Part B Eng., vol. 227, pp. 109393, 2021. DOI: 10.1016/j.compositesb.2021.109393.

[138] T. Thomas and G. Tiwari, Crushing behavior of honeycomb structure: a review, Int. J. Crashworthiness., vol. 24, no. 5, pp. 555–579, 2019. DOI: 10.1080/13588265.2018.1480471.

[139] E. Montgomery-Liljeroth, S. Schievano, and G. Burriesci, Elastic properties of 2D auxetic honeycomb structures- a review, Appl. Mater. Today., vol. 30, pp. 101722, 2023. DOI: 10.1016/j.apmt.2022.101722.

[140] W. Tao and M.C. Leu, Design of lattice structure for additive manufacturing, International Symposium on Flexible Automation (ISFA), Cleveland, OH, USA, pp. 325–332, 2016. DOI: 10.1109/ISFA.2016.7790182.

[141] M. Sajjad and W. Lu, Honeycomb-based heterostructures: an emerging platform for advanced energy applications: A review on energy systems, Electrochem Sci Adv., vol. 2, pp. e202100075, 2022. DOI: 10.1002/ELSA.202100075.

[142] M.-Y. Ma, D. Han, N.-K. Chen, D. Wang, and X.-B. Li, Recent progress in double-layer honeycomb structure: a new type of two-dimensional material, Materials., vol. 15, no. 21, pp. 7715, 2022. DOI: 10.3390/MA15217715.

[143] M.W. Chuan, K.L. Wong, A. Hamzah, S. Rusli, N.E. Alias, C.S. Lim, and M.L.P. Tan, 2D honeycomb silicon: a review on theoretical advances for silicone field-effect transistors, CNANO., vol. 16, no. 4, pp. 595–607, 2020. DOI: 10.2174/1573413715666190709120019.

[144] X. Zhao, R.R. Liang, S.Y. Jiang, and A. Ru-Han, Two-dimensional covalent organic frameworks with hierarchical porosity, Chem. Soc. Rev., vol. 49, no. 12, pp. 3920–3951, 2020. DOI: 10.1039/D0CS00049C.

[145] N. Vogel, M. Retsch, C.-A. Fustin, A. Del Campo, and U. Jonas, advances in colloidal assembly: the design of structure and hierarchy in two and three dimensions, Chem. Rev., vol. 115, no. 13, pp. 6265–6311, 2015., DOI: 10.1021/CR400081D/ASSET/CR400081D.FP.PNG_V03.

[146] J.-E. Kim, J.-H. Oh, M. Kotal, N. Koratkar, and I.-K. Oh, Self-assembly and morphological control of three-dimensional macroporous architectures built of two-dimensional materials, Nano Today., vol. 14, pp. 100–123, 2017. DOI: 10.1016/j.nantod.2017.04.008.

[147] Z. Wang, Z. Lei, Z. Li, K. Yuan, and X. Wang, Mechanical reinforcement mechanism of a hierarchical Kagome honeycomb, Thin-Walled Struct., vol. 167, pp. 108235, 2021. DOI: 10.1016/j.tws.2021.108235.

[148] Y. Tao, W. Li, K. Wei, S. Duan, W. Wen, L. Chen, Y. Pei, and D. Fang, Mechanical properties and energy absorption of 3D printed square hierarchical honeycombs under in-plane axial compression, Compos. Part B Eng. vol. 176, pp. 107219, 2019. DOI: 10.1016/j.compositesb.2019.107219.

[149] H. Yin, X. Huang, F. Scarpa, G. Wen, Y. Chen, and C. Zhang, In-plane crashworthiness of bio-inspired hierarchical honeycombs, Compos Struct. vol. 192, pp. 516–527, 2018. DOI: 10.1016/j.compstruct.2018.03.050.

[150] Q. He, J. Feng, and H. Zhou, A numerical study on the in-plane dynamic crushing of self-similar hierarchical honeycombs, Mech. Mater., vol. 138, pp. 103151, 2019. DOI: 10.1016/j.mechmat.2019.103151.

[151] W. Zhang, S. Yin, T.X. Yu, and J. Xu, Crushing resistance and energy absorption of pomelo peel inspired hierarchical honeycomb, Int. J. Impact Eng., vol. 125, pp. 163–172, 2019. DOI: 10.1016/j.ijimpeng.2018.11.014.

[152] F. Sun, C. Lai, H. Fan, and D. Fang, Crushing mechanism of hierarchical lattice structure, Mech Mater., vol. 97, pp. 164–183, 2016. DOI: 10.1016/j.mechmat.2016.02.016.

[153] R. Peng, Y. Ma, Q. Wu, B. Huang, and Y. Dai, Two-dimensional materials with intrinsic auxeticity: progress and perspectives, Nanoscale., vol. 11, no. 24, pp. 11413–11428, 2019. DOI: 10.1039/C9NR03546J.

[154] X. Ren, R. Das, P. Tran, T.D. Ngo, and Y.M. Xie, Auxetic metamaterials and structures: a review, Smart Mater. Struct., vol. 27, no. 2, pp. 023001, 2018. DOI: 10.1088/1361-665X/aaa61c.

[155] L. Cabras and M. Brun, Auxetic two-dimensional lattices with Poisson's ratio arbitrarily close to −1, Proc. R Soc. A., vol. 470, no. 2172, pp. 20140538, 2014. DOI: 10.1098/rspa.2014.0538.

[156] Y. Suzuki, G. Cardone, D. Restrepo, P.D. Zavattieri, T.S. Baker, and F.A. Tezcan, Self-assembly of coherently dynamic, auxetic, two-dimensional protein crystals, Nat., vol. 533, no. 7603, pp. 369–373, 2016. DOI: 10.1038/nature17633.

[157] Y. Xue, P. Gao, L. Zhou, and F. Han, An enhanced three-dimensional auxetic lattice structure with improved property, Materials, vol. 13, no. 4, pp. 1008, 2020. DOI: 10.3390/MA13041008.

[158] S.N. Orhan, and Ş. Erden, Numerical investigation of the mechanical properties of 2D and 3D auxetic structures, Smart Mater. Struct., vol. 31, no. 6, pp. 065011, 2022. DOI: 10.1088/1361-665X/ac6918.]

[159] L.-C. Zhang, G. Qin, W.-Z. Fang, H.-J. Cui, Q.-R. Zheng, Q.-B. Yan, and G. Su, Tinselenidene: a two-dimensional auxetic material with ultralow lattice thermal conductivity and ultrahigh hole mobility, Sci. Rep., vol. 6, pp. 19830, 2016. DOI: 10.1038/srep19830.

[160] M. Bruggi and A. Corigliano, Optimal 2D auxetic microstructures with band gap, Meccanica., vol. 54, no. 13, pp. 2001–2027, 2019. DOI: 10.1007/S11012-019-00981-W/TABLES/4.

[161] P. Suttakul and T. Fongsamootr, Numerical study on bending response of auxetic 2D-lattice plates, IOP Conf. Ser. Mater. Sci. Eng., vol. 1137, no. 1, pp. 012025, 2021. DOI: 10.1088/1757-899X/1137/1/012025.

[162] Y. Wu and L. Yang, The effect of unit cell size and topology on tensile failure behavior of 2D lattice structures, Int. J.

Mech. Sci., vol. 170, pp. 105342, 2020. DOI: 10.1016/j.ijmecsci.2019.105342.
[163] Y. Gao, X. Wei, X. Han, Z. Zhou, and J. Xiong, Novel 3D auxetic lattice structures developed based on the rotating rigid mechanism, Int. J. Solids Struct., vol. 233, pp. 111232, 2021. DOI: 10.1016/j.ijsolstr.2021.111232.
[164] N.K. Choudhry, B. Panda, and S. Kumar, Enhanced energy absorption performance of 3D printed 2D auxetic lattices, Thin-Walled Struct., vol. 186, pp. 110650, 2023. DOI: 10.1016/j.tws.2023.110650.
[165] R. Brighenti, A. Spagnoli, M. Lanfranchi, and F. Soncini, Nonlinear deformation behaviour of auxetic cellular materials with re-entrant lattice structure, Fatigue Fract. Eng. Mat. Struct., vol. 39, no. 5, pp. 599–610, 2016. DOI: 10.1111/ffe.12381.
[166] W. Zhang, H. Yin, Y. Wu, Q. Jin, L. Wu, G. Wen, J. Liu, and X. Wu, A novel auxetic 3D lattice structure for enhancing energy absorption, Compos. Struct., vol. 326, pp. 117620, 2023. DOI: 10.1016/j.compstruct.2023.117620.
[167] Z. Wu, L. Xia, S. Wang, and T. Shi, Topology optimization of hierarchical lattice structures with substructuring, Comput. Methods Appl. Mech. Eng., vol. 345, pp. 602–617, 2019. DOI: 10.1016/j.cma.2018.11.003.
[168] M. Al Nashar and A. Sutradhar, Design of hierarchical architected lattices for enhanced energy absorption, Materials, vol. 14, no. 18, pp. 5384, 2021. DOI: 10.3390/MA14185384.
[169] J. Hou, D. Li, Z. Zhang, H. Ruan, and H. Liu, Bandgap enhancement of two-dimensional lattice metamaterial via re-entrant hierarchy, Smart Mater. Struct., vol. 31, no. 9, pp. 095012, 2022. DOI: 10.1088/1361-665X/ac7e0d.
[170] L. Liu, D. Li, and L. Dong, Mechanical properties of 2D hierarchical re-entrant cellular structures with Voronoi sub-structures, EPL., vol. 123, no. 1, pp. 16002, 2018. DOI: 10.1209/0295-5075/123/16002.
[171] L. Brely, F. Bosia, and N.M. Pugno, A hierarchical lattice spring model to simulate the mechanics of 2-D materials-based composites, Front. Mater., vol. 2, pp. 129760, 2015. DOI: 10.3389/FMATS.2015.00051/BIBTEX.
[172] J. Hou, D. Li, and L. Dong, Study on band-gap behaviors of 2D hierarchical re-entrant lattice structures, Physica Status Solidi (b)., vol. 256, no. 5, pp. 1800693, 2019. DOI: 10.1002/pssb.201800693.
[173] M.K. Khan, T. Baig, and S. Mirza, Experimental investigation of in-plane and out-of-plane crushing of aluminum honeycomb, Mater Sci Eng A., vol. 539, pp. 135–142, 2012. DOI: 10.1016/j.msea.2012.01.070.
[174] S.D. Papka and S. Kyriakides, Experiments and full-scale numerical simulations of in-plane crushing of a honeycomb, Acta Mater. vol. 46, no. 8, pp. 2765–2776, 1998.)00453-9 DOI: 10.1016/S1359-6454(97.
[175] R.K. McFarland, Hexagonal cell structures under post-buckling axial load, AIAA J., vol. 1, pp. 1380–1385, 1963. DOI: 10.2514/3.1798.
[176] M. Mahmoudabadi, A theoretical and experimental study on metal hexagonal honeycomb crushing under quasi-static and low velocity impact loading, Mater. Sci. Eng. A., vol. 528, pp. 4958–4966, 2011. DOI: 10.1016/j.msea.2011.03.009.
[177] Z. Li, T. Wang, Y. Jiang, L. Wang, and D. Liu, Design-oriented crushing analysis of hexagonal honeycomb core under in-plane compression, Compos. Struct., vol. 187, pp. 429–438, 2018. DOI: 10.1016/j.compstruct.2017.12.066.
[178] T. Tancogne-Dejean, Elastically-isotropic truss lattice materials of reduced plastic anisotropy. Int. J. Solids Struct., vol. 138, pp. 24–39, 2018. DOI: 10.1016/j.ijsolstr.2017.12.025.
[179] X. Ren, J. Shen, P. Tran, T.D. Ngo, and Y.M. Xie, Design and characterisation of a tuneable 3D buckling-induced auxetic metamaterial, Mater. Des. 2018•Elsevier., vol. 139, pp. 336–342, 2018. DOI: 10.1016/j.matdes.2017.11.025.
[180] L.R. Meza, A.J. Zelhofer, N. Clarke, A.J. Mateos, D.M. Kochmann, and J.R. Greer, Resilient 3D hierarchical architected metamaterials, Proc. Natl. Acad. Sci. USA., vol. 112, no. 37, pp. 11502–11507, 2015. DOI: 10.1073/PNAS.1509120112.
[181] I. Maskery, N.T. Aboulkhair, A.O. Aremu, C.J. Tuck, I.A. Ashcroft, R.D. Wildman, and R.J.M. Hague, A mechanical property evaluation of graded density Al-Si10-Mg lattice structures manufactured by selective laser melting. Mater. Sci. Eng. A, vol. 670, pp. 264–274, 2016. DOI: 10.1016/j.msea.2016.06.013.
[182] T. Tancogne-Dejean, M. Diamantopoulou, M.B. Gorji, et al., 3D plate-lattices: an emerging class of low-density metamaterial exhibiting optimal isotropic stiffness. Adv. Mater. vol. 30, no. 8, 2018. DOI: 10.1002/adma.201803334.
[183] J. Andrew, J. Schneider, J. Ubaid, et al., Energy absorption characteristics of additively manufactured plate-lattices under low-velocity impact loading. Int. J. Impact Eng. vol. 149, 103768, 2021. DOI: 10.1016/j.ijimpeng.2020.103768.
[184] S. Wang, Z. Zheng, C. Zhu, Y. Ding, and J. Yu, Crushing and densification of rapid prototyping polylactide foam: meso-structural effect and a statistical constitutive model, Mech. Mater., vol. 127, pp. 65–76, 2018. DOI: 10.1016/j.mechmat.2018.09.003.
[185] M. Zhao, D.Z. Zhang, F. Liu, Z. Li, Z. Ma, and Z. Ren, Mechanical and energy absorption characteristics of additively manufactured functionally graded sheet lattice structures with minimal surfaces. Int. J. Mech. Sci., vol. 167, pp. 105262, 2020. DOI: 10.1016/j.ijmecsci.2019.105262.
[186] C. Bonatti and D.M.-A. Materialia, U Smooth-shell metamaterials of cubic symmetry: anisotropic elasticity, yield strength and specific energy absorption, Acta Mater., vol. 164, pp. 301–321, 2019. DOI: 10.1016/j.actamat.2018.10.034.
[187] X. Fan, Q. Tang, Q. Feng, et al., Design, mechanical properties and energy absorption capability of graded-thickness triply periodic minimal surface structures fabricated by selective laser. Int. J. Mech. Sci., vol. 204, 106586, 2021. DOI: 10.1016/j.ijmecsci.2021.106586.
[188] R. Hensleigh, H. Cui, J. Oakdale, et al., Additive manufacturing of complex micro-architected graphene aerogels. Mater. Horiz., vol. 5, no. 6, pp. 1035–1041, 2018. •pubs.rsc.org
[189] C.M. Suryawanshi, R. Bhallamudi, and S. Mishra, Design and additive manufacturing of metamaterials for orthopedic implants and its mechanical characterization, Mech. Adv. Mater. Struct., vol. 0, pp. 1–19, 2025. DOI: 10.1080/15376494.2025.2471033.
[190] H. Yin, Z. Liu, J. Dai, G. Wen, and C. Zhang, Crushing behavior and optimization of sheet-based 3D periodic cellular structures, Compos. Part B Eng., vol. 182, pp. 107565, 2020., DOI: 10.1016/j.compositesb.2019.107565.
[191] Y. Wang, X. Ren, Z. Chen, et al., Numerical and experimental studies on compressive behavior of Gyroid lattice cylindrical shells. Materials Des., vol. 186, 108340, 2020.
[192] M. Zhang, Y. Yang, W. Qin, S. Wu, J. Chen, and C. Song, Optimizing the pinch-off problem for gradient triply periodic minimal surface cellular structures manufactured by selective laser melting, RPJ., vol. 26, no. 10, pp. 1771–1781, 2020., DOI: 10.1108/RPJ-11-2019-0298/FULL/HTML.
[193] E. Cetin, Energy absorption of thin-walled tubes enhanced by lattice structures. Int. J. Mech. Sci., vol. 157–158, pp. 471–484, 2019.
[194] F. Concli, U Numerical and experimental assessment of the static behavior of 3D printed reticular Al structures produced by selective laser melting: progressive damage, Procedia Struct. Integr., vol. 12, pp. 204–212, 2018. DOI: 10.1016/j.prostr.2018.11.094.
[195] L. Yang, R. Mertens, M. Ferrucci, C. Yan, Y. Shi, and S. Yang, Continuous graded Gyroid cellular structures fabricated by selective laser melting: design, manufacturing and mechanical properties, Mater. Des. vol. 162, pp. 394–404, 2019. DOI: 10.1016/j.matdes.2018.12.007.

[196] B. Nečemer, S. Glodež, N. Novak, et al., Numerical modelling of a chiral auxetic cellular structure under multiaxial loading conditions, Elsevier, Theor Appl Fract Mech., vol. 107, pp. 102514, 2020. DOI: 10.1016/j.tafmec.2020.102514.

[197] G.N. Labeas and M.M. Sunaric, Investigation on the static response and failure process of metallic open lattice cellular structures, Strain., vol. 46, no. 2, pp. 195–204, 2010. DOI: 10.1111/j.1475-1305.2008.00498.x.

[198] M. Leary, M. Mazur, H. Williams, et al., Inconel 625 lattice structures manufactured by selective laser melting (SLM): mechanical properties, deformation and failure modes. Materials Des., vol. 157, pp. 179–199, 2018.

[199] T. Zhong, K. He, H. Li, and L. Yang, Mechanical properties of lightweight 316L stainless steel lattice structures fabricated by selective laser melting, Mater. Des., vol. 181, pp. 108076, 2019. DOI: 10.1016/j.matdes.2019.108076.

[200] C. Li, H.-S. Shen, and H. Wang, Postbuckling behavior of sandwich plates with functionally graded auxetic 3D lattice core, Compos. Struct., vol. 237, pp. 111894, 2020. DOI: 10.1016/j.compstruct.2020.111894.

[201] M. McGregor, S. Patel, S. McLachlin, and M. Vlasea, Architectural bone parameters and the relationship to titanium lattice design for powder bed fusion additive manufacturing. Addit. Manuf., vol. 47, pp. 102273, 2021. DOI: 10.1016/j.addma.2021.102273.

[202] G. Maliaris, and E. Sarafis, Mechanical behavior of 3D printed stochastic lattice structures, SSP., vol. 258, pp. 225–228, 2016. DOI: 10.4028/www.scientific.net/SSP.258.225.

[203] H. Liu, L. Chen, Y. Jiang, D. Zhu, Y. Zhou, and X. Wang, Multiscale optimization of additively manufactured graded non-stochastic and stochastic lattice structures, Compos. Struct., vol. 305, pp. 116546, 2023. DOI: 10.1016/j.compstruct.2022.116546.

[204] R. Raj, M. Jiyalal Prajapati, J.-T. Tsai, A. Kumar, and J.-Y. Jeng, Design and additive manufacturing of novel hybrid lattice metamaterial for enhanced energy absorption and structural stability, Mater. Des., vol. 245, pp. 113268, 2024. DOI: 10.1016/j.matdes.2024.113268.

[205] C. Bhat, A. Kumar, S.C. Lin, and J.Y. Jeng, Design, fabrication, and properties evaluation of novel nested lattice structures, Addit. Manuf., vol. 68, pp. 103510, 2023. DOI: 10.1016/j.addma.2023.103510.

[206] F. Alawwa, I. Barsoum, and R.K. Abu Al-Rub, Modeling, testing, and optimization of novel lattice structures for enhanced mechanical performance, Mech. Adv. Mater. Struct., vol. 31, no. 26, pp. 8691–8714, 2023. DOI: 10.1080/15376494.2023.2262987.

[207] C. Zhang, J. Liu, Z. Yuan, S. Xu, B. Zou, L. Li, and Y. Ma, A novel lattice structure topology optimization method with extreme anisotropic lattice properties, J. Comput. Des. Eng., vol. 8, no. 5, pp. 1367–1390, 2021. DOI: 10.1093/jcde/qwab051.

[208] X. Chen, W. Ren, Y. Sun, J. Zhang, J. Yang, K. Wang, Y. Gong, Z. Zhang, and L. Bai, Adjusting unit cell three-dimensional posture and mirror array: a novel lattice structure design approach, Mater. Des., vol. 221, pp. 110852, 2022. DOI: 10.1016/j.matdes.2022.110852.

[209] A. Armanfar and E. Gunpinar, G-lattices: a novel lattice structure and its generative synthesis under additive manufacturing constraints, J Mech Des., vol. 145, no. 1, 011702, 2023. DOI: 10.1115/1.4054675/1141288.

[210] Y. Han and W.F. Lu, A novel design method for nonuniform lattice structures based on topology optimization, J Mech Des., vol. 140, no. 9, 091403, 2018. DOI: 10.1115/1.4040546/473015.

[211] Y. Deng, B. Li, Z. Huang, Y. Lin, and Y. Li, Experimental and numerical studies on the compression responses of novel mixed lattice structures, Mater. Today Commun., vol. 33, pp. 104439, 2022. DOI: 10.1016/j.mtcomm.2022.104439.

[212] X. Ma, N. Zhang, C. Zhang, and X. Tian, Mechanical behavior of a novel lattice structure with two-step deformation, Thin-Walled Struct., vol. 197, pp. 111580, 2024. DOI: 10.1016/j.tws.2024.111580.

[213] M. Zhao, B. Ji, D.Z. Zhang, H. Li, and H. Zhou, Design and mechanical performances of a novel functionally graded sheet-based lattice structure, Addit. Manuf., vol. 52, pp. 102676, 2022. DOI: 10.1016/j.addma.2022.102676.

[214] S.A. Hassanieh, A. Alhantoobi, K.A. Khan, and M.A. Khan, Mechanical properties and energy absorption characteristics of additively manufactured lightweight novel re-entrant plate-based lattice structures, Polym., vol. 13, pp. 3882, 2021. DOI: 10.3390/POLYM13223882.

[215] A. Nazir, M. Ali, and J.-Y. Jeng, Investigation of compression and buckling properties of a novel surface-based lattice structure manufactured using multi jet fusion technology, Materials, vol. 14, no. 10, pp. 2599, 2021. DOI: 10.3390/MA14102599.

[216] N.K. Choudhry, T.K. Nguyen, V. Nguyen-Van, B. Panda, and P. Tran, Auxetic lattice reinforcement for tailored mechanical properties in cementitious composite: experiments and modelling, Constr. Build. Mater., vol. 438, pp. 137252, 2024. DOI: 10.1016/j.conbuildmat.2024.137252.

[217] X. Guo, X. Li, E. Wang, J.Y.H. Fuh, W.F. Lu, and W. Zhai, Bioinspired hierarchical diamond triply periodic minimal surface lattices with high energy absorption and damage tolerance, Addit. Manuf., vol. 76, pp. 103792, 2023. DOI: 10.1016/j.addma.2023.103792.

[218] D.J. McGregor, S. Tawfick, and W.P. King, Mechanical properties of hexagonal lattice structures fabricated using continuous liquid interface production additive manufacturing, Addit. Manuf., vol. 25, pp. 10–18, 2019. DOI: 10.1016/j.addma.2018.11.002.

[219] H.N.G. Wadley, Multifunctional periodic cellular metals, Philos. Trans. A Math. Phys. Eng. Sci., vol. 364, no. 1838, pp. 31–68, 2006. DOI: 10.1098/RSTA.2005.1697.

[220] G. Li, M. Zhang, C. Zhao, et al., Design method of function-structure integrated lattice structure. IOP Conf. Ser. Mater. Sci. Eng., vol. 686, 2019. DOI: 10.1088/1757-899X/686/1/012009.

[221] M. Heidari-Rarani, Mechanical characterization of FDM 3D printing of continuous carbon fiber reinforced PLA composites, Composit. Part B Eng., vol. 175, 107147, 2019.

[222] Y.-H. Lee, B.-K. Lee, I. Jeon, and K.-J. Kang, Wire-woven bulk Kagome truss cores, Acta Mater., vol. 55, no. 18, pp. 6084–6094, 2007. DOI: 10.1016/j.actamat.2007.07.023.

[223] J.H. Koo, R. Ortiz, B. Ong, and H. Wu, Polymer nanocomposites for laser additive manufacturing, Laser Addit Manuf., pp. 205–235, 2017. DOI: 10.1016/B978-0-08-100433-3.00008-7.

[224] B. Bhushan and M. Caspers, An overview of additive manufacturing (3D printing) for microfabrication, Microsyst. Technol., vol. 23, no. 4, pp. 1117–1124, 2017. DOI: 10.1007/S00542-017-3342-8/FIGURES/6.

[225] J. Manapat and Q. Chen, 3D printing of polymer nanocomposites via stereolithography. Macromolecular Mater. Eng. vol. 302, 1600553, 2017. DOI: 10.1002/mame.201600553.

[226] J.-Y. Lee, J. An, and C.K. Chua, Fundamentals and applications of 3D printing for novel materials. Appl. Mater Today, vol. 7, pp. 120–133, 2017. DOI: 10.1016/j.apmt.2017.02.004.

[227] F. Jabri, A. Ouballouch, L. Lasri, and R. EL Alaiji, A Review on Selective Laser Sintering 3D Printing Technology for Polymer Materials. In: Zarbane, K., Beidouri, Z. (eds) Proceedings of CASICAM 2022. CASICAM 2022. Springer Tracts in Additive Manufacturing. Springer, Cham. DOI: 10.1007/978-3-031-32927-2_6.

[228] A. Nouri, A. Rohani Shirvan, Y. Li, and C. Wen, Additive manufacturing of metallic and polymeric load-bearing biomaterials using laser powder bed fusion: a review, J. Mater. Sci. Technol., vol. 94, pp. 196–215, 2021. DOI: 10.1016/j.jmst.2021.03.058.

[229] A. Awad, F. Fina, A. Goyanes, S. Gaisford, and A.W. Basit, 3D printing: principles and pharmaceutical applications of

selective laser sintering., Int. J. Pharm., vol. 586, pp. 119594, 2020. DOI: 10.1016/J.IJPHARM.2020.119594.
[230] F. Fina, A. Goyanes, S. Gaisford, and A.W. Basit, Selective laser sintering (SLS) 3D printing of medicines, Int. J. Pharm., vol. 529, no. 1–2, pp. 285–293, 2017. DOI: 10.1016/J.IJPHARM.2017.06.082.
[231] F. Fina, A. Goyanes, C.M. Madla, A. Awad, S.J. Trenfield, J.M. Kuek, P. Patel, S. Gaisford, and A.W. Basit, 3D printing of drug-loaded gyroid lattices using selective laser sintering., Int. J. Pharm., vol. 547, no. 1–2, pp. 44–52, 2018. DOI: 10.1016/J.IJPHARM.2018.05.044.
[232] F. Fina, C.M. Madla, A. Goyanes, J. Zhang, S. Gaisford, and A.W. Basit, Fabricating 3D printed orally disintegrating printlets using selective laser sintering, Int. J. Pharm., vol. 541, no. 1–2, pp. 101–107, 2018., DOI: 10.1016/J.IJPHARM.2018.02.015.
[233] X. Gan, G. Fei, J. Wang, et al., Powder quality and electrical conductivity of selective laser sintered polymer composite components, Structure and Properties of Additive Manufactured Polymer Components Woodhead Publishing Series in Composites Science and Engineering Part 2, pp. 149–185, 2020. DOI: 10.1016/B978-0-12-819535-2.00006-5.
[234] A.-M. Schwager, J. Bliedtner, K. Götze, and A. Bruder, Production of glass filters by selective laser sintering. 3D Print Opt. Addit. Photonic Manuf., vol. 22, pp. 22, 2018. DOI: 10.1117/12.2305695.
[235] R. Dou, T. Wang, Y. Guo, and B. Derby, Ink-jet printing of zirconia: coffee staining and line stability, J. Am. Ceram. Soc., vol. 94, no. 11, pp. 3787–3792, 2011. DOI: 10.1111/j.1551-2916.2011.04697.x.
[236] S. Singh, S. Ramakrishna, and F. Berto, 3D printing of polymer composites: a short review, Mater. Des. Process Commun., vol. 2, pp. e97, 2020. DOI: 10.1002/MDP2.97.
[237] I. Grida and J.R.G. Evans, Extrusion free forming of ceramics through fine nozzles, J. Eur. Ceram. Soc., vol. 23, no. 5, pp. 629–635, 2003. DOI: 10.1016/S0955-2219(02)00163-2.
[238] F. Pati, J. Jang, J. Lee, et al., Extrusion bioprinting, Biofabrication Transl., pp. 123–152, 2015. DOI: 10.1016/B978-0-12-800972-7.00007-4.
[239] A.K. Sood, R.K. Ohdar, and S.S. Mahapatra, Parametric appraisal of mechanical property of fused deposition modelling processed parts, Mater. Des., vol. 31, no. 1, pp. 287–295, 2010. DOI: 10.1016/j.matdes.2009.06.016.
[240] J.S. Chohan, R. Singh, K.S. Boparai, R. Penna, and F. Fraternali, Dimensional accuracy analysis of coupled fused deposition modeling and vapour smoothing operations for biomedical applications, Compos Part B Eng., vol. 117, pp. 138–149, 2017. DOI: 10.1016/j.compositesb.2017.02.045.
[241] A. Boschetto and L. Bottini, Accuracy prediction in fused deposition modeling, Int. J. Adv. Manuf. Technol., vol. 73, no. 5–8, pp. 913–928, 2014. DOI: 10.1007/S00170-014-5886-4/METRICS.
[242] F. Ning, W. Cong, Y. Hu, and H. Wang, Additive manufacturing of carbon fiber-reinforced plastic composites using fused deposition modeling: effects of process parameters on tensile properties, J. Compos. Mater., vol. 51, no. 4, pp. 451–462, 2017. DOI: 10.1177/0021998316646169.
[243] J. Cesarano, A review of robocasting technology, MRS Online Proc. Libr., vol. 542, pp. 133–139, 1998. DOI: 10.1557/PROC-542-133.
[244] H. Xia, J. Meng, J. Liu, X. Ao, S. Lin, and Y. Yang, Evaluation of the equivalent mechanical properties of lattice structures based on the finite element method, Materials, vol. 15, no. 9, pp. 2993, 2022. DOI: 10.3390/MA15092993.
[245] A. Seharing, A.H. Azman, and S. Abdullah, Finite element analysis of gradient lattice structure patterns for bone implant design, IJSI., vol. 11, no. 4, pp. 535–545, 2020. DOI: 10.1108/IJSI-03-2020-0028/FULL/HTML.
[246] H. Chen, Q. Han, C. Wang, Y. Liu, B. Chen, and J. Wang, Porous scaffold design for additive manufacturing in orthopedics: a review, Front. Bioeng. Biotechnol., vol. 8, pp. 609, 2020. DOI: 10.3389/FBIOE.2020.00609/FULL.
[247] L.K. Pratama, S.P. Santosa, T. Dirgantara, and D. Widagdo, Design and numerical analysis of electric vehicle li-ion battery protections using lattice structure undergoing ground impact, WEVJ., vol. 13, no. 1, pp. 10, 2021. DOI: 10.3390/wevj13010010.
[248] Z. Xue, X. Geng, X. Li, Y. Cao, J. Zhang, A. Aydeng, and J. Liu, Compressive mechanical properties of lattice structures filled with silicone rubber, Mech. Adv. Mater. Struct., vol. 31, no. 27, pp. 9062–9072, 2024. DOI: 10.1080/15376494.2023.2265354.
[249] S.-I. Park, D.W. Rosen, S-k Choi, and C.E. Duty, Effective mechanical properties of lattice material fabricated by material extrusion additive manufacturing, Addit. Manuf., vol. 1–4, pp. 12–23, 2014. DOI: 10.1016/j.addma.2014.07.002.
[250] I. Gibson, and A.M. Farries, The mechanics of three-dimensional cellular materials, Proc. R. Soc. Lond., A38243–59, vol. 382, no. 1782, 1982. DOI: 10.1098/rspa.1982.0088.
[251] C. Beyer and D. Figueroa, Design and analysis of lattice structures for additive manufacturing, J. Manuf. Sci. Eng. Trans. ASME., vol. 138, no. 12, 121014, 2016. DOI: 10.1115/1.4033957.
[252] L.G.-M. Bulletin, Cellular solids. Bull., vol. 28, pp. 270–274, 2003. DOI: 10.1557/mrs2003.79.
[253] X. Ren, L. Xiao, and Z. Hao, Multi-property cellular material design approach based on the mechanical behaviour analysis of the reinforced lattice structure, Mater. Des., vol. 174, pp. 107785, 2019. DOI: 10.1016/j.matdes.2019.107785.
[254] A. Kumar, L. Collini, A. Daurel, and J.Y. Jeng, Design and additive manufacturing of closed cells from supportless lattice structure, Addit. Manuf., vol. 33, pp. 101168, 2020. DOI: 10.1016/j.addma.2020.101168.
[255] C. Yang, K. Xu, and S. Xie, Comparative study on the uniaxial behaviour of topology-optimised and crystal-inspired lattice materials, Metals, vol. 10, no. 4, pp. 491, 2020. DOI: 10.3390/met10040491.
[256] C. Zhang, A. Banerjee, A. Hoe, A. Tamraparni, J.R. Felts, P.J. Shamberger, and A. Elwany, Design for laser powder bed additive manufacturing of AlSi12 periodic mesoscale lattice structures, Int. J. Adv. Manuf. Technol., vol. 113, no. 11-12, pp. 3599–3612, 2021. DOI: 10.1007/s00170-021-06817-w.
[257] K. Hazeli, B.B. Babamiri, J. Indeck, A. Minor, and H. Askari, Microstructure-topology relationship effects on the quasi-static and dynamic behavior of additively manufactured lattice structures, Mater. Des., vol. 176, pp. 107826, 2019. DOI: 10.1016/j.matdes.2019.107826.
[258] L. Bai, J. Zhang, Y. Xiong, X. Chen, Y. Sun, C. Gong, H. Pu, X. Wu, and J. Luo, Influence of unit cell pose on the mechanical properties of Ti6Al4V lattice structures manufactured by selective laser melting, Addit. Manuf., vol. 34, pp. 101222, 2020. DOI: 10.1016/j.addma.2020.101222.
[259] R.R. Fernandes and A.Y. Tamijani, Design optimization of lattice structures with stress constraints, Mater. Des., vol. 210, pp. 110026, 2021. DOI: 10.1016/j.matdes.2021.110026.
[260] A. Zargarian, M. Esfahanian, J. Kadkhodapour, S. Ziaei-Rad, and D. Zamani, On the fatigue behavior of additive manufactured lattice structures, Theor. Appl. Fract. Mech., vol. 100, pp. 225–232, 2019. DOI: 10.1016/j.tafmec.2019.01.012.
[261] W. Tao, A. Sutton, K. Kolan, et al., Design of lattice structures with graded density fabricated by additive manufacturing, Proc. Int. Symp. Flex. Autom., vol. 2018, pp. 122–125, 2018. DOI: 10.11509/isfa.2018.122.
[262] A.A. Zadpoor, Mechanical performance of additively manufactured meta-biomaterials., Acta Biomater., vol. 85, pp. 41–59, 2019. DOI: 10.1016/J.ACTBIO.2018.12.038.
[263] Y. Wang, Z. Chi, and J. Liu, On buckling behaviors of a typical bending-dominated periodic lattice, Compos. Struct., vol. 258, pp. 113204, 2021. DOI: 10.1016/j.compstruct.2020.113204.

[264] A. Parisien, M.S.A. ElSayed, and H. Frei, Mechanoregulation modelling of stretching versus bending dominated periodic cellular solids, Mater. Today Commun., vol. 33, pp. 104315, 2022. DOI: 10.1016/j.mtcomm.2022.104315.

[265] M.A. Wagner, T.S. Lumpe, T. Chen, and K. Shea, Programmable, active lattice structures: unifying stretch-dominated and bending-dominated topologies, Extrem Mech Lett., vol. 29, pp. 100461, 2019. DOI: 10.1016/j.eml.2019.100461.

[266] O. Eren, H.K. Sezer, and N. Yalçın, Effect of lattice design on mechanical response of PolyJet additively manufactured cellular structures, J Manuf Process., vol. 75, pp. 1175–1188, 2022. DOI: 10.1016/j.jmapro.2022.01.063.

[267] M. Alaña, A. Cutolo, S. Ruiz de Galarreta, and B. Van Hooreweder, Influence of relative density on quasi-static and fatigue failure of lattice structures in Ti6Al4V produced by laser powder bed fusion., Sci. Rep., vol. 11, no. 1, pp. 19314, 2021. DOI: 10.1038/s41598-021-98631-3.

[268] P. Płatek, J. Sienkiewicz, J. Janiszewski, and F. Jiang, Investigations on mechanical properties of lattice structures with different values of relative density made from 316L by selective laser melting (SLM)., Materials., vol. 13, no. 9, 2020. DOI: 10.3390/ma13092204.

[269] E. Alabort and D. Barba, Design of metallic bone by additive manufacturing, Scripta Mater., vol. 164, pp. 110–114, 2019. DOI: 10.1016/j.scriptamat.2019.01.022.

[270] C. Ling, A. Cernicchi, M.D. Gilchrist, and P. Cardiff, Mechanical behaviour of additively-manufactured polymeric octet-truss lattice structures under quasi-static and dynamic compressive loading, Mater. Des., vol. 162, pp. 106–118, 2019. DOI: 10.1016/j.matdes.2018.11.035.

[271] M.K. Kandasamy, A. Ganesan, and L. Srinivasan, Influence of relative density and strain rate on mechanical behavior and energy absorption of additively manufactured lattice structure, Trans. Indian Inst. Met., vol. 76, no. 2, pp. 505–510, 2023. DOI: 10.1007/S12666-022-02780-6/FIGURES/5.

[272] U.A. Dar, H.H. Mian, M. Abid, M.B. Nutkani, A. Jamil, and M.Z. Sheikh, Quasi-static compression and deformation behavior of additively manufactured flexible polymeric lattice structure, J. Materi. Eng. Perform., vol. 31, no. 4, pp. 3107–3119, 2022. DOI: 10.1007/S11665-021-06419-3/FIGURES/18.

[273] Y. Chen, M.-H. Fu, H. Hai, et al., A novel three-dimensional auxetic lattice meta-material with enhanced stiffness, Smart Mater. Struct., vol. 26, no. 10, pp. 105029, 2017. DOI: 10.1088/1361-665X/aa819e.

[274] G. Ye, H. Bi, Z. Li, and Y. Hu, Compression performances and failure modes of 3D printed pyramidal lattice truss composite structures, Compos. Commun., vol. 24, pp. 100615, 2021. DOI: 10.1016/j.coco.2020.100615.

[275] M. Al Khalil, N. Lebaal, F. Demoly, and S. Roth, A design and optimization framework of variable-density lattice structures for additive manufacturing, Mech. Adv. Mater. Struct., vol. 29, no. 26, pp. 4711–4725, 2022. DOI: 10.1080/15376494.2021.1936704.

[276] V.S. Sufiiarov, A.V. Orlov, E.V. Borisov, V.V. Sokolova, M.O. Chukovenkova, A.V. Soklakov, D.S. Mikhaluk, and A.A. Popovich, Design and mechanical properties simulation of graded lattice structures for additive manufacturing endoprostheses, Mech. Adv. Mater. Struct., vol. 28, no. 16, pp. 1656–1662, 2021. DOI: 10.1080/15376494.2019.1700432.

[277] S. Palaniyappan, D. Veeman, S. Narain Kumar, G.J. Surendhar, and L. Natrayan, Effect of printing characteristics for the incorporation of hexagonal-shaped lattice structure on the PLA polymeric material, J. Thermoplast. Compos. Mater., vol. 36, no. 5, pp. 2009–2030, 2023. DOI: 10.1177/08927057221089832/ASSET/IMAGES/LARGE/10.1177_08927057221089832-FIG8.JPEG.

[278] L. Kothandaraman and N.K. Balasubramanian, Optimization of FDM printing parameters for square lattice structures: improving mechanical characteristics, Mater Today Proc., 2024. DOI: 10.1016/j.matpr.2024.04.033.

[279] G. Dong, G. Wijaya, Y. Tang, and Y.F. Zhao, Optimizing process parameters of fused deposition modeling by Taguchi method for the fabrication of lattice structures, Addit. Manuf., vol. 19, pp. 62–72, 2018. DOI: 10.1016/j.addma.2017.11.004.

[280] A. Hussein, L. Hao, C. Yan, R. Everson, and P. Young, Advanced lattice support structures for metal additive manufacturing, J. Mater. Process. Technol., vol. 213, no. 7, pp. 1019–1026, 2013. DOI: 10.1016/j.jmatprotec.2013.01.020.

[281] X. Yang, Q. Yang, Y. Shi, L. Yang, S. Wu, C. Yan, and Y. Shi, Effect of volume fraction and unit cell size on manufacturability and compressive behaviors of Ni-Ti triply periodic minimal surface lattices, Addit. Manuf., vol. 54, pp. 102737, 2022. DOI: 10.1016/j.addma.2022.102737.

[282] Z. Chen, X. Wang, Y. Tao, S. Wen, Y. Zhou, and Y. Shi, Volume fraction effect on the mechanical and shape memory properties of NiTi gyroid lattice structure fabricated by laser powder bed fusion, JOM., vol. 76, no. 3, pp. 1715–1725, 2024. DOI: 10.1007/S11837-024-06372-1/FIGURES/11.

[283] I. Maskery, A.O. Aremu, L. Parry, R.D. Wildman, C.J. Tuck, and I.A. Ashcroft, Effective design and simulation of surface-based lattice structures featuring volume fraction and cell type grading, Mater. Des., vol. 155, pp. 220–232, 2018. DOI: 10.1016/j.matdes.2018.05.058.

[284] Y. Nie, Q. Tang, M. Zhao, and J. Song, Effect of heat treatment on mechanical properties, failure modes and energy absorption characteristics of lattice skeleton and sheet structures fabricated by SLM, J. Mater. Res. Technol., vol. 26, pp. 4925–4941, 2023. DOI: 10.1016/j.jmrt.2023.08.264.

[285] M. Galati, A. Saboori, S. Biamino, F. Calignano, M. Lombardi, G. Marchiandi, P. Minetola, P. Fino, and L. Iuliano, Ti-6Al-4V lattice structures produced by EBM: heat treatment and mechanical properties, Procedia CIRP., vol. 88, pp. 411–416, 2020. DOI: 10.1016/j.procir.2020.05.071.

[286] D. Li, R. Qin, J. Xu, B. Chen, and X. Niu, Effect of heat treatment on AlSi10Mg lattice structure manufactured by selective laser melting: microstructure evolution and compression properties, Mater. Charact., vol. 187, pp. 111882, 2022. DOI: 10.1016/j.matchar.2022.111882.

[287] M. Ali, R.K. Sari, U. Sajjad, M. Sultan, and H.M. Ali, Effect of annealing on microstructures and mechanical properties of PA-12 lattice structures proceeded by multi jet fusion technology, Addit. Manuf., vol. 47, pp. 102285, 2021. DOI: 10.1016/j.addma.2021.102285.

[288] M. Liu, N. Takata, A. Suzuki, and M. Kobashi, Effect of heat treatment on gradient microstructure of AlSi10Mg lattice structure manufactured by laser powder bed fusion, Materials, vol. 13, no. 11, pp. 2487, 2020. DOI: 10.3390/MA13112487.

[289] Y. Wang, S. Jing, Y. Liu, et al., Generative design method for lattice structure with hollow struts of variable wall thickness, Adv Mech Eng., vol. 10, no. 3, 2018. DOI: 10.1177/1687814017752482/ASSET/IMAGES/LARGE/10.1177_1687814017752482-FIG16.JPEG.

[290] K.M. Park, K.S. Min, and Y.S. Roh, Design optimization of lattice structures under compression: study of unit cell types and cell arrangements, Materials., vol. 15, no. 1, 2021. DOI: 10.3390/ma15010097.

[291] H.S. Abdulhadi and A. Mian, Effect of strut length and orientation on elastic mechanical response of modified body-centered cubic lattice structures, Proc Inst Mech Eng Part L J Mater Des Appl., vol. 233, pp. 2219–2233, 2019. DOI: 10.1177/1464420719841084/ASSET/IMAGES/LARGE/10.1177_1464420719841084-FIG14.JPEG.

[292] C. Britt, C.J. Montgomery, M.J. Brand, Z.-K. Liu, J.S. Carpenter, and A.M. Beese, Effect of processing parameters and strut dimensions on the microstructures and hardness of stainless steel 316L lattice-emulating structures made by powder bed fusion, Addit. Manuf., vol. 40, pp. 101943, 2021. DOI: 10.1016/j.addma.2021.101943.

[293] H. Fan, F. Jin, and D. Fang, Characterization of edge effects of composite lattice structures, Compos. Sci. Technol., vol. 69, no. 11–12, pp. 1896–1903, 2009. DOI: 10.1016/j.compscitech.2009.04.007.

[294] W.P. Syam, W. Jianwei, B. Zhao, I. Maskery, W. Elmadih, and R. Leach, Design and analysis of strut-based lattice structures for vibration isolation, Precis. Eng., vol. 52, pp. 494–506, 2018. DOI: 10.1016/j.precisioneng.2017.09.010.

[295] S.L. Sing, W.Y. Yeong, F.E. Wiria, and B.Y. Tay, Characterization of titanium lattice structures fabricated by selective laser melting using an adapted compressive test method, Exp. Mech., vol. 56, no. 5, pp. 735–748, 2016. DOI: 10.1007/S11340-015-0117-Y/TABLES/12.

[296] C.S. Shin and Y.C. Chang, Fabrication and compressive behavior of a micro-lattice composite by high resolution DLP stereolithography, Polymers., vol. 13, no. 5, pp. 785, 2021. DOI: 10.3390/POLYM13050785.

[297] S.O. Obadimu and K.I. Kourousis, Compressive behaviour of additively manufactured lattice structures: a review, Aerosp., vol. 8, no. 8, 2021. 207. DOI: 10.3390/aerospace8080207.

[298] ISO/ASTM DIS 52959(en), Additive manufacturing of metals—test artefacts—compression validation coupons for lattice designs. Available from https://www.iso.org/obp/ui/en/#iso:std:iso-astm:52959:dis:ed-1:v1:en (accessed 21 Oct 2024).

[299] International Organization for Standardization, 2011. ISO 13314:2011 mechanical testing of metals – ductility testing – compression test for porous and cellular metals (ISO Standard No. 13314:2011(E)). www.iso.org (accessed 21 Oct 2024).

[300] Y. Xue, W. Wang, and F. Han, Enhanced compressive mechanical properties of aluminum based auxetic lattice structures filled with polymers, Compos. Part B Eng., vol. 171, pp. 183–191, 2019. DOI: 10.1016/j.compositesb.2019.05.002.

[301] Z.H. Lin, J.H. Pan, and H.Y. Li, Mechanical strength of triply periodic minimal surface lattices subjected to three-point bending, Polymers., vol. 14, no. 14, pp. 2885, 2022. DOI: 10.3390/POLYM14142885.

[302] C. Bellini, R. Borrelli, V. Di Cocco, et al., Damage analysis of Ti6Al4V lattice structures manufactured by electron beam melting process subjected to bending load, Mater. Des. Process Commun., vol. 3, pp. e223, 2021. DOI: 10.1002/MDP2.223.

[303] ASTM Standard E8/E8M-13a, Standard test methods for tension testing of metallic materials. In: ASTM Int. http://www.astm.org/Standards/E8.htm (accessed 21 Oct 2024).

[304] M. Ast, D638, Standard test method for tensile properties of plastics, 2013 http://scholar.google.com/scholar?hl=en&btnG=Search&q=intitle:Standard+Test+Method+for+Tensile+Properties+of+Plastics#0 (accessed 21 Oct 2024).

[305] M. Bolan, M. Dean, and A. Bardelcik, The energy absorption behavior of 3D-printed polymeric octet-truss lattice structures of varying strut length and radius, Polymers, vol. 15, no. 3, pp. 713, 2023. DOI: 10.3390/POLYM15030713.

[306] X. Geng, Y. Lu, C. Liu, W. Li, and Z. Yue, Fracture characteristic analysis of cellular lattice structures under tensile load, Int. J. Solids Struct., vol. 163, pp. 170–177, 2019. DOI: 10.1016/j.ijsolstr.2019.01.006.

[307] M. Marco, R. Belda, M.H. Miguélez, and E. Giner, Numerical analysis of mechanical behaviour of lattice and porous structures, Compos. Struct., vol. 261, pp. 113292, 2021. DOI: 10.1016/j.compstruct.2020.113292.

[308] A. Zargarian, M. Esfahanian, J. Kadkhodapour, and S. Ziaei-Rad, Numerical simulation of the fatigue behavior of additive manufactured titanium porous lattice structures, Mater. Sci. Eng. C Mater. Biol. Appl., vol. 60, pp. 339–347, 2016. DOI: 10.1016/J.MSEC.2015.11.054.

[309] R.M. Gorguluarslan, O.U. Gungor, S. Yıldız, and E. Erem, Energy absorption behavior of stiffness optimized graded lattice structures fabricated by material extrusion, Meccanica., vol. 56, no. 11, pp. 2825–2841, 2021. DOI: 10.1007/S11012-021-01404-5/TABLES/6.

[310] Z.P. Sun, Y.B. Guo, and V.P.W. Shim, Deformation and energy absorption characteristics of additively-manufactured polymeric lattice structures—Effects of cell topology and material anisotropy, Thin-Walled Struct., vol. 169, pp. 108420, 2021. DOI: 10.1016/j.tws.2021.108420.

[311] A. Nazir, A.B. Arshad, and J.Y. Jeng, Buckling and post-buckling behavior of uniform and variable-density lattice columns fabricated using additive manufacturing, Materials, vol. 12, no. 21, pp. 3539, 2019. DOI: 10.3390/MA12213539.

[312] ASTM, F2971 – standard practice for reporting data for test specimens prepared by additive manufacturing, 2013. https://www.astm.org/f2971-13r21.html (accessed 21 Oct 2024).

[313] B. Yi, Y. Zhou, G.H. Yoon, and K. Saitou, Topology optimization of functionally-graded lattice structures with buckling constraints, Comput. Methods Appl. Mech. Eng., vol. 354, pp. 593–619, 2019. DOI: 10.1016/j.cma.2019.05.055.

[314] Z. Chang, Z. Wan, Y. Xu, E. Schlangen, and B. Šavija, Convolutional neural network for predicting crack pattern and stress-crack width curve of air-void structure in 3D printed concrete, Eng. Fract. Mech., vol. 271, pp. 108624, 2022. DOI: 10.1016/j.engfracmech.2022.108624.

[315] A.M.E. Arefin, N.R. Khatri, N. Kulkarni, and P.F. Egan, Polymer 3D printing review: materials, process, and design strategies for medical applications, Polymers, vol. 13, no. 9, pp. 1499, 2021. DOI: 10.3390/POLYM13091499.

[316] L. Azzouz, Y. Chen, M. Zarrelli, J.M. Pearce, L. Mitchell, G. Ren, and M. Grasso, Mechanical properties of 3-D printed truss-like lattice biopolymer non-stochastic structures for sandwich panels with natural fibre composite skins, Compos. Struct., vol. 213, pp. 220–230, 2019. DOI: 10.1016/j.compstruct.2019.01.103.

[317] A.I. Ansari and N.A. Sheikh, Simulation and Experimental Assesment of acrylonitrile butadiene styrene polymer based new lattice design, J. Inst. Eng. India. Ser. C., vol. 104, no. 3, pp. 593–604, 2023. DOI: 10.1007/S40032-023-00928-X/TABLES/5.

[318] M.T. Mansour, K. Tsongas, and D. Tzetzis, 3D printed hierarchical honeycombs with carbon fiber and carbon nanotube reinforced acrylonitrile butadiene styrene, J. Compos. Sci., vol. 5, no. 2, pp. 62, 2021. DOI: 10.3390/jcs5020062.

[319] R. Hedayati, M. Alavi, and M. Sadighi, Effect of degradation of polylactic acid (PLA) on dynamic mechanical response of 3D printed lattice structures, Materials, vol. 17, no. 15, pp. 3674, 2024. DOI: 10.3390/MA17153674/S1.

[320] R. Jain and N. Gupta, Design optimization of PLA lattice in 3D printing, Mater Today Proc., vol. 59, pp. 1577–1583, 2022. DOI: 10.1016/j.matpr.2022.02.186.

[321] X. Gao, H. Wang, X. Zhang, X. Gu, Y. Liu, G. Zhou, and S. Luan, Preparation of amorphous poly(aryl ether nitrile ketone) and its composites with nano hydroxyapatite for 3D artificial bone printing, ACS Appl. Bio Mater., vol. 3, no. 11, pp. 7930–7940, 2020. DOI: 10.1021/ACSABM.0C01044/SUPPL_FILE/MT0C01044_SI_001.PDF.

[322] C. Kummert, H.J. Schmid, L. Risse, and G. Kullmer, Mechanical characterization and numerical modeling of laser-sintered TPE lattice structures, J. Mater. Res., vol. 36, no. 16, pp. 3182–3193, 2021. DOI: 10.1557/S43578-021-00321-3/FIGURES/8.

[323] S. Bhandari, and R. Lopez-Anido, Finite element analysis of thermoplastic polymer extrusion 3D printed material for mechanical property prediction, Addit. Manuf., vol. 22, pp. 187–196, 2018. DOI: 10.1016/j.addma.2018.05.009.

[324] E.H. Backes, S.V. Harb, L.A. Pinto, N.K. de Moura, G.F. de Melo Morgado, J. Marini, F.R. Passador, and L.A. Pessan, Thermoplastic polyurethanes: synthesis, fabrication techniques, blends, composites, and applications, J. Mater. Sci., vol. 59, no. 4, pp. 1123–1152, 2024. DOI: 10.1007/s10853-023-09077-z.

[325] T.C. Cheung, S.Y. Choi, and S. Jiang, Influence of thermoplastic polyurethane and elastomer polymers on self-folding behaviour of 4D-printed polymer-textile composites, Addit.

Manuf., vol. 79, pp. 103909, 2024. DOI: 10.1016/j.addma.2023.103909.
[326] P.K. Mishra, S. Salve, and T. Jagadesh, Investigations into impact behavior of 3D printed nylon short carbon fiber composite, J. Inst. Eng. India. Ser. D., vol. 105, no. 2, pp. 1047–1058, 2024. DOI: 10.1007/S40033-023-00551-1/FIGURES/9.
[327] M. Arioli, J. Puiggalí, and L. Franco, Nylons with applications in energy generators, 3D printing and biomedicine, Molecules, vol. 29, no. 11, pp. 2443, 2024. DOI: 10.3390/MOLECULES29112443.
[328] A.S. Alaboodi and S. Sivasankaran, Experimental design and investigation on the mechanical behavior of novel 3D printed biocompatibility polycarbonate scaffolds for medical applications, J Manuf Process., vol. 35, pp. 479–491, 2018. DOI: 10.1016/j.jmapro.2018.08.035.
[329] B.A. Aloyaydi and S. Sivasankaran, Low-velocity impact characteristics of 3D-printed poly-lactic acid thermoplastic processed by fused deposition modeling, Trans. Indian Inst. Met., vol. 73, no. 6, pp. 1669–1677, 2020. DOI: 10.1007/S12666-020-01952-6/FIGURES/5.
[330] W. Wu, K. Zeng, B. Zhao, F. Duan, and F. Jiang, New considerations on the determination of the apparent shear viscosity of polymer melt with micro capillary dies, Polymers, vol. 13, no. 24, pp. 4451, 2021. DOI: 10.3390/POLYM13244451.
[331] A. Thabet, and Y. Mobarak, Predictable models and experimental measurements for electric properties of polypropylene nanocomposite films, IJECE., vol. 6, no. 1, pp. 120–129, 2016. DOI: 10.11591/ijece.v6i1.9108.
[332] R.V. Morgan, B. McReynolds, K. Husmann, et al., Markforged continuous fiber composite material testing, 2020. DOI: 10.2172/1641543.
[333] F.M. Mwania, M. Maringa, and J. Nsengimana, Investigating the effect of process parameters on the degree of fusion of two adjacent tracks produced through fused deposition modelling of acrylonitrile butadiene styrene, Polym. Test., vol. 121, pp. 107981, 2023. DOI: 10.1016/j.polymertesting.2023.107981.
[334] A.R. Zanjanijam, I. Major, J.G. Lyons, U. Lafont, and D.M. Devine, Fused filament fabrication of PEEK: a review of process-structure-property relationships, Polymers, vol. 12, no. 8, pp. 1665, 2020. DOI: 10.3390/POLYM12081665.
[335] S. Singh, C. Prakash, and S. Ramakrishna, 3D printing of polyether-ether-ketone for biomedical applications, Eur. Polym. J., vol. 114, pp. 234–248, 2019. DOI: 10.1016/j.eurpolymj.2019.02.035.
[336] A.L. De la Colina-Martínez, G. Martínez-Barrera, C.E. Barrera-Díaz, et al., Characterization of recycled polycarbonate from electronic waste and its use in hydraulic concrete: improvement of compressive performance, Adv. Concr. Constr., vol. 5, pp. 563–573, 2017. DOI: 10.12989/ACC.2017.5.6.563.
[337] Y. He, J. Zhang, Y. Jiang, Z. Liu, Y. Qi, and W. Zhao, Interfacial effects on the dynamic stresses in high speed cutting of heterogeneous materials, Procedia CIRP., vol. 77, pp. 151–154, 2018. DOI: 10.1016/j.procir.2018.08.263.
[338] R.I. Eom, H. Lee, and Y. Lee, Evaluation of thermal properties of 3D spacer technical materials in cold environments using 3D printing technology, Polymers, vol. 11, no. 9, pp. 1438, 2019. DOI: 10.3390/POLYM11091438.
[339] T.A. Lin, C.-W. Lou, and J.-H. Lin, The effects of thermoplastic polyurethane on the structure and mechanical properties of modified polypropylene blends, Appl. Sci., vol. 7, no. 12, pp. 1254, 2017. DOI: 10.3390/app7121254.
[340] J. Xie, Y. Xu, Z. Wan, A. Ghaderiaram, E. Schlangen, and B. Šavija, Auxetic cementitious cellular composite (ACCC) PVDF-based energy harvester, Energy Build., vol. 298, pp. 113582, 2023. DOI: 10.1016/j.enbuild.2023.113582.
[341] Y. Xu, E. Schlangen, M. Luković, and B. Šavija, Tunable mechanical behavior of auxetic cementitious cellular composites (CCCs): experiments and simulations, Constr. Build. Mater., vol. 266, pp. 121388, 2021. DOI: 10.1016/j.conbuildmat.2020.121388.
[342] X. Zhang, P. Liu, and L. Wu, Study on flexural properties of 3D printing functionally graded lattice structure cement composites, Mater. Lett., vol. 375, pp. 137231, 2024. DOI: 10.1016/j.matlet.2024.137231.
[343] J.G.M. van Mier, Fracture Processes of Concrete (1st ed.). CRC Press, Boca Raton, 2017. DOI: 10.1201/b22384.
[344] J.G.M. van Mier, Concrete Fracture: A Multiscale Approach (1st ed.). CRC Press, Boca Raton, 2012. DOI: 10.1201/b12968.
[345] J.E. Bolander, S. Choi, and S.R. Duddukuri, Fracture of fiber-reinforced cement composites: effects of fiber dispersion, Int. J. Fract., vol. 154, no. 1–2, pp. 73–86, 2008. DOI: 10.1007/s10704-008-9269-4.
[346] P. Stähli, R. Custer, and J.G.M. Van Mier, On flow properties, fibre distribution, fibre orientation and flexural behaviour of FRC, Mater. Struct., vol. 41, no. 1, pp. 189–196, 2008. DOI: 10.1617/s11527-007-9229-x.
[347] A. Abrishambaf, J.A.O. Barros, and V.M. Cunha, Relation between fibre distribution and post-cracking behaviour in steel fibre reinforced self-compacting concrete panels. Cement Concr. Res., vol. 51, pp. 57–66, 2013. DOI: 10.1016/j.cemconres.2013.04.009.
[348] E.V. Sarmiento, M.R. Geiker, and T. Kanstad, Influence of fibre distribution and orientation on the flexural behaviour of beams cast from flowable hybrid polymer–steel FRC, Constr Build Mater., vol. 109, pp. 166–176, 2016. DOI: 10.1016/j.conbuildmat.2016.02.005.
[349] B. Zhou and Y. Uchida, Relationship between fiber orientation/distribution and post-cracking behaviour in ultra-high-performance fiber-reinforced concrete (UHPFRC), Cem. Concr. Compos., vol. 83, pp. 66–75, 2017. DOI: 10.1016/j.cemconcomp.2017.07.007.
[350] P. Stähli and J.G.M. van Mier, Manufacturing, fibre anisotropy and fracture of hybrid fibre concrete, Eng. Fract. Mech. vol. 74, no. 1-2, pp. 223–242, 2007. DOI: 10.1016/j.engfracmech.2006.01.028.
[351] W. Hao, J. Liu, and H. Kanwal, Compressive properties of cementitious composites reinforced by 3D printed PA 6 lattice, Polym. Test., vol. 117, pp. 107811, 2023. DOI: 10.1016/j.polymertesting.2022.107811.
[352] A.W. Alshaer and D.J. Harland, An investigation of the strength and stiffness of weight-saving sandwich beams with CFRP face sheets and seven 3D printed cores, Compos. Struct., vol. 257, pp. 113391, 2021. DOI: 10.1016/j.compstruct.2020.113391.
[353] L.K. Johnson, C. Richburg, M. Lew, W.R. Ledoux, P.M. Aubin, and E. Rombokas, 3D Printed lattice microstructures to mimic soft biological materials, Bioinspir. Biomim., vol. 14, no. 1, pp. 016001, 2018. DOI: 10.1088/1748-3190/aae10a.
[354] J.D. Kang and S. Kim, Development of a 3D printing method for the textile hybrid structure, IJCST., vol. 34, no. 2, pp. 262–272, 2022. DOI: 10.1108/IJCST-09-2020-0134.
[355] Y. Xu, H. Zhang, E. Schlangen, M. Luković, and B. Šavija, Cementitious cellular composites with auxetic behavior, Cem. Concr. Compos., vol. 111, pp. 103624, 2020. DOI: 10.1016/j.cemconcomp.2020.103624.
[356] G.J. Gibbons, R. Williams, P. Purnell, and E. Farahi, 3D printing of cement composites, Adv. Appl. Ceram., vol. 109, no. 5, pp. 287–290, 2010. DOI: 10.1179/174367509X12472364600878.
[357] R.A. Buswell, W.R. Leal de Silva, S.Z. Jones, and J. Dirrenberger, 3D printing using concrete extrusion: a roadmap for research, Cem. Concr. Res., vol. 112, pp. 37–49, 2018. DOI: 10.1016/j.cemconres.2018.05.006.
[358] D. Asprone, F. Auricchio, C. Menna, and V. Mercuri, 3D printing of reinforced concrete elements: technology and design approach, Constr. Build. Mater., vol. 165, pp. 218–231, 2018. DOI: 10.1016/j.conbuildmat.2018.01.018.
[359] Y. Xu, Y. Gan, Z. Chang, Z. Wan, E. Schlangen, and B. Šavija, Towards understanding deformation and fracture in cementitious lattice materials: insights from multiscale experiments

and simulations, Constr. Build. Mater., vol. 345, pp. 128409, 2022. DOI: 10.1016/j.conbuildmat.2022.128409.
[360] D. Bourell, J.P. Kruth, M. Leu, G. Levy, D. Rosen, A.M. Beese, and A. Clare, Materials for additive manufacturing, CIRP Ann - Manuf Technol., vol. 66, no. 2, pp. 659–681, 2017. DOI: 10.1016/j.cirp.2017.05.009.
[361] K.S. Prakash, T. Nancharaih, and V.V.S. Rao, Additive manufacturing techniques in manufacturing -an overview, Mater Today Proc., vol. 5, no. 2, pp. 3873–3882, 2018. DOI: 10.1016/j.matpr.2017.11.642.
[362] S. Singh, S. Ramakrishna, and R. Singh, Material issues in additive manufacturing: a review, J Manuf Process., vol. 25, pp. 185–200, 2017. DOI: 10.1016/j.jmapro.2016.11.006.
[363] N. Li, S. Huang, G. Zhang, R. Qin, W. Liu, H. Xiong, G. Shi, and J. Blackburn, Progress in additive manufacturing on new materials: a review, J. Mater. Sci. Technol., vol. 35, no. 2, pp. 242–269, 2019. DOI: 10.1016/j.jmst.2018.09.002.
[364] G. Imbalzano, P. Tran, T.D. Ngo, and P.V.S. Lee, Three-dimensional modelling of auxetic sandwich panels for localised impact resistance, J. Sandwich Struct. Mater., vol. 19, no. 3, pp. 291–316, 2017. DOI: 10.1177/1099636215618539.
[365] P. Zhang, D. Qi, R. Xue, K. Liu, W. Wu, and Y. Li, Mechanical design and energy absorption performances of rational gradient lattice metamaterials, Compos. Struct., vol. 277, pp. 114606, 2021. DOI: 10.1016/j.compstruct.2021.114606.
[366] S.C. Han, D.S. Kang, and K. Kang, Two nature-mimicking auxetic materials with potential for high energy absorption, Mater. Today., vol. 26, pp. 30–39, 2019. DOI: 10.1016/j.mattod.2018.11.004.
[367] K.M. Conway, C. Kunka, B.C. White, G.J. Pataky, and B.L. Boyce, Increasing fracture toughness via architected porosity, Mater. Des., vol. 205, pp. 109696, 2021. DOI: 10.1016/j.matdes.2021.109696.
[368] A.J.D. Shaikeea, H. Cui, M. O'Masta, X.R. Zheng, and V.S. Deshpande, The toughness of mechanical metamaterials, Nat. Mater., vol. 21, no. 3, pp. 297–304, 2022. DOI: 10.1038/s41563-021-01182-1.
[369] J. Shi, and A.H. Akbarzadeh, 3D Hierarchical lattice ferroelectric metamaterials, Int. J. Eng. Sci., vol. 149, pp. 103247, 2020. DOI: 10.1016/j.ijengsci.2020.103247.
[370] Z. Jia, F. Liu, X. Jiang, and L. Wang, Engineering lattice metamaterials for extreme property, programmability, and multifunctionality, J Appl Phys., vol. 127, no. 15, 150901, 2020. DOI: 10.1063/5.0004724.
[371] Z. Vangelatos, K. Komvopoulos, J. Spanos, M. Farsari, and C. Grigoropoulos, Anisotropic and curved lattice members enhance the structural integrity and mechanical performance of architected metamaterials, Int. J. Solids Struct., vol. 193-194, pp. 287–301, 2020. DOI: 10.1016/j.ijsolstr.2020.02.023.
[372] R. Johnston, and Z. Kazancı, Analysis of additively manufactured (3D printed) dual-material auxetic structures under compression, Addit. Manuf., vol. 38, pp. 101783, 2021. DOI: 10.1016/j.addma.2020.101783.
[373] A. Alammar, J.C. Kois, M. Revilla-León, and W. Att, Additive manufacturing technologies: current status and future perspectives, J. Prosthodont., vol. 31, no. S1, pp. 4–12, 2022. DOI: 10.1111/jopr.13477.
[374] B.A. Praveena, N. Lokesh, A. Buradi, et al., A comprehensive review of emerging additive manufacturing (3D printing technology): methods, materials, applications, challenges, trends and future potential, Mater Today Proc., vol. 52, pp. 1309–1313, 2022. DOI: 10.1016/j.matpr.2021.11.059.
[375] J. Saroia, Y. Wang, Q. Wei, M. Lei, X. Li, Y. Guo, and K. Zhang, A review on 3D printed matrix polymer composites: its potential and future challenges, Int. J. Adv. Manuf. Technol., vol. 106, no. 5–6, pp. 1695–1721, 2020. DOI: 10.1007/s00170-019-04534-z.
[376] V. Mechtcherine, J. Grafe, V.N. Nerella, E. Spaniol, M. Hertel, and U. Füssel, 3D-printed steel reinforcement for digital concrete construction – manufacture, mechanical properties and bond behaviour, Constr. Build. Mater., vol. 179, pp. 125–137, 2018. DOI: 10.1016/j.conbuildmat.2018.05.202.
[377] I. Farina, F. Fabbrocino, G. Carpentieri, M. Modano, A. Amendola, R. Goodall, L. Feo, and F. Fraternali, On the reinforcement of cement mortars through 3D printed polymeric and metallic fibers, Compos Part B Eng., vol. 90, pp. 76–85, 2016. DOI: 10.1016/j.compositesb.2015.12.006.
[378] I. Farina, F. Fabbrocino, F. Colangelo, L. Feo, and F. Fraternali, Surface roughness effects on the reinforcement of cement mortars through 3D printed metallic fibers, Compos Part B Eng., vol. 99, pp. 305–311, 2016. DOI: 10.1016/j.compositesb.2016.05.055.
[379] C. Tang, J. Liu, W. Hao, and Y. Wei, Flexural properties of 3D printed graded lattice reinforced cementitious composites using digital image correlation, Mater. Des., vol. 227, pp. 111734, 2023. DOI: 10.1016/j.matdes.2023.111734.
[380] B. Salazar, I. Williams, P. Aghdasi, et al., Bending and crack characteristics of polymer lattice-reinforced mortar, Int. Congr. Polym. Concr., pp. 261–266, 2018. DOI: 10.1007/978-3-319-78175-4_32.
[381] J.A. Rosewitz, H.A. Choshali, and N. Rahbar, Bioinspired design of architected cement-polymer composites, Cem. Concr. Compos., vol. 96, pp. 252–265, 2019. DOI: 10.1016/j.cemconcomp.2018.12.010.
[382] S. Jang and S. Cho, The effects of polyaniline nanofibers and graphene flakes on the electrical properties and mechanical properties of ABS-like resin composites obtained by DLP 3D printing, Polymers, vol. 15, no. 14, pp. 3079, 2023. DOI: 10.3390/POLYM15143079/S1.
[383] C109/C109M, Standard test method for compressive strength of hydraulic cement mortars (using 2-in. or [50-mm] cube specimens). https://www.astm.org/c0109_c0109m-20.html (accessed 27 Sep 2024).
[384] ASTM C1609/C1609M-07, Standard test method for flexural performance of fiber-reinforced concrete (using beam with third-point loading), 2010. ASTM Int. www.astm.org (accessed 27 Sep 2024).
[385] B. Xie, X. Li, X. Zhao, and N. Hu, Tunable properties and responses of architected lattice-reinforced cementitious composite components induced by versatile cell topology and distributions, Compos. Struct., vol. 312, pp. 116850, 2023. DOI: 10.1016/j.compstruct.2023.116850.
[386] J. Li, S. Cao, and W. Song, Flexural behavior of cementitious backfill composites reinforced by various 3D printed polymeric lattices, Compos. Struct., vol. 323, pp. 117489, 2023. DOI: 10.1016/j.compstruct.2023.117489.
[387] S. Qin, S. Cao, and E. Yilmaz, Employing U-shaped 3D printed polymer to improve flexural properties of cementitious tailings backfills, Constr. Build. Mater., vol. 320, pp. 126296, 2022. DOI: 10.1016/j.conbuildmat.2021.126296.
[388] S. Zou, S. Cao, and E. Yilmaz, Enhancing flexural property and mesoscopic mechanism of cementitious tailings backfill fabricated with 3D-printed polymers, Constr. Build. Mater., vol. 414, pp. 135009, 2024. DOI: 10.1016/j.conbuildmat.2024.135009.
[389] V. Nguyen-Van, N.K. Choudhry, B. Panda, H. Nguyen-Xuan, … P. Tran, Performance of concrete beam reinforced with 3D printed bioinspired primitive scaffold subjected to three-point bending, Autom. Constr., vol. 134, pp. 104060, 2022. DOI: 10.1016/j.autcon.2021.104060.
[390] H. Singh, R.S. Ambekar, D. Das, V.A. Danam, N.K. Katiyar, B. Kanti Das, C.S. Tiwary, and J. Bhattacharya, Enhancing structural resilience by using 3D printed complex polymer reinforcement for high damage tolerant structures, Constr. Build. Mater., vol. 425, pp. 136085, 2024., DOI: 10.1016/j.conbuildmat.2024.136085.
[391] Z. Wu, Y. Xu, and B. Šavija, Mechanical properties of lightweight cementitious cellular composites incorporating micro-encapsulated phase change material, Materials., vol. 14, no. 24, pp. 7586, 2021. DOI: 10.3390/MA14247586.

[392] M. Pelanconi and A. Ortona, Nature-inspired, ultra-lightweight structures with gyroid cores produced by additive manufacturing and reinforced by unidirectional carbon fiber ribs, Materials., vol. 12, no. 24, pp. 4134, 2019. DOI: 10.3390/ma12244134.

[393] M. Chen, X. Yao, L. Zhu, M. Yin, Y. Xiong, and N. Hu, Geometric design and performance of single and dual-printed lattice-reinforced cementitious composite, Cem. Concr. Compos., vol. 143, pp. 105266, 2023., DOI: 10.1016/j.cemconcomp.2023.105266.

[394] P. Aghdasi, I.D. Williams, B. Salazar, N. Panditi, H.K. Taylor, and C.P. Ostertag, An Octet-Truss Engineered Concrete (OTEC) for lightweight structures, Compos. Struct., vol. 207, pp. 373–384, 2019., DOI: 10.1016/j.compstruct.2018.09.011.

[395] B. Xie, R. Tian, H. Zhao, T. Ye, Y. Zhang, and N. Hu, Controlling crack propagation in layered beams with architected lattice-reinforced composite interlayer designs, Constr. Build. Mater., vol. 426, pp. 136174, 2024., DOI: 10.1016/j.conbuildmat.2024.136174.

[396] P. Dong, J. Hu, C. Lin, W. Ding, J. Liu, and Y. Liu, Topology-optimized lattice enhanced cementitious composites, Mater. Des., vol. 244, pp. 113155, 2024., DOI: 10.1016/j.matdes.2024.113155.

[397] Y. Xu and B. Šavija, Auxetic cementitious composites (ACCs) with excellent compressive ductility: experiments and modeling, Mater. Des., vol. 237, pp. 112572, 2024. DOI: 10.1016/j.matdes.2023.112572.

[398] N.K. Choudhry, B. Panda, and S. Kumar, In-plane energy absorption characteristics of a modified re-entrant auxetic structure fabricated via 3D printing, Compos. Part B Eng. vol. 228, pp. 109437, 2022. DOI: 10.1016/j.compositesb.2021.109437.

[399] A. Palos, N.A. D'Souza, C. Snively, … R.F. Reidy, III, Modification of cement mortar with recycled ABS, Cem. Concr. Res. vol. 31, no. 7, pp. 1003–1007, 2001. DOI: 10.1016/S0008-8846(01)00531-2.

[400] A. Alomarah, S.H. Masood, and D. Ruan, Out-of-plane and in-plane compression of additively manufactured auxetic structures, Sci. Technol., vol. 106, pp. 106107, 2020. DOI: 10.1016/j.ast.2020.106107.

[401] Y. Xu, Z. Meng, R.J.M. Bol, and B. Šavija, Spring-like behavior of cementitious composite enabled by auxetic hyperelastic frame, Int. J. Mech. Sci., vol. 275, pp. 109364, 2024. DOI: 10.1016/j.ijmecsci.2024.109364.

[402] T. Zahra, and M. Dhanasekar, Characterisation of cementitious polymer mortar – auxetic foam composites, Constr. Build. Mater., vol. 147, pp. 143–159, 2017. DOI: 10.1016/j.conbuildmat.2017.04.151.

[403] M. Chen, S. Fang, G. Wang, Y. Xuan, D. Gao, and M. Zhang, Compressive and flexural behaviour of engineered cementitious composites based auxetic structures: an experimental and numerical study, J Build Eng., vol. 86, pp. 108999, 2024. DOI: 10.1016/j.jobe.2024.108999.

[404] G. Zhao, Y. Fan, C. Tang, Y. Wei, and W. Hao, Preparation and compressive properties of cementitious composites reinforced by 3D printed cellular structures with a negative Poisson's ratio, Dev Built Environ., vol. 17, pp. 100362, 2024. DOI: 10.1016/j.dibe.2024.100362.

[405] A. Ingrole, A. Hao, and R. Liang, Design and modeling of auxetic and hybrid honeycomb structures for in-plane property enhancement, Mater. Des., vol. 117, pp. 72–83, 2017. DOI: 10.1016/j.matdes.2016.12.067.

[406] M. Chen, Z. Chen, Y. Xuan, T. Zhang, and M. Zhang, Static and dynamic compressive behaviour of 3D printed auxetic lattice reinforced ultra-high performance concrete, Cem. Concr. Compos., vol. 139, pp. 105046, 2023., DOI: 10.1016/j.cemconcomp.2023.105046.

[407] Z. Meng, Y. Xu, J. Xie, W. Zhou, R.J.M. Bol, Q-f Liu, and B. Šavija, Unraveling the reinforcing mechanisms for cementitious composites with 3D printed multidirectional auxetic lattices using X-ray computed tomography, Mater. Des., vol. 246, pp. 113331, 2024. DOI: 10.1016/j.matdes.2024.113331.

[408] D. Edmund, T. Zahra, M. Asad, and J. Thamboo, Experimental investigation on tensile characteristics of 3D printed auxetic embedded cementitious composites and shear bonding behaviour to masonry, J Build Eng., vol. 97, pp. 110749, 2024. DOI: 10.1016/j.jobe.2024.110749.

[409] P. Tran, S. Linforth, T.D. Ngo, R. Lumantarna, and T.Q. Nguyen, Design analysis of hybrid composite anti-ram bollard subjected to impulsive loadings, Compos Struct, vol. 189, pp. 598–613, 2018. DOI: 10.1016/j.compstruct.2018.01.093.

[410] K. Ko, S. Jin, S.E. Lee, and J.-W. Hong, Impact resistance of nacre-like composites diversely patterned by 3D printing. Composite Struct., vol. 238, pp. 111951, 2020. DOI: 10.1016/j.compstruct.2020.111951.

[411] S. Maduliat, T.D. Ngo, and P. Tran, Energy absorption of steel hollow tubes under bending, Proc. Inst. Civ. Eng. Struct. Build., vol. 168, no. 12, pp. 930–942, 2015. DOI: 10.1680/jstbu.14.00109.]

[412] M.M. Sychov, L.A. Lebedev, S.V. Dyachenko, and L.A. Nefedova, Mechanical properties of energy-absorbing structures with triply periodic minimal surface topology, Acta Astronaut, vol. 150, pp. 81–84, 2018. DOI: 10.1016/j.actaastro.2017.12.034.

[413] H.H. Tsang, and S. Raza, Impact energy absorption of bio-inspired tubular sections with structural hierarchy, Compos Struct, vol. 195, pp. 199–210, 2018. DOI: 10.1016/j.compstruct.2018.04.057.

[414] I. Maskery, N.T. Aboulkhair, A.O. Aremu, C.J. Tuck, and I.A. Ashcroft, Compressive failure modes and energy absorption in additively manufactured double gyroid lattices, Addit. Manuf., vol. 16, pp. 24–29, 2017. DOI: 10.1016/j.addma.2017.04.003.

[415] D.-W. Lee, K.A. Khan, and R.K. Abu Al-Rub, Stiffness and yield strength of architectured foams based on the Schwarz Primitive triply periodic minimal surface. International J Plast, vol. 95, pp. 1–20, 2017. DOI: 10.1016/j.ijplas.2017.03.005.

[416] Biomaterials DY, U Porous scaffold design using the distance field and triply periodic minimal surface models. Biomaterials, vol. 32, no. 31, pp. 7741–7754, 2011. DOI: 10.1016/j.biomaterials.2011.07.019.

[417] Z. Wan, Y. Xu, Y. Zhang, S. He, and B. Šavija, Mechanical properties and healing efficiency of 3D-printed ABS vascular based self-healing cementitious composite: EXPERIMENTS and modelling, Eng. Fract. Mech., vol. 267, pp. 108471, 2022. DOI: 10.1016/j.engfracmech.2022.108471.

[418] T. Kien Nguyen, M. Shazwan Suhaizan, H. Nguyen-Xuan, and P. Tran, Mechanical responses of buoyant bio-inspired foamed concrete structures, Constr. Build. Mater., vol. 391, pp. 131731, 2023. DOI: 10.1016/j.conbuildmat.2023.131731.

[419] V. Nguyen-Van, P. Tran, C. Peng, L. Pham, G. Zhang, and H. Nguyen-Xuan, Bioinspired cellular cementitious structures for prefabricated construction: hybrid design & performance evaluations, Autom. Constr., vol. 119, pp. 103324, 2020. DOI: 10.1016/j.autcon.2020.103324.

[420] V. Nguyen-Van, C. Wu, F. Vogel, G. Zhang, H. Nguyen-Xuan, and P. Tran, Mechanical performance of fractal-like cementitious lightweight cellular structures: numerical investigations, Compos. Struct., vol. 269, pp. 114050, 2021. DOI: 10.1016/j.compstruct.2021.114050.

[421] J. Song, M. Cao, L. Cai, Y. Zhou, J. Chen, S. Liu, B. Zhou, Y. Lu, J. Zhang, W. Long, and L. Li, 3D printed polymeric formwork for lattice cementitious composites, J Build Eng., vol. 43, pp. 103074, 2021. DOI: 10.1016/j.jobe.2021.103074.

[422] Y. Wang, G. Zhang, H. Ren, G. Liu, and Y. Xiong, Fabrication strategy for joints in 3D printed continuous fiber reinforced composite lattice structures, Compos. Commun., vol. 30, pp. 101080, 2022., DOI: 10.1016/j.coco.2022.101080.

[423] Y. Chen, L. Ye, A.J. Kinloch, and Y.X. Zhang, 3D printed carbon-fibre reinforced composite lattice structures with good

thermal-dimensional stability, Compos. Sci. Technol., vol. 227, pp. 109599, 2022. DOI: 10.1016/j.compscitech.2022.109599.
[424] Y. Chen, L. Ye, and H. Dong, Lightweight 3D carbon fibre reinforced composite lattice structures of high thermal-dimensional stability, Compos. Struct., vol. 304, pp. 116471, 2023. DOI: 10.1016/j.compstruct.2022.116471.
[425] P. Zhang, Z. Han, X. Ran, S. Sun, and H. Fu, Path design and compression behavior of 3D printed continuous carbon fiber reinforced composite lattice sandwich structures, Compos. Struct., vol. 296, pp. 115893, 2022. DOI: 10.1016/j.compstruct.2022.115893.
[426] W. Hao, Y. Liu, T. Wang, G. Guo, H. Chen, and D. Fang, Failure analysis of 3D printed glass fiber/PA12 composite lattice structures using DIC, Compos. Struct., vol. 225, pp. 111192, 2019. DOI: 10.1016/j.compstruct.2019.111192.
[427] X. Peng, M. Zhang, Z. Guo, L. Sang, and W. Hou, Investigation of processing parameters on tensile performance for FDM-printed carbon fiber reinforced polyamide 6 composites, Elsevier, Compos Commun., vol. 22, pp. 100478, 2020. DOI: 10.1016/j.coco.2020.100478.
[428] N. Shahrubudin, T.C. Lee, and R. Ramlan, An overview on 3D printing technology: technological, materials, and Applications, Procedia Manuf., vol. 35, pp. 1286–1296, 2019. DOI: 10.1016/j.promfg.2019.06.089.
[429] G. Qi, B. Ji, and L. Ma, Mechanical response of pyramidal lattice truss core sandwich structures by additive manufacturing, vol. 6494, no. 15, pp. 1298–1306, 2019. DOI: 10.1080/15376494.2018.1432805.
[430] J.H. Martin, B.D. Yahata, J.M. Hundley, J.A. Mayer, T.A. Schaedler, and T.M. Pollock, 3D printing of high-strength aluminium alloys, Nature, vol. 549, no. 7672, pp. 365–369, 2017. DOI: 10.1038/nature23894.
[431] L. Hitzler, F. Alifui-Segbaya, P. Williams, et al., Additive manufacturing of cobalt-based dental alloys: analysis of microstructure and physicomechanical properties. Adv. Mater. Sci. Eng., pp. 12, 2018. DOI: 10.1155/2018/8213023.
[432] L.E. Murr, Frontiers of 3D printing/additive manufacturing: from human organs to aircraft fabrication, J. Mater. Sci. Technol., vol. 32, no. 10, pp. 987–995, 2016. DOI: 10.1016/j.jmst.2016.08.011.
[433] E. Uhlmann, R. Kersting, T.B. Klein, M.F. Cruz, and A.V. Borille, Additive manufacturing of titanium alloy for aircraft components, Procedia CIRP., vol. 35, pp. 55–60, 2015. DOI: 10.1016/j.procir.2015.08.061.
[434] H.E.L. Etri, A.K. Singla, M.T. Özdemir, M.E. Korkmaz, R. Demirsöz, M.K. Gupta, J.B. Krolczyk, and N.S. Ross, Wear performance of Ti-6Al-4 V titanium alloy through nano-doped lubricants, ArchivCivMechEng., vol. 23, no. 3, 2023. DOI: 10.1007/s43452-023-00685-9.
[435] Q. Zhou, X. Xing, X. Gong, Z. Zhou, X. Zhang, and X. Hu, Enhanced compressive mechanical properties of different topological lattice structures fabricated by additive manufacturing, Mech. Adv. Mater. Struct., vol. 32, no. 9, pp. 1868–1881, 2025. DOI: 10.1080/15376494.2024.2372458.
[436] Y.E. Mukhrish, M. Asad, M. Azhar, and A. Khan, Experimental investigations on wire arc additive manufacturing process using an Inconel 625 alloy wire, Mech. Adv. Mater. Struct., vol. 31, no. 26, pp. 8242–8253, 2024. DOI: 10.1080/15376494.2023.2256336.
[437] M.R. Kamranfard, H. Darijani, and S. Khademzadeh, Mechanical behavior of Ti6Al4V lattice structures; numerical and experimental analysis, Mech. Adv. Mater. Struct., vol. 31, no. 4, pp. 735–748, 2024. DOI: 10.1080/15376494.2022.2120651.
[438] G. Tzortzinis, A. Gross, and S. Gerasimidis, Auxetic boosting of confinement in mortar by 3D reentrant truss lattices for next generation steel reinforced concrete members, Extrem Mech Lett., vol. 52, pp. 101681, 2022. DOI: 10.1016/j.eml.2022.101681.
[439] C. Luo, X. Ren, D. Han, X.G. Zhang, R. Zhong, X.Y. Zhang, and Y.M. Xie, A novel concrete-filled auxetic tube composite structure: design and compressive characteristic study, Eng. Struct., vol. 268, pp. 114759, 2022. DOI: 10.1016/j.engstruct.2022.114759.
[440] P. Morel, Automated casting systems for spatial concrete lattices, Modelling Behav. Des. Model Symp. pp. 213–223, 2015. DOI: 10.1007/978-3-319-24208-8_18.
[441] Z. Chang, Y. Chen, E. Schlangen, and B. Šavija, A review of methods on buildability quantification of extrusion-based 3D concrete printing: from analytical modelling to numerical simulation, Dev Built Environ., vol. 16, pp. 100241, 2023. DOI: 10.1016/j.dibe.2023.100241.
[442] Z. Chang, M. Liang, S. He, E. Schlangen, and B. Šavija, Lattice modelling of early-age creep of 3D printed segments with the consideration of stress history, Mater. Des., vol. 234, pp. 112340, 2023., DOI: 10.1016/j.matdes.2023.112340.
[443] Z. Wan, Y. Xu, S. He, E. Schlangen, and B. Šavija, The use of additive manufacturing in self-healing cementitious materials: a state-of-the-art review, Dev Built Environ., vol. 17, pp. 100334, 2024. DOI: 10.1016/j.dibe.2024.100334.
[444] A. Du Plessis, A.J. Babafemi, S.C. Paul, B. Panda, J.P. Tran, and C. Broeckhoven, Biomimicry for 3D concrete printing: a review and perspective, Addit. Manuf., vol. 38, pp. 101823, 2021, DOI: 10.1016/j.addma.2020.101823.
[445] L. Wang, H. Jiang, Z. Li, and G. Ma, Mechanical behaviors of 3D printed lightweight concrete structure with hollow section, ArchivCivMechEng., vol. 20, no. 1, pp. 1–17, 2020. DOI: 10.1007/s43452-020-00017-1.
[446] Y. Chen, Z. Chang, S. He, O. Çopuroğlu, B. Šavija, and E. Schlangen, Effect of curing methods during a long time gap between two printing sessions on the interlayer bonding of 3D printed cementitious materials, Constr. Build. Mater., vol. 332, pp. 127394, 2022. DOI: 10.1016/j.conbuildmat.2022.127394.
[447] A.L. van Overmeir, B. Šavija, F.P. Bos, and E. Schlangen, Effects of 3D concrete printing phases on the mechanical performance of printable strain-hardening cementitious composites, vol. 13, no. 10, pp. 2483, 2023. DOI: 10.3390/buildings13102483.
[448] Z. Chang, M. Liang, Y. Xu, E. Schlangen, and B. Šavija, 3D concrete printing: lattice modeling of structural failure considering damage and deformed geometry, Cem. Concr. Compos., vol. 133, pp. 104719, 2022. DOI: 10.1016/j.cemconcomp.2022.104719.
[449] F.P. Bos, C. Menna, M. Pradena, E. Kreiger, W.R.L. da Silva, A.U. Rehman, D. Weger, R.J.M. Wolfs, Y. Zhang, L. Ferrara, and V. Mechtcherine, The realities of additively manufactured concrete structures in practice, Cem. Concr. Res., vol. 156, pp. 106746, 2022. DOI: 10.1016/j.cemconres.2022.106746.
[450] G. Ma, R. Buswell, W.R. Leal da Silva, L. Wang, J. Xu, and S.Z. Jones, Technology readiness: a global snapshot of 3D concrete printing and the frontiers for development, Cem. Concr. Res., vol. 156, pp. 106774, 2022. DOI: 10.1016/j.cemconres.2022.106774.
[451] Z. Chang, H. Zhang, M. Liang, E. Schlangen, and B. Šavija, Numerical simulation of elastic buckling in 3D concrete printing using the lattice model with geometric nonlinearity, Autom. Constr., vol. 142, pp. 104485, 2022. DOI: 10.1016/j.autcon.2022.104485.
[452] Anon, Innovative rapid prototyping process makes large sized, smooth surfaced complex shapes in a wide variety of materials, Mater Technol., vol. 13, pp. 53–56, 1998. DOI: 10.1080/10667857.1998.11752766.
[453] B. Khoshnevis, D. Hwang, K.T. Yao, and Z. Yeh, Mega-scale fabrication by contour crafting, IJISE., vol. 1, no. 3, pp. 301–320, 2006. DOI: 10.1504/IJISE.2006.009791.
[454] B. Khoshnevis, R. Russell, H. Kwon, and S. Bukkapatnam, Crafting large prototypes. IEEE Robot. Automat. Mag., vol. 8, no. 3, pp. 33–42, 2001. DOI: 10.1109/100.956812.

[455] B. Khoshnevis, Automated construction by contour crafting – related robotics and information technologies, Autom. Constr., vol. 13, no. 1, pp. 5–19, 2004. DOI: 10.1016/j.autcon.2003.08.012.

[456] T.A.M. Salet, Z.Y. Ahmed, F.P. Bos, and H.L.M. Laagland, Design of a 3D printed concrete bridge by testing, *Virtual Phys Prototyp., vol. 13, no. 3, pp. 222–236, 2018. DOI: 10.1080/17452759.2018.1476064.

[457] M. Nodehi, F. Aguayo, S.E. Nodehi, A. Gholampour, T. Ozbakkaloglu, and O. Gencel, Durability properties of 3D printed concrete (3DPC), Autom. Constr., vol. 142, pp. 104479, 2022. DOI: 10.1016/j.autcon.2022.104479.]

[458] S. Bhattacherjee, A.S. Basavaraj, A.V. Rahul, M. Santhanam, R. Gettu, B. Panda, E. Schlangen, Y. Chen, O. Copuroglu, G. Ma, L. Wang, M.A. Basit Beigh, and V. Mechtcherine, Sustainable materials for 3D concrete printing, Cem. Concr. Compos., vol. 122, pp. 104156, 2021., DOI: 10.1016/j.cemconcomp.2021.104156.

[459] A. Bhardwaj, S.Z. Jones, N. Kalantar, Z. Pei, J. Vickers, T. Wangler, P. Zavattieri, and N. Zou, Additive manufacturing processes for infrastructure construction: a review, J. Manuf. Sci. Eng., vol. 141, no. 9, pp. 13, 2019. DOI: 10.1115/1.4044106.

[460] T. Wangler, N. Roussel, F.P. Bos, T.A.M. Salet, and R.J. Flatt, Digital concrete: a review, Cem Concr Res 2019•Elsevier., vol. 123, pp. 105780, 2019. DOI: 10.1016/j.cemconres.2019.105780.

[461] I. Perkins and M. Skitmore, Three-dimensional printing in the construction industry: a review, Int J Constr Manag., vol. 15, no. 1, pp. 1–9, 2015. DOI: 10.1080/15623599.2015.1012136.

[462] B. Panda, Y.W.D. Tay, S.C. Paul, and M.J. Tan, Current challenges and future potential of 3D concrete printing, Materialwissenschaft Werkst., vol. 49, no. 5, pp. 666–673, 2018. DOI: 10.1002/mawe.201700279.

[463] S. Hou, Z. Duan, J. Xiao, and J. Ye, A review of 3D printed concrete: performance requirements, testing measurements and mix design, Constr. Build. Mater., vol. 273, pp. 121745, 2021. DOI: 10.1016/j.conbuildmat.2020.121745.

[464] Z. Chang, Y. Xu, Y. Chen, Y. Gan, E. Schlangen, and B. Šavija, A discrete lattice model for assessment of buildability performance of 3D-printed concrete, Computer. Aided Civil Eng., vol. 36, no. 5, pp. 638–655, 2021. DOI: 10.1111/mice.12700.

[465] D. Liu, Z. Zhang, X. Zhang, and Z. Chen, 3D printing concrete structures: state of the art, challenges, and opportunities, Constr. Build. Mater., vol. 405, pp. 133364, 2023. DOI: 10.1016/j.conbuildmat.2023.133364.

[466] R. Dilawar Riaz, M. Usman, A. Ali, U. Majid, M. Faizan, and U. Jalil Malik, Inclusive characterization of 3D printed concrete (3DPC) in additive manufacturing: a detailed review, Constr. Build. Mater., vol. 394, pp. 132229, 2023. DOI: 10.1016/j.conbuildmat.2023.132229.

[467] S. Kristombu Baduge, S. Navaratnam, Y. Abu-Zidan, T. McCormack, K. Nguyen, P. Mendis, G. Zhang, and L. Aye, Improving performance of additive manufactured (3D printed) concrete: a review on material mix design, processing, interlayer bonding, and reinforcing methods, Structures., vol. 29, pp. 1597–1609, 2021. DOI: 10.1016/j.istruc.2020.12.061.

[468] S. Luhar, T. Suntharalingam, S. Navaratnam, I. Luhar, J. Thamboo, K. Poologanathan, and P. Gatheeshgar, Sustainable and renewable bio-based natural fibres and its application for 3d printed concrete: a review, Sustain., vol. 12, no. 24, pp. 10485, 2020. DOI: 10.3390/su122410485.

[469] T. Ding, J. Xiao, and V. Mechtcherine, Microstructure and mechanical properties of interlayer regions in extrusion-based 3D printed concrete: a critical review, Cem. Concr. Compos., vol. 141, pp. 105154, 2023. DOI: 10.1016/j.cemconcomp.2023.105154.

[470] K. Liu, K. Takasu, J. Jiang, K. Zu, and W. Gao, Mechanical properties of 3D printed concrete components: a review, Dev Built Environ., vol. 16, pp. 100292, 2023. DOI: 10.1016/j.dibe.2023.100292.

[471] B. Bhushan Jindal, and P. Jangra, 3D Printed Concrete: a comprehensive review of raw material's properties, synthesis, performance, and potential field applications, Constr. Build. Mater., vol. 387, pp. 131614, 2023. DOI: 10.1016/j.conbuildmat.2023.131614.

[472] J. Zhang, J. Wang, S. Dong, X. Yu, and B. Han, A review of the current progress and application of 3D printed concrete, Compos. Part A Appl. Sci. Manuf., vol. 125, pp. 105533, 2019. DOI: 10.1016/j.compositesa.2019.105533.

[473] J. Xiao, G. Ji, Y. Zhang, G. Ma, V. Mechtcherine, J. Pan, L. Wang, T. Ding, Z. Duan, and S. Du, Large-scale 3D printing concrete technology : current status and future opportunities, Cem. Concr. Compos., vol. 122, pp. 104115, 2021. DOI: 10.1016/j.cemconcomp.2021.104115.

[474] M.T. Souza, I.M. Ferreira, E. Guzi de Moraes, L. Senff, and A.P. Novaes de Oliveira, 3D printed concrete for large-scale buildings: an overview of rheology, printing parameters, chemical admixtures, reinforcements, and economic and environmental prospects, J. Build. Eng., vol. 32, pp. 101833, 2020., DOI: 10.1016/j.jobe.2020.101833.

[475] S.K. Kaliyavaradhan, P.S. Ambily, P.R. Prem, and S.B. Ghodke, Test methods for 3D printable concrete, Autom. Constr., vol. 142, pp. 104529, 2022. DOI: 10.1016/j.autcon.2022.104529.

[476] C. Zhang, V.N. Nerella, A. Krishna, S. Wang, Y. Zhang, V. Mechtcherine, and N. Banthia, Mix design concepts for 3D printable concrete: a review, Cem. Concr. Compos., vol. 122, pp. 104155, 2021., DOI: 10.1016/j.cemconcomp.2021.104155.]

[477] F. Lyu, D. Zhao, X. Hou, L. Sun, and Q. Zhang, Overview of the development of 3D-printing concrete: a review, Appl Sci., vol. 11, no. 21, pp. 9822, 2021. DOI: 10.3390/app11219822.

[478] S.A. Khan, M. Koç, and S.G. Al-Ghamdi, Sustainability assessment, potentials and challenges of 3D printed concrete structures: a systematic review for built environmental applications, J Clean Prod., vol. 303, pp. 127027, 2021. DOI: 10.1016/j.jclepro.2021.127027.

[479] A.K. Tiwari, P.P. Pratapa, and M. Santhanam, Lattice concrete: 3D printed periodic cellular structures through selective cement hydration, J Build Eng., vol. 86, pp. 108946, 2024. DOI: 10.1016/j.jobe.2024.108946.

[480] D. Dey, V.N. Van, H.N. Xuan, D. Srinivas, B. Panda, and P. Tran, Flexural performance of 3D printed concrete structure with lattice infills, Dev Built Environ., vol. 16, pp. 100297, 2023. DOI: 10.1016/j.dibe.2023.100297.

[481] J. Ye, Y. Weng, H. Du, M. Li, J. Yu, and M. Nasir Uddin, Feasibility of using ultra-high ductile concrete to print self-reinforced hollow structures, RILEM Bookseries., vol. 37, pp. 133–138, 2022., DOI: 10.1007/978-3-031-06116-5_20.

[482] A.A. AlZahrani, A.A. Alghamdi, and A.A. Basalah, Computational optimization of 3D-printed concrete walls for improved building thermal performance, Buildings., vol. 12, no. 12, pp. 2267, 2022. DOI: 10.3390/buildings12122267.

[483] D. Nemova, E. Kotov, D. Andreeva, S. Khorobrov, V. Olshevskiy, I. Vasileva, D. Zaborova, and T. Musorina, Experimental study on the thermal performance of 3D-printed enclosing structures, Energies, vol. 15, no. 12, pp. 4230, 2022. DOI: 10.3390/en15124230.

[484] T. Suntharalingam, P. Gatheeshgar, I. Upasiri, K. Poologanathan, B. Nagaratnam, H. Rajanayagam, and S. Navaratnam, Numerical study of fire and energy performance of innovative light-weight 3d printed concrete wall configurations in modular building system, Sustain., vol. 13, no. 4, pp. 2314, 2021. DOI: 10.3390/su13042314.

[485] J. Ye, J. Zhang, J. Yu, J. Yu, and K. Yu, Flexural behaviors of 3D printed lightweight engineered cementitious composites (ECC) slab with hollow sections, Eng. Struct., vol. 299, pp. 117113, 2024., DOI: 10.1016/j.engstruct.2023.117113.

[486] X. Han, J. Yan, M. Liu, L. Huo, and J. Li, Experimental study on large-scale 3D printed concrete walls under axial compression, Autom. Constr., vol. 133, pp. 103993, 2022. DOI: 10.1016/j.autcon.2021.103993.

[487] K. Cuevas, J. Strzałkowski, J.-S. Kim, C. Ehm, T. Glotz, M. Chougan, S.H. Ghaffar, D. Stephan, and P. Sikora, Towards development of sustainable lightweight 3D printed wall building envelopes – Experimental and numerical studies, Case Stud. Constr. Mater., vol. 18, pp. e01945, 2023., DOI: 10.1016/j.cscm.2023.e01945.

[488] Y. Yang, H. Wu, L. Han, Q. Huang, S. Yang, J. Bai, and M. Feng, Investigation on geometric and surface finish quality of 3D concrete printed walls with hollow section, Adv. Struct. Eng., vol. 27, no. 3, pp. 386–401, 2024. DOI: 10.1177/13694332231222088.

[489] W. Wang, D. Feng, L. Yang, S. Li, and C.C.L. Wang, Topology optimization of self-supporting lattice structure, Addit. Manuf., vol. 67, pp. 103507, 2023. DOI: 10.1016/j.addma.2023.103507.

[490] H.E. Etri, Graphene: a state-of-the-art review of types, properties and applications in different sectors tribological behavior of titanium view project graphene: a state-of-the-art review of types, properties and applications in different sectors, Prabha Mater. Sci. Lett., vol. 2, no. 2, pp. 98–139, 2023. DOI: 10.33889/PMSL.2023.2.2.009.]

[491] P. Wang, F. Yang, B. Zheng, et al., Breaking the tradeoffs between different mechanical properties in bioinspired hierarchical lattice metamaterials, Adv. Funct. Mater., vol. 33, pp. 1–13, 2023. DOI: 10.1002/adfm.202305978.

[492] S. Mubarak, D. Dhamodharan, M.B. Kale, et al., A novel approach to enhance mechanical and thermal properties of SLA 3D printed structure by incorporation of metal–metal oxide nanoparticles, Nanomater., vol. 10, pp. 217, 2020. DOI: 10.3390/NANO10020217.

[493] K. Markandan and C.Q. Lai, Enhanced mechanical properties of 3D printed graphene-polymer composite lattices at very low graphene concentrations, Compos Part A Appl Sci Manuf., vol. 129, pp. 105726, 2020. DOI: 10.1016/j.compositesa.2019.105726.

[494] X. Geng, M. Wang, and B. Hou, Experiment investigation of the compression behaviors of nickel-coated hybrid lattice structure with enhanced mechanical properties, Micromachines, vol. 14, no. 10, pp. 1959, 2023. DOI: 10.3390/MI14101959.

[495] H. Kazemi, A. Vaziri, and J.A. Norato, Multi-material topology optimization of lattice structures using geometry projection, Comput. Methods Appl. Mech. Eng., vol. 363, pp. 112895, 2020. DOI: 10.1016/j.cma.2020.112895.

[496] R-q Feng, F-c Liu, W-j Xu, M. Ma, and Y. Liu, Topology optimization method of lattice structures based on a genetic algorithm, Int. J. Steel Struct., vol. 16, no. 3, pp. 743–753, 2016. DOI: 10.1007/S13296-015-0208-8/METRICS.

[497] Z. Xiao, Y. Yang, R. Xiao, Y. Bai, C. Song, and D. Wang, Evaluation of topology-optimized lattice structures manufactured via selective laser melting, Mater. Des., vol. 143, pp. 27–37, 2018., DOI: 10.1016/j.matdes.2018.01.023.

[498] R.N. Oosterbeek, G. Sirbu, S. Hansal, K. Nai, and J.R.T. Jeffers, Effect of chemical–electrochemical surface treatment on the roughness and fatigue performance of porous titanium lattice structures, Addit. Manuf., vol. 78, pp. 103896, 2023. DOI: 10.1016/j.addma.2023.103896.

[499] J.P. Wahl, S. An, R. Foest, N. Emminghaus, and J. Hermsdorf, Surface treatment of additively manufactured stainless steel 316L lattice structures by plasma electrolytic polishing, Procedia CIRP., vol. 124, pp. 669–672, 2024. DOI: 10.1016/j.procir.2024.08.198.

[500] N. Soro, N. Saintier, H. Attar, and M.S. Dargusch, Surface and morphological modification of selectively laser melted titanium lattices using a chemical post treatment, Surf Coatings Technol., vol. 393, pp. 125794, 2020. DOI: 10.1016/j.surfcoat.2020.125794.

[501] B.J. Mohan, A. Vasudevan, and C.H.C. Alexandar, A comparative analysis of flexural strength between 3D printed lattice structures (ABS) compared with and without the silica nanoparticle, Proc 5TH Int Conf Sustain Innov Eng Technol 2023. vol. 3161, pp. 020256, 2024. DOI: 10.1063/5.0229659/3310708.

[502] S.E. Taher, J.M. Ashraf, K. Liao, and R.K. Abu Al-Rub, Mechanical properties of graphene-based gyroidal sheet/shell architected lattices, Graphene and 2D Mater., vol. 8, no. 3–4, pp. 161–178, 2023. DOI: 10.1007/s41127-023-00066-2.